

የኢፌዲሪ የቴክኒክና ሙያ ስልጠና ኢንስቲትዩት
FDRE TECHNICAL & VOCATIONAL TRAINING INSTITUTE

TECHNICAL AND VOCATIONAL TRAINING INSTITUTION (TVTI)

School of Graduate Studies

FACULTY OF ELECTRICAL AND ELECTRONICS TECHNOLOGY AND INFORMATION AND COMMUNICATION TECHNOLOGY

(DEPARTMENT OF ELECTRONICS AND COMMUNICATION TECHNOLOGY MANAGEMENT)

THESIS ON: DESIGN AND APPLICATIONS OF MASSIVE MIMO ANTENNA WITH METASURFACE FOR 5G WIRELESS COMMUNICATIONS SYSTEM

Thesis for the Partial Fulfillment of Master of Science (MSc.) in Electronics and communication Technology Management

By,

Abinet Oche Alemu (TTMR/014/16)

Supervisor,

Anand Anbalagan, PhD

June 2026

Addis Ababa, Ethiopia

የኢፌዲሪ የቴክኒክና ሙያ ስልጠና ኢንስቲትዩት
FDRE TECHNICAL & VOCATIONAL TRAINING INSTITUTE

DESIGN AND APPLICATIONS OF MASSIVE MIMO ANTENNA WITH METASURFACE FOR 5G WIRELESS COMMUNICATIONS SYSTEM

A Thesis submitted to:

TECHNICAL AND VOCATIONAL TRAINING INSTITUTE (TVTI)
FACULTY OF ELECTRICAL AND ELECTRONICS TECHNOLOGY AND INFORMATION AND COMMUNICATION TECHNOLOGY (DEP'T OF ELECTRICAL AND ELECTRONICS TECHNOLOGY)
IN PARTIAL FULFILLMENT FOR THE

MASTER OF SCIENCE IN ELECTRONICS AND COMMUNICATION TECHNOLOGY MANAGEMENT

By,

Abinet Oche (TTMR/014/16)

Supervisor,

Anand Anbalagan, PhD

Jan 2026

Addis Ababa, Ethiopia

DECLARATIONS

I hereby declare that this thesis paper is my original work, has not been presented for a degree in this or any other university, and all necessary sources of materials used for the thesis have been duly acknowledged.

Name: Abinet Oche Signature Date

Declared by: _____ _____

Place: Addis Ababa, Ethiopia

Submission Approval

This thesis entitled **"Design and Applications of Massive MIMO Antenna with Meta surface for 5G Wireless Communications System**" submitted in partial fulfillment of the requirements for the MSc. in Electronics and Communication Technology Management at the School of Electrical and Electronics Technology, written by Abinet Oche. Has been submitted for thesis examination with my approval as TVTI advisor.

Anand Anbalagan, PhD

Signature: _____

Submission Date: _____

ACKNOWLEDGMENT

First and foremost, I thank God for giving me strength, health, and guidance throughout this research journey. I would like to express my deepest gratitude to my supervisor, Dr. Anand Anbalagan, for his continuous support, valuable guidance, and patience during this research. His knowledge, advice, and encouragement were essential in completing this thesis. I am also grateful to the faculty and staff of the Department of Electronics and Communication Technology Management at TVTI for providing the necessary resources and support throughout my study. My sincere thanks go to my friends and colleagues who supported me and shared ideas during this work.

Finally, I thank my family for their love, understanding, and endless encouragement. Without them, this work would not have been possible.

የኢፌዲሪ የቴክኒክና ሙያ ስልጠና ኢንስቲትዩት
FDRE TECHNICAL & VOCATIONAL TRAINING INSTITUTE

Faculty of Electrical & Electronics Technology and Information & Communication Technology (Dept. of Electrical and Electronics Technology)

Thesis on

Design and Applications of Massive MIMO Antenna with Meta surface for 5G Wireless Communications System

Prep. By,

Abinet Oche

APPROVED BY THESIS ADVISORY COMMITTEE

Name of the Advisor	**Signature**	**Date**
----------	----------	----------

Name of the Examiner, Internal	**Signature**	**Date**
----------	----------	----------

Name of the Examiner, External

----------	----------	----------

Name of the Chairperson

----------	----------	----------

TABLE OF CONTENTS

DECLARATIONS i
ACKNOWLEDGMENT ii
LIST OF TABLE viii
LIST OF FIGURE ix
LIST OF ACRONYM xi
ABSTRACT xii
CHAPTER ONE 1
INTRODUCTION 1
1.1 Background of Study 1
1.2. Statement of Problems 1
1.3. Objectives 2
1.3.1. General Objective 2
1.3.2. Specific Objective 2
1.4. Significance of Thesis 2
1.5. Scope of Thesis 3
1.6. Limitations of Thesis 3
1.7. Thesis Outlines 4
CHAPTER TWO 5
LITERATURE REVIEWS 5
2.1 Introductions to Literature Reviews 5
2.2. Reviews of Related Works 5
2.3. Literature Summary 15
2.4. Gap Summary 17
CHAPTER THREE 18
THEORETICAL BACKGROUND AND METHOD OF ANALYSIS 18
3.1 Introduction to chapter three 18
3.2. Methodology and Materials 18
3.2.1. Methodology 18
3.2.2. Flow Chart 19

3.2.3 Material 20
3.3. Trapezoidal micro strip patch antenna 21
3.4. Mata Material 22
3.4.1. Application of metamaterial 22
3.4.2. Meta material Unit Cell 23
3.4.3. Corporation Metamaterial into antenna design 23
3.4.4. Advantage of Metamaterials for Antenna Design 24
3.5. MIMO Antenna 24
3.5.1. Advantage of MIMO Antenna for 5G WCS 25
3.6. Analyzing Method 26
3.6.1 Meta material Unit Cell Analyzing Methods 26
3.6.2 Physical Interpretation 27
3.6.3. Conductor Thickness 30
3.7. Trapezoidal Patch Analyzing Methods 33
3.7.1. Transmission Line Modeling 33
3.7.2. Cavity Modeling 36
CHAPTER FOUR 38
DESIGN MASSIVE MIMO ANTENNA WITH METASURFACE FOR 5G WCS 38
4.1. Design Considerations 38
4.2. Design Trapezoidal Patch Antenna 38
4.2.1 Design Procedures 38
4.3. Design Trapezoidal Array Layout for Massive MIMO 41
4.3.1. Design Procedures 41
4.4. Design Meta surface 41
4.4.1 Design Procedures 41
CHAPTER FIVE 45
SIMULATION RESULT, DISCUSSIONS AND ANALYSIS 45
5.1. Result and Discussions 45
5.2. Simulation Results of single Trapezoidal patch antenna 45
5.2.1. Gain of single Trapezoidal patch antenna 45
5.2.2. Directivity of single Trapezoidal patch antenna 46

5.2.3. S11 of single Trapezoidal patch antenna 47
5.2.4. Voltage Standing Wave Ratio of Single Trapezoidal Patch Antenna 48
5.2.5. Radiation Patterns of Single Trapezoidal Patch Antenna 49
5.2.6. 3D Polar Plot of Single Trapezoidal Patch Antenna 50
5.3. Simulation Results of Single Trapezoidal patch antenna with Meta surface 51
5.3.1. Gain of single Trapezoidal patch antenna with Met surface 51
5.3.2. Directivity of single Trapezoidal patch antenna with Met surface 52
5.3.3. S11 of single Trapezoidal patch antenna with Met surface 53
5.3.4. Voltage Standing Wave Ratio of Single Trapezoidal Patch Antenna with Metasurface 54
5.3.5. Radiation Patterns of Single Trapezoidal Patch Antenna with Met surface 55
5.3.6. 3D Polar Plot of Single Trapezoidal Patch Antenna with Met surface 56
5.4. Simulation Results of 2x4 MIMO Trapezoidal patch antenna for 5G WCS 57
5.4.1. Gain of 2x4 MIMO Trapezoidal patch antenna for 5G WCS 57
5.4.2. Directivity of 2x4 MIMO Trapezoidal patch antenna for 5G WCS 58
5.4.3. S11 of 2x4 MIMO Trapezoidal patch antenna for 5G WCS 59
5.4.4. VSWR of 2x4 MIMO Trapezoidal Patch Antenna 60
5.4.5. Radiation Patterns of 2x4 MIMO Trapezoidal Patch Antenna 61
5.4.6. 3D Polar Plot of 2x4 MIMO Trapezoidal Patch Antenna 61
5.5. Simulation Results of 2x4 MIMO Trapezoidal patch antenna for 5G WCS with Meta surface 62
5.5.1. Gain of 2x4 MIMO Trapezoidal patch antenna for 5G WCS with Meta surface 63
5.5.2. Directivity of 2x4 MIMO Trapezoidal patch antenna for 5G WCS with Metasurface 63
5.5.3. S11 of 2x4 MIMO Trapezoidal patch antenna for 5G WCS with Meta surface 64
5.5.4. VSWR of 2x4 MIMO Trapezoidal Patch Antenna with Meta surface 65
5.5.5. Radiation Patterns of 2x4 MIMO Trapezoidal Patch Antenna with Meta surface 65
5.5.6. 3D Polar Plot of 2x4 MIMO Trapezoidal Patch Antenna with Meta surface 66
5.6. Simulation Results of 4x4 MIMO Trapezoidal patch antenna without Meta surface 67
5.6.1. Gain of 4x4 MIMO Trapezoidal patch antenna without Meta surface 68

5.6.2. Directivity of 4x4 MIMO Trapezoidal patch antenna without Meta surface ...68
5.6.3. S11of 4x4 MIMO Trapezoidal patch antenna without Meta surface 69
5.6.4. VSWR of 4x4 MIMO Trapezoidal Patch Antenna without Meta surface 70
5.6.5. Radiation Patterns of 4x4 MIMO Trapezoidal Patch Antenna.....70
5.6.6. 3D Polar Plot of 4x4 MIMO Trapezoidal Patch Antenna 71
5.7. Simulation Results of 4x4 MIMO Trapezoidal patch antenna with Meta surface..72
5.7.1. Gain of 4x4 MIMO Trapezoidal patch antenna with Met surface 72
5.7.2. Directivity of 4x4 MIMO Trapezoidal patch antenna with Meta surface 73
5.7.3. S11 of 4x4 MIMO Trapezoidal patch antenna without Met surface.....74
5.7.4. Voltage Standing Wave Ratio of 4x4 MIMO Trapezoidal Patch Antenna with Meta surface 74
5.7.5. Radiation Patterns of 4x4 MIMO Trapezoidal Patch Antenna with Met surface 75
5.7.6. 3D Polar Plot of 4x4 MIMO Trapezoidal Patch Antenna 76
5.8. Performance Comparisons of Designed Antenna for 5G mobile CS.....77
5.8.1 Discussion.....78
5.9. Performance Comparisons of proposed work with previously related works for 5G MCS 79
5.9.1. Discussions.....80
CHAPTER SIX:.....81
CONCLUSION AND FUTURE RECOMMENDATIONS 81
6.1. CONCLUSION.....81
6.2. Thesis contribution.....81
6.3. Future Direction 82
REFERENCE.....83

LIST OF TABLES

Table 1 Literature Summary 15
Table 2. Performance Comparisons of Designed Antenna for 5G mobile CS 77
Table 3. Performance Comparisons of proposed work with previously related works for 5G MC 79

LIST OF FIGURES

Figure 1. Flow chart of Thesis 19
Figure 2. The LC resonant circuit of the unit cell 27
Figure 3. Trapezoidal Patch Antenna 33
Figure 4. Electric Field Distributions 36
Figure 5. Single Trapezoidal patch antenna 45
Figure 6. Total Gains of single TPA 46
Figure 7.Total Directivity of single TPA 47
Figure 8. Reflection Coefficient of single TPA 48
Figure 9. Reflection Coefficient of single TPA 49
Figure 10. Radiation Patterns of Single TPA 50
Figure 11. 3D Polar plots of Single TPA 51
Figure 12. Single TPA with Meta surface 51
Figure 13. Total Gains of single TPA with Meta surface 52
Figure 14. Total Directivity of single TPA with Met surface 53
Figure 15. Reflection Coefficient of single TPA with Met surface 54
Figure 16. Reflection Coefficient of single TPA with Met surface 55
Figure 17. Radiation Patterns of Single TPA with Met surface 56
Figure 18.3D Polar plots of Single TPA with Met surface 57
Figure 19.2x4 MIMO TPA for 5G WCS 57
Figure 20. Total Gains of 2x4 MIMO TPA 58
Figure 21. Total Directivity of 2x4 MIMO TPA 59
Figure 22. Reflection Coefficient of 2x4 MIMO TPA 60
Figure 23. Voltage Standing Wave Ratio of 2x4 MIMO TPA 60
Figure 24. Radiation Patterns of 2x4 MIMO TPA 61
Figure 25. 3D Polar plots of 2x4 MIMO TPA 62
Figure 26. 2x4 MIMO TPA for 5G WCS with Meta surface 63
Figure 27. Total Gains of 2x4 MIMO TPA with Meta surface 63
Figure 28. Total Directivity of 2x4 MIMO TPA with meta surface 64
Figure 29. Reflection Coefficient of 2x4 MIMO TPA with Met surface 65
Figure 30. VSWR of 2x4 MIMO TPA with Met surface 65
Figure 31. Radiation Patterns of 2x4 MIMO TPA with Meta surface 66
Figure 32. 3D Polar plots of 2x4 MIMO TPA with Meta surface 67
Figure 33. 3D Polar plots of 4x4 MIMO TPA without Meta surface 67
Figure 34. Total Gains of 4x4 MIMO TPA without Meta surface 68
Figure 35. Total Directivity of 4x4 MIMO TPA without Meta surface 69
Figure 36. Reflection Coefficient of 4x4 MIMO TPA without Met surface 69
Figure 37. VSWR of 4x4 MIMO TPA 70
Figure 38. Radiation Patterns of 4x4 MIMO TPA 71
Figure 39. 3D Polar plots of 4x4 MIMO TPA without metasurface 72
Figure 40. 3D Polar plots of 4x4 MIMO TPA with Met surface 72
Figure 41. Total Gains of 4x4 MIMO TPA with Met surface 73
Figure 42. Total Directivity of 4x4 MIMO TPA with Met surface 73

Figure 43. Reflection Coefficient of 4x4 MIMO TPA with Met surface 74
Figure 44. VSWR of 4x4 MIMO TPA with Meta surface 75
Figure 45.Radiation Patterns of 4x4 MIMO TPA 76
Figure 46. 3D Polar plots of 4x4 MIMO TPA.....76

LIST OF ACRONYMS

Abbr.	Meaning	Abbr.	Meaning
5G	Fifth Generation (Wireless Network)	IRS	Intelligent Reflecting Surface
6G	Sixth Generation (Wireless Network)	ITS	Intelligent Transmitting Surface
AR	Axial Ratio	LA	Lens Array
BW	Bandwidth	Mm Wave	Millimeter Wave
CMA	Characteristic Mode Analysis	MIA	Meta material-Inspired Antenna
CP	Trapezoidal Polarization	MIMO	Multiple Input Multiple Output
CSAA	Connected Slot Antenna Array	MPA	Micro strip Patch Antenna
D2D	Drone-to-Drone	MTM	Meta material
D2G	Drone-to-Ground	MTS	Metamaterial
D2S	Drone-to-Satellite	NZRI	Near-Zero Refractive Index
DG	Diversity Gain	OSB	Open Stop Band
DGS	Defected Ground Structure	RF	Radio Frequency
DNG	Double-Negative (Meta material)	SAR	Specific Absorption Rate
ECC	Envelope Correlation Coefficient	SNR	Signal-to-Noise Ratio
ENG	Epsilon-Negative (Meta material)	SRR	Split Ring Resonator
FD	Fully Digital (Pre coder)	S-parameters	Scattering Parameters

ABSTRACT

The increasing demands for network expansion require Multiple-Input Multiple-Output (MIMO) technology which needs Multiple-Input Multiple-Output (MIMO) technology that can deploy extensive antenna systems. The study investigated the complete characteristics of a large MIMO antenna together with its adaptable Meta surface which supports innovative 5G wireless communication technology. The proposed design uses Meta materials to achieve electromagnetic control which solves three major problems such as mutual coupling, bandwidth constraints, and ineffective beam formation that affect standard MIMO systems. A trapezoidal patch antenna array was developed and optimized to function in the sub-6 GHz frequency range specifically at 3.5 GHz which serves as a vital 5G access network frequency. The Meta surface augmented design achieves significant performance improvements over traditional patch arrays in three key areas design delivers notable gains in isolation, directivity, and gain, which full wave simulations demonstrate through comprehensive testing. The antenna demonstrates wide impedance bandwidth which extends beyond 1GHz the voltage standing wave ratio (VSWR) reached 1.9dB while its return loss (S11) dropped below -19dB at 3.5GHz. The Meta surface integration delivers exceptional diversity performance through its 90% efficiency maintenance and 0.001 ECC reductions. The design enables urban areas to have dense deployments through its combination of better spectrum efficiency and reliable connections and energy-saving design. The findings showcase massive MIMO systems with Meta surface support as effective solutions which enable fast data transfer and low latency and strong coverage in tough environments to evolve into next-generation wireless networks. This research supports the creation of flexible sustainable antenna technologies which will benefit 5G networks and all future communication technologies.

Key Words*:* Massive MIMO Antenna, Meta surface, Sub 6 GHz (3.5 GHz) Band, 5G Wireless Communication Systems

CHAPTER ONE

INTRODUCTION

1.1 Background of Study

Wireless communication technologies need to develop faster data rates and better coverage and increased network capacity because they are advancing toward 5G and beyond. The requirements for network expansion will be fulfilled through network demands which need Multiple-Input Multiple-Output (MIMO) technology that can deploy extensive antenna systems. The typical MIMO systems face three main challenges which operate their system performance through energy efficiency, antenna size and interference management in difficult operational environments[1].

The challenges can be solved through the implementation of artificial materials which possess distinct electromagnetic characteristics as Met materials in large MIMO array systems. Met materials enable beam forming enhancement through their ability to control electromagnetic waves in innovative ways which enable real-time signal transmission management. The research aims to develop a large MIMO antenna through Met material technology because it will bring substantial performance improvements for spatial diversity and energy efficiency and signal quality enhancements[2].

The design combines Massive MIMO benefits with Met material attributes to create wireless communication systems that reach higher performance levels which scalability, and adaptability in a range of challenging scenarios. The study develops advanced antennas which will support 5G and future wireless technologies [3].

1.2. Statement of Problems

The increasing demand for the high-performance antenna systems which enable multiple users to communicate simultaneously without experiencing cross-signal interference has become critical because 5G networks and IoT devices and urban areas experience their highest mobile data usage.

The performance of conventional single-element antennas and small-scale MIMO arrays suffers from multiple limitations which include restricted bandwidth capabilities and their low gain performance and directivity limitations and their ability to spatially multiplex signals.

The performance of dense MIMO arrays experiences detrimental effects from electromagnetic losses, surface-wave propagation and mutual coupling between antennas. The development of scalable MIMO antennas requires high-gain wideband designs which create efficient radiation performance to meet the needs of sub-6 GHz 5G wireless systems.

1.3. Objectives

1.3.1. General Objective

- Design and Applications of Trapezoidal Massive MIMO Antenna Array with Met surface for 5G Wireless Communications System"

1.3.2. Specific Objective

- To design single and multi element trapezoidal patch antennas with and without metas urfaces for the 3.5 GHz sub-6 GHz 5G band.
- To analyze and optimize the gain, directivity, S11, VSWR, and bandwidth of massive MIMO antennas for high-efficiency 5G wireless communication systems.
- To standardize the proposed antenna designs must be evaluated through testing against current sub-6 GHz and mm Wave MIMO systems to determine which configuration works best for real-world 5G implementations.

1.4. Significance of Thesis

The wireless communication field requires advanced antenna technologies which deliver ultra-reliable connections with high-speed performance and energy-efficient operation to support its transition from current technologies to 5G and 6G networks. The traditional Massive MIMO systems achieve better spectral efficiency yet face hardware limitations and beam formation challenges and power consumption problems which become worse during high-density dynamic situations.

The thesis introduces an innovative approach to Massive MIMO antenna systems through the integration of Met materials which delivers a compact design that enables users to control beam patterns and perform precise wave control. The upcoming wireless systems will receive their major advancement through this integration which will boost system adaptability and energy-efficient operations and spatial coverage while solving crucial challenges.

The study supports the creation of antenna systems which deliver high performance while being scalable and sustainable to achieve widespread connectivity and environmentally friendly communication. The research findings support academic smart antenna system research while advancing industry smart antenna system deployment which enables the development of wireless infrastructure that remains operational for future wireless technology.

1.5. Scope of Thesis

The main goals of this thesis work which establishes design procedures for Massive MIMO antenna systems that use Meta material to create 5G and future wireless systems. The study aims to enhance traditional Massive MIMO systems through energy-efficient beam forming and spatial coverage improvements which use reconfigurable Meta materials for electromagnetic manipulation.

The research examines downlink transmission performance at millimeter-wave (mm Wave) and sub-6 5G frequency bands which serve as essential links to next-generation testing networks. The project includes performance simulations which use standard wireless channel models and Met material electromagnetic modeling and hybrid antenna design development. The research employs software simulations to evaluate system performance instead of using physical hardware implementation and real-time system testing.

The proposed design assessment uses key performance metrics which include energy consumption and beam forming accuracy and signal-to-noise ratio (SNR) and spectral efficiency measurements. The thesis presents a comparison between the proposed Met material-assisted system and traditional MIMO antenna arrays for different deployment scenarios.

1.6. Limitations of Thesis

The research on metamaterial-loaded MIMO antennas is conducted theoretically, as there is no space to practically test their performance in real life. The performance testing is conducted in a controlled environment, which is not comparable to the real challenges faced due to interference or signal fading in real life. The research focuses on a specific 5G communication frequency range which limits its applicability to different wireless frequency bands. The process of integrating and fabricating met materials creates

challenges that threaten to make large-scale production unfeasible. The optimization process concentrates on essential antenna characteristics which include isolation and gain and bandwidth instead of testing all aspects which include mechanical durability and thermal behavior.

1.7. Thesis Outlines

This thesis is organized into six chapters

- **Chapter 1: Introduction**: Provides background, motivation, problem statement, and research objectives.
- **Chapter 2: Literature Review**: Reviews existing MIMO antenna designs and met material applications in 5G communication.
- **Chapter 3: Theoretical Background**: Discusses fundamental concepts of met materials, MIMO systems, antenna theory and Method of Analysis.
- **Chapter 4: Design:** Details the proposed antenna design methodology, simulation setup, and performance analysis.
- **Chapter 5: Results and Discussion**: Presents simulation results, compares with existing designs, and analyzes performance metrics.
- **Chapter 6: Conclusion and Future Work**: Summarizes findings, highlights contributions, and suggests directions for further research.

CHAPTER TWO

LITERATURE REVIEWS

2.1 Introductions to Literature Reviews

This chapter reviews related works of Massive MIMO Antenna with Metamaterial for Ne xt Generations 5G Wireless Communication Systems.

2.2. Reviews of Related Works

In this Literature, a broadband Meta material-based MIMO antenna has been proposed. The proposed MIMO antenna has applications in 5G technology at millimeter wave frequencies. The proposed MIMO antenna has a configuration of 1×2 elements to increase the gain of the antenna. A 9×6 SRR-based Meta material cell has been stacked on top of the antenna to increase gain and reduce coupling effect [4]. The antenna and the Met material are fabricated using Rogers's 5880 substrate with 0.787 mm and 1.6 mm thickness, respectively. The antenna's performance is evaluated using S-parameters, MIMO, and radiation patterns. The antenna design is applicable in 5G technology since it operates in the mm-wave frequency spectrum, specifically in the Ka-band, with an increased gain and improved isolation using the Meta material [5].

Unmanned Antenna Vehicles (UAVs) need high data rates, which can be achieved by using the mm-wave and sub-THz frequency bands. In this paper, we propose a two-port leaky wave MIMO antenna using the coplanar proximity technique with capacitive and inductive loading. The mesh slot and vertical slot are used to overcome the open stop band issues, providing broadside and bidirectional radiation. H-shaped slots are used to increase the isolation between ports, while the coffee bean Meta material (MTS) is used to increase the efficiency of the radiation. The simulations are carried out in different scenarios, showing the beam steering, Trapezoidal polarization (CP), and high-gain features of the proposed MIMO antenna, with a maximum gain of 13.8 dBi, an axial ratio of less than 2.9, a diversity gain of more than 9.98 dB, and an envelope correlation coefficient of less than 0.003. The proposed MIMO antenna can be used for D2G, D2D, and D2S communications [5].

In this article, a new low-profile Meta material antenna is proposed, targeted for use in 5G mm-wave communications. The antenna is developed with a base slot antenna, along with a Meta material structure placed on top, comprising a 3x3 patch array structure. By placing slits and stubs in the patches, higher-order modes are eliminated, along with problems like beam splitting and beam squint. Experimental results show that it covers a bandwidth of 25.14% (23.3-30 GHz, 5G) with a peak gain of 8dB[6].

This Literature deals with the design and performance analysis of meta-material inspired millimeter wave antenna arrays, specifically designed for 5G wireless communication systems at a frequency of 38 5G. The antenna elements are designed using Rogers' 5880 substrate with a dielectric constant of 2.2 and a thickness of 0.35 mm. The paper analyzes single-element, 2 x 1-element, and 4 x 1-element MIA arrays. The parameters taken into consideration are return loss, bandwidth, gain, voltage standing wave ratio, and total efficiency. The advancements in the design of the MIA arrays over traditional micro-strip patch antennas are discussed in the paper. The impact of using meta-material structures on the design of antennas and their radiation characteristics is also discussed[7].

This Article proposes two new innovative massive multiple-input multiple-output transmitter architectures, specifically suited for millimeter wave communications systems. In these proposed transmitter architectures, a small number of active antennas, with their own dedicated radio frequency chains, illuminate a nearby large intelligent reflecting/transmitting surface. The intelligent reflecting/transmitting surface is comprised of many low-cost, low-power, passive antennas that can reflect or transmit the phase-shifted version of the impinging electromagnetic waves. In contrast to the lens array antennas, where the number of active antennas must increase linearly with the number of passive antennas, the IRS/ITS-aided antennas can increase the number of radiating passive antennas without increasing the number of active antennas proportionally, based on the configurability of the intelligent surface. The paper addresses the special constraints that pre-coders of IRS/ITS-aided antennas must meet, which are different from those of conventional MIMO systems[8]. With the above constraints in mind, two efficient pre-coders are proposed: one based on maximizing mutual information, and another based on approximating the optimal unconstrained FD pre-coder with the help of the orthogonal matching pursuit algorithm. Moreover, a power consumption model is developed for IRS/ITS-aided antennas, considering spillover loss, taper loss, aperture loss, phase shifter loss, etc. From the simulation results, it can be concluded that the

position of the active antennas with regard to the IRS/ITS plays an important role in achieving better results. From the simulation results, it can be concluded that, unlike other MIMO systems, IRS/ITS-aided antennas are highly efficient in terms of power consumption, as well as highly scalable with regard to the number of antennas used for transmission, making them suitable for achieving the full potential of mm Wave ultra-massive MIMO systems [9].

With the above constraints, two efficient pre-coding schemes are proposed: one that maximizes mutual information and another that approximates the optimal unconstrained frequency domain pre-coder using the orthogonal matching pursuit algorithm. Moreover, a power consumption model for the IRS/ITS-assisted antennas is developed, considering spillover loss, taper loss, aperture loss, phase shifter loss, etc. The simulation results show that the position of the active antennas with respect to the IRS/ITS plays an important role in the overall performance. Moreover, the simulation results show that, unlike other MIMO systems, IRS/ITS-assisted antennas offer better power efficiency with respect to the number of transmitting antennas, thus unlocking the full potential of millimeter-wave ultra-m Massive MIMO systems [10].

Another study discusses the use of Meta materials for the development of extensive antenna arrays for the purpose of massive MIMO devices used in 5G networks. The compact nature of these antennas makes it easier to integrate these devices into extensive arrays because of the smaller size of the antennas. The parameters that are analyzed include S-parameters, radiation characteristics, and derivations related to the envelope correlation coefficient (ECC) and diversity gain[11].

In one study, a novel planar scalar impedance holographic Meta material is proposed and discussed. The proposed Meta material has the capability to enable directional beam forming with controlled polarization and gain. The Meta material is composed of simple geometric patches and mainly operates in the transverse magnetic (TM) surface wave mode with some transverse electric (TE) component. The TE component is used to enable beam forming at non-phase crossover frequencies[12].

Another contribution proposes a high-gain and low-profile antenna design using a dual-layer metamaterial. The metamaterial structure comprises square patch cell elements arranged on different dielectric substrates. The feeding mechanism is achieved by using an aperture coupling technique on the bottom layer. The design allows the antenna to

function in dual modes at two close frequency points. The design parameters are optimized using a genetic algorithm. The optimized design exhibits an impedance bandwidth of 44%, or 4.08-6.38 GHz at -10 dB. The 3 dB gain bandwidth of the optimized design is 45%, or 4.16-6.56 GHz. The optimized design also exhibits a peak gain of 11.6 dB[13].

Yet another study presents a compact broadband mushroom antenna with a metamaterial structure. The structure comprises mushroom elements along with a ground plane having a slot-fed micro strip line. The slot is placed at the bottom of the central part of the mushroom gap. The performance of the proposed structure is determined by a transmission line model with composite right/left-handed dispersion. The proposed structure operates at 5G frequency with a bandwidth of 25% at S11 < -10 dB, with a gain of 9.9 dBi, along with efficiencies of over 76%, along with cross-polarization suppression of over 20 dB[14].

In another study, a metamaterial lens antenna is proposed, which is specifically designed for full-dimensional massive MIMO systems with multi-beam functionality in sub-6 GHz 5G frequency bands. In the proposed design, an 8x8 dual-polarized patch array is integrated with a lightweight Jerusalem-cross-based metamaterial, which achieves a scanning range of ±25°, peak gain of 22.4 dB, and gain bandwidth of 3.3 dB at 5.6 GHz. The multi-layer, low-cost nature of the proposed design outperforms the conventional dielectric lenses in terms of compactness and ease of implementation for 5G beam forming [15].

A literature source presents a versatile antenna design with the intention of supporting 4G and 5G on mobile devices. The design combines a slot antenna with tunable frequency support for the 4G/WLAN band of 2.05-2.7 GHz with a connected slot antenna array supporting the 23-29 GHz band for 5G devices. The slot antenna array utilizes a reactor diode to offer tenability, while the connected slot array utilizes eight feeders on a small Rogers 5880 substrate of dimensions 70 x 60 x 0.381 mm^3. The orthogonal orientation of the slots allows for MIMO functionality, with an envelope correlation coefficient as low as 0.01, along with isolation between ports of more than 20 dB[16].

In another study, a method to reduce mutual coupling by placing parasitic L-shaped strips between closely spaced antenna elements has been proposed. The proposed method has

been shown to provide isolation levels higher than 30 dB without compromising radiation characteristics[17].

A micro strip patch MIMO array optimized for 5.8 GHz 5G WLAN operation is proposed, which combines characteristic mode analysis with defected ground structures having crossed slots. The proposed MIMO array presents low mutual coupling, as low as -32 dB, along with good gain performance of about 5.3 dB per element. With good MIMO performance, as indicated by an envelope correlation coefficient of 0.0001 along with a diversity gain of about 10 dB, the proposed MIMO array presents strong promise for its application in next-generation systems[18].

Finally, a MIMO antenna with a metamaterial structure suitable for millimeter Wave 5G communication systems is shown in the paper. The structure has four elements with a rotation of 90 degrees to create a compact structure. The addition of a 2x2 mm Wave structure enhances the gain from 7 dB to 10.44 dBs The structure has an efficiency of above 80%. The structure has been validated using CST simulations and physical implementations with good ECC, DG, and no channel capacity loss[19].

This paper proposes a metamaterial-enhanced MIMO antenna design optimized for use in 5G systems at the 28 GHz millimeter wave band. In order to achieve a compact MIMO antenna, the design consists of four antennas placed in a square similar arrangement with a 90-degree phase shift. To improve the isolation and radiation properties, the metamaterial structure which is made up of trapezoidal split ring resonators is placed at the bottom of the antennas. The dimensions of the proposed antenna are 24 x 24 mm, and the frequency range of operation extends from 23.5 to 29.4 GHz. The results obtained from both simulation and measurement indicate that the antenna has a peak gain of 10.44 dBi and efficiencies above 80%, while the MIMO antenna metrics indicate satisfactory performance[20].

The purpose of this paper is to develop a broadband antenna using a metamaterial structure with the aim of minimizing cross-polarization levels to extremely low values, with the antenna design process guided by characteristic mode analysis (CMA). With the inclusion of a metamaterial structure, it is possible to significantly suppress higher-order modes, thus resulting in a high performance antenna with a wide range of frequency operation. In this regard, the approach is to tune the modal characteristics to achieve

minimum cross-polarization, an essential aspect in improving signal quality in wireless communication systems[21].

A metamaterial structure above the radiators transforms linear polarization into trapezoidal (circular-like) polarization in this innovative dual-port printed MIMO antenna for 28 GHz 5G mm-wave communication. For polarization conversion, the proposed metamaterial unit cell is formed by a square conducting strip with corners connected diagonally in order to produce a $\pi/2$ phase difference between Ex and Ey electric fields. The proposed antenna size is $12 \times 8.5 \times 0.8$ mm³ and the dimensions of this antenna are optimized by machine learning to enhance throughput performance. To prove MIMO diversity performance, experimental validation is given and confirmed that the proposed antenna can work for 5G mm-wave communication[22].

In this article, a broadband Metamaterial-based MIMO antenna has been proposed to increase gain and isolation characteristics. The proposed MIMO antenna has a 1x2 array configuration with a concurrent feed line. A stacked structure consisting of a 9x6 SRR elongated cell has been used to increase gain characteristics. The MIMO antenna has been realized on Rogers 5880 substrates with thickness values of 0.787 mm and 1.6 mm. The proposed MIMO antenna has been optimized to operate in the Ka-band frequency range of the mm-wave spectrum. The proposed MIMO antenna has shown an increase in gain characteristics with the integration of metamaterial structures. The proposed MIMO antenna has potential applications in 5G technology [23].

An MIMO antenna with multiband characteristics for 5G and Wi-Fi6E applications is presented. In order to obtain the tri-band resonance, the structure consists of SRRs and cosine type monopole. Archimedean spiral metamaterial and folded SRR are employed for further band-extending. These metamaterials provide good decoupling of surface and space waves. The Archimedean spiral metamaterial (ASM) is used to decouple the space waves in the tri-frequency bands. The proposed MIMO antenna exhibits a better decoupling in the measurements. It can be observed that the decoupling at 3.5 GHz (5G), 5.8 GHz (5G) and 6.9 GHz (5G) increased by 3.5 dB, 36.47 dB and 6.42 dB respectively. The average efficiency of the proposed design is 89%. The design also shows an ECC of 0.0025 on average. Using metamaterial, the peak gain is improved by 4.3 dB at 3.5 GHz, 3.8 dB at 5.8 GHz and 1.9 dB at 6.9 GHz respectively. The designed metamaterial MIMO antenna offers a significant enhancement in decoupling and peak gain[24].

The literature introduces an MIMO antennas system using metamaterial for smartphone 5G technology applications. The proposed antenna is a combination of two dual-band compact antennas, which ensures that the entire operation band, covering 5G bands such as millimeter wave and others are covered. Metamaterial is introduced in the antenna design to improve the isolation between the antenna ports, and that enables an effective reduction of inter-port coupling for this type of antenna system. The metamaterial design is built up by a resonator array and it enhances the isolation while maintaining the efficiency of the entire antenna system. The antenna configuration exhibits high efficiency, etch area, couple band for the impedance bandwidth of 5.2-6 GHz and 7.4-8 GHz a low Envelope Correlation Coefficient (ECC), so that it is suitable to be implemented in handheld devices for 5G applications. Based on the simulation results, the performance of the design in terms of isolation, bandwidth and overall efficiency of antenna system are demonstrated. The compact size of the antenna system and its enhanced isolation renders it suitable for future wireless communication technologies[25].

This paper proposes multi-frequency, multiple-input, multiple-output antenna design, specifically targeted towards 5G technology and Wi-Fi 6E applications. The design makes use of a cosine-shaped monopole antenna, along with the use of split-ring resonators, to achieve tri-band resonance. To improve the bandwidth, folded split-ring resonators, as well as an Archimedean spiral metamaterial, are integrated into the design to achieve both surface wave decoupling as well as space wave decoupling. The use of an Archimedean spiral metamaterial helps improve space wave decoupling over the three frequencies of operation. At 3.5 GHz, 5.8 GHz, and 6.9 GHz, the measurements' results demonstrate enhanced decoupling by 3.5 dB, 36.47 dB and 6.42 dB, respectively. The antenna also achieves an average efficiency of 89%, with an average envelope correlation coefficient of 0.0025. The gain of the antenna increases by 4.3 dB, 3.8 dB, and 1.9 dB at 3.5 GHz, 5.8 GHz, and 6.9 GHz, respectively, with the use of the metamaterial in the design, thereby improving the overall performance of the MIMO antenna[26].

The article presents a MIMO antenna system which uses a metamaterial component to achieve high isolation between its antenna elements, enabling the system to function correctly in 5G smartphone applications. The article presents a compact MIMO antenna system which operates in 5G frequency bands, including millimeter wave bands, through its use of a metamaterial component which provides high isolation between its antenna

elements, thus enabling 5G smartphone applications. In this proposed antenna, high isolation is achieved between antenna elements using a metamaterial component, thus making it suitable for a 5G device. In addition, it is highly efficient, covers a wide frequency band, and exhibits a low envelope correlation coefficient, making it suitable for a 5G device. Simulations have been conducted to validate the proposed antenna with regard to isolation, frequency band, and radiation performance, thus making it suitable for a 5G device. In addition, it is compact in size, making it suitable for a 5G device[25].

The literature discussed in this section focuses on the design and performance evaluation of metamaterial-inspired millimeter wave antenna arrays for fifth-generation (5G) wireless communication systems with a center frequency of 38 GHz. In this work, single-element, 2x1 and 4x1 micro strip patch antenna (MPA) arrays are examined. A Rogers RO5880 substrate with a thickness of 0.35 mm and a dielectric constant of 2.2 is used to create the MPA array. In order to decrease losses on the ground plane and enhance the fringing field at the patch borders, metamaterials specifically split-ring resonators, or SRRs are integrated to affect the current distribution on the radiating patch. The simulation results reveal significant improvements in performance with return losses of -82.95 dB, -67.1 dB, and -69.12 dB; bandwidths of 1.971 5G, 2.278 5G, and 4.704 5G; gains of 7.36 dBi, 9.11 dBi, and 11.4 dBi; voltage standing wave ratios (VSWR) of 1.001432, 1.0009, and 1.0007; and total efficiencies of 95.55%, 94.01%, and 95.87% for single-element, 2×1, and 4×1 MPA arrays, respectively. The improvements are due to the effect of the metamaterial on both the radiator and ground plane of the MPAs. The proposed metamaterial-inspired antenna arrays solve the limitations of conventional MPAs by improving bandwidth, VSWR, and return losses. The improvements are consistent with the stringent requirements of 5G communication systems[25].

This literature describes the design of four 178 × 178 mm^2 wideband, high-gain, and highly efficient metamaterial-based 4T4R MIMO antennas with highly isolated ports. The proposed antennas will operate over the middle and part of the upper sub-6 GHz 5G frequency spectrum. As such, these antennas will be highly effective in 5G-enabled technologies such as Internet of Things (IoT) technologies, vehicular networks (such as rooftop antennas installed on vehicles like automobiles and trains), and smart environments in industries like agriculture and manufacturing. The radiators use an aperture-coupled technique with dumbbell-shaped slots and a truncated square patch with U-slots and metamaterial. The proposed MIMO antennas comprise four identical

radiators arranged in a 2 × 2 array configuration with successive 90° rotations to generate orthogonal electromagnetic fields. The antennas have a 6 mm element spacing. The decoupling technique comprises two vertical and two horizontal slots cut in the ground plane. The simulation results show that Ant_1, Ant_2, and Ant_3 have gain ranges of 6.2-9.4 dBi, 8.2-11.6 dBi, and 6.2-9.5 dBi, and isolation levels below -35 dB, -25 dB, and -33 dB. The antennas have diversity gain levels of approximately 10 dB over 2.8-4.7 GHz (5G), 2.8-4.5 GHz (5G), and 2.7-4.9 GHz (5G) frequency ranges. As part of the design, Ant_4 was fabricated and tested. The results obtained indicate that the antenna has gain levels ranging from 6.28-10.45 dBi, isolation levels below -23 dB, and an ECC of 0.001 over the 2.7-4.3 GHz 5G band. The results obtained validate that the proposed antennas meet the fundamental requirements[26].

To enhance performance in fifth-generation communication systems, the current study presents the suggested design of a low-profile multiple-input, multiple-output antenna based on metamaterials. In order to reduce unwanted radiation patterns and increase efficiency, a metamaterial is used in this study to eliminate higher-order modes. Furthermore, without sacrificing performance in terms of bandwidth, gain, and isolation all crucial for fifth-generation communication systems the suggested antenna is made to be small. According to simulation, it is found that the proposed antenna is effective in the required frequency bands, thus improving isolation between ports while minimizing coupling between ports. In addition, the proposed antenna is low-profile, thus addressing space issues, which is a problem in modern communication systems. In order to sum up this study is important for the creation of small effective antennas for fifth generation communication systems where size and performance are crucial [27].

This literature offers a metamaterial-based multiple input multiple output (MIMO) antenna for fifth-generation (5G) communication systems, specifically targeting mm Wave frequency ranges. The proposed antenna uses a 4-element MIMO array, with each element being a 1x2 array with a corporate feed network. The metamaterial layer, comprising a total of 9x6 trapezoidal split-ring resonators, is integrated on top of the MIMO array, which improves its performance by increasing isolation between the array elements and overall gain of the proposed antenna. The simulation results show that the proposed antenna operates well within the 24.55-26.5 GHz range, which is the frequency range for 5G communication, with a maximum measured gain of 10.27 dBi. In addition, a 5 dB improvement is also seen with the integration of a metamaterial layer over

conventional antennas. The proposed antenna's performance, specifically for a MIMO system, is also discussed by analyzing Envelope Correlation Coefficient, Diversity Gain, Channel Capacity Loss, and Mean Effective Gain, which show promising results for a 5G system. The proposed antenna's compact size and improved performance make it a suitable candidate for future 5G mm Wave communication systems [28].

2.3. Literature Summary

Table 1 Literature Summary

Ref	Techniques	Research Gap	Year	Simulation Results
[4]	1×2 MIMO antenna with 9×6 SRR Meta material on Rogers 5880	Need for higher gain and coupling reduction in Ka-band 5G	2023	Gain enhanced with Metamaterial, improved isolation for mm Wave 5G
[5]	Leaky wave MIMO with proximity coupling, H-slot, coffee bean Meta material	Limited Trapezoidal polarization and OSB in UAV Communications	2023	Gain: 13.8dBi, AR < 2.9, DG > 9.98 dB, ECC < 0.003
[6]	Slot antenna + 3×3 patch Metamaterial with slits/stubs	Beam squint, cross-polarization, and size limitations in Metamaterial Antennas	2022	BW: 25.14% (23.3–30 5G), Gain: 8.1 dB, Isolation high in 2×2 MIMO
[7]	Meta material-inspired antenna	Improve radiation and suppress surface waves in mmWave	2022	Improved VSWR, gain, return loss, and efficiency at 38 5G
[8]	IRS/ITS-aided MIMO with RF-limited active antennas	Power inefficiency a	2023	Enhanced performance via optimized pre coding and positioning
[9]	32-element m MIMO with ENG	Gain and isolation in dense		S11 < −10 dB, Isolation

	+ SRR MTM for sub-6 5G	base stations	2023	> 35 dB, ECC < 0.0001,
[10]	Meta material MIMO antennas with compact design	Miniaturization and diversity enhancement for 5G	2021	Strong ECC and diversity gain with compact antenna Geometry
[11]	Scalar impedance holographic Metamaterial	Phase crossover limitations in traditional HAIS	2022	Effective beam forming with custom polarization at TM mode
[12]	Dual-layer Metamaterial with aperture feeding and GA optimization	Limited bandwidth in high-gain antennas	2021	BW: 44% (S11), Gain BW: 45%, Peak Gain: 11.6dBi
[13]	Broadband mushroom antenna using composite MTM	High profile and narrowband in Metamaterial antennas	2022	BW: 25%, Gain: 9.9 dBi, Efficiency > 76%, X-pol
[14]	Metamaterial lens with 8×8 dual-polarized array	Bulky 3D lenses for	2023	Gain: 12.4 dBi, Beam scanning ±25°, Gain variation 3.3 dB

2.4. Gap Summary

The literature review indicates that there are significant gaps in the research in terms of the development of Meta material-based and Meta material-based MIMO antennas for 5G and beyond. One of the common problems that researchers have tried to solve in the development of MIMO antennas is how to increase the antenna's gain and isolation, especially in Ka band and compact mm Wave MIMO antennas [1], [6], [15]. In addition, researchers have tried to solve problems related to mutual coupling in compact MIMO antennas using different techniques such as parasitic elements, defected ground structures, and compact meta material structures [13], [14]. Trapezoidal polarization stability problems, OSB effects, beam forming problems like beam squint and cross-polarization effects are critical problems in UAV antennas and planar antennas [2], [3]. In addition, researchers have tried to solve problems related to surface waves in millimeter-wave antennas by using metamaterial structures [4], [9], [10]. In addition, researchers have tried to solve problems related to antenna miniaturization for mobile phones that support both 5G and millimeter-wave frequencies [7], [12]. In addition, researchers have tried to solve problems related to 3D lens beam forming systems that are bulky and complex in nature by using meta material structures for beam forming [11]. In addition, researchers have tried to solve problems related to scalability and power inefficiency in massive MIMO antennas by using intelligent IRS/ITS [5]. In addition, researchers have tried to solve problems related to phase crossover problems in Meta material antennas by using Material **[8].**

CHAPTER THREE

THEORETICAL BACKGROUND AND METHOD OF ANALYSIS

3.1 Introduction to chapter three

The theoretical foundation of antenna design will be described in this chapter through various design concepts. The discussion will cover met materials through their electromagnetic material properties and their material and methodology. The discussion will cover multiple-input multiple-output technology through its ability to enhance data transmission capacity. The discussion will explore different antenna concepts through their various antenna properties. The chapter will end with a description of all the analytical and numerical methods that engineers use to assess antenna design.

3.2. Methodology and Materials

3.2.1. Methodology

The first step of the methodology involves creating and assessing a Meta material-enhanced Massive MIMO antenna design that functions at optimal levels for 5G wireless communication networks. The first step to comprehend recent advancements in Meta material antennas requires executing a comprehensive literature review which explores common design techniques and all relevant frequency bands and the common issues of mutual coupling and bandwidth limitations. The key design parameters which include operating frequency and antenna type and number of antenna elements and Metamaterial configuration and substrate selection and desired performance metrics which include gain and isolation and correlation coefficients will be determined through those insights. Through sophisticated simulation tools which include all metamaterial components the design team creates the antenna structure during core design phase to achieve maximum radiation and reduced interference and increased gain.

3.2.2. Flow Chart

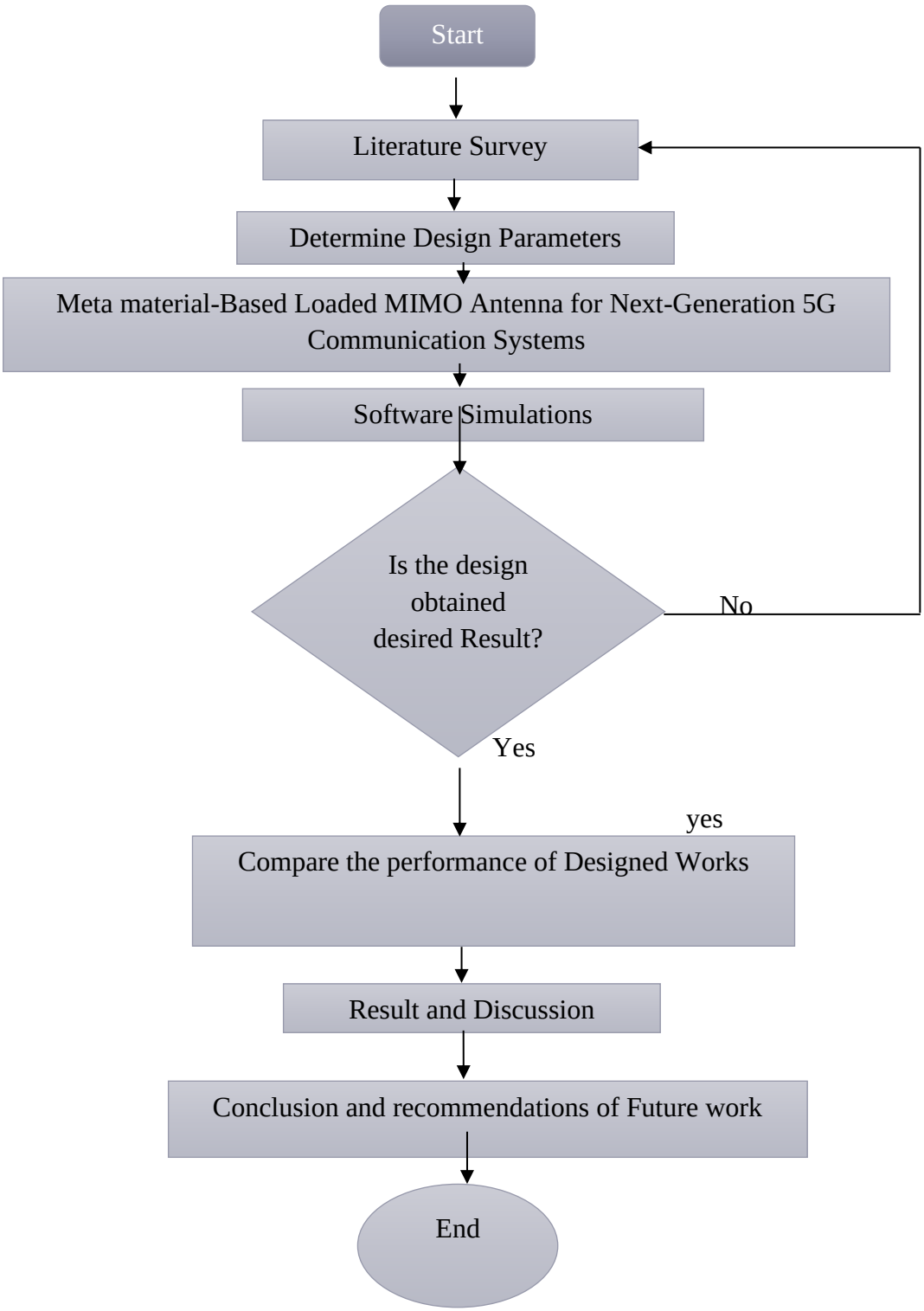


Figure 1. Flow chart of Thesis

3.2.3 Material

List of materials and tools commonly used for the simulation of a Meta material-based loaded MIMO antenna for next-generation 5G communication systems, along with specifications [31]:

1. Simulation Software

- ❖ Tool: CST Microwave Studio (or Ansys HFSS, FEKO, or COMSOL Multiphysics)
- ❖ Purpose: 3D electromagnetic simulation for antenna design and performance evaluation.
- ➢ Key Features:
  - ✓ Full-wave electromagnetic solver
  - ✓ S-parameters, far-field, and near-field analysis
  - ✓ Time-domain and frequency-domain solvers
  - ✓ Compatibility with Meta material modeling and parametric sweeps

2. Substrate Material

- ❖ Material: Rogers RT/Duroid 5880 (or FR4 for low-cost prototyping)
- ❖ Dielectric Constant (εr): 2.2 ± 0.02 (for RT/Duroid)
- ❖ Loss Tangent: 0.0009 @ 10 5G
- ❖ Thickness: 0.79 mm or 1.575 mm (standard options)
- ❖ Purpose: Acts as the base layer for the antenna and Meta material elements, chosen for its low loss at high frequencies.

3. Meta material Unit Cell

- ➢ Structure Types: Split-ring resonators (SRRs), Complementary SRRs (CSRRs), or Artificial Magnetic Conductors (AMCs)
- ➢ Material Composition:
  - ✓ Conductor: Copper (thickness ~35 μm, conductivity = 5.8×10^7 S/m)
  - ✓ Dielectric: Same as substrate or air gap based
  - ✓ Unit Cell Dimensions: Typically, in sub-wavelength scale (λ/10 or smaller)

4. Antenna Elements

- Type: Micro strip patch, monopole, or printed dipole arrays
- Material: Copper cladding for radiation patches
- Design Frequency Bands:
    - ✓ Sub-6 5G: 3.3–4.2 5G (n77/n78 bands)
    - ✓ Mm Wave: 26–28 5G or 38 5G bands

5. Boundary Conditions and Ports (in Simulation)

- Boundary: Open (add space) or Perfectly Matched Layer (PML)
- Excitation: Wave ports or lumped ports for multi-port MIMO excitation
- Meshing: Adaptive meshing with minimum cell size ~λ/30

6. Output Parameters Analyzed

- ❖ S-parameters (S11, S21, etc.)
- ❖ Radiation pattern (2D & 3D)
- ❖ Gain and directivity
- ❖ Envelope Correlation Coefficient (ECC)
- ❖ Diversity Gain (DG)
- ❖ Mutual coupling
- ❖ Total coupling

3.3. Trapezoidal micro strip patch antenna

Since they can be easily designed and manufactured, micro strip transmission lines along with flat, compact, and mechanically feasible radiating antennas have become the preferred method of coupling electromagnetic energy into the human body. When the micro strip antenna is intended to penetrate human tissues as efficiently as possible, it becomes physically larger in size and is likely to suffer from radiation leakage in a narrow bandwidth. The major difference in designing micro strip antennas for medical and non-medical applications is that they need to operate in a lossy medium, while non-medical micro strip antennas usually radiate in free space. To increase the bandwidth of micro strip antennas, various approaches can be employed: increase in substrate height, impedance matching, reduction in permittivity of the substrate material, and the use of multiple resonances.

3.4. Mata Material

Meta materials are artificially created three-dimensional structures composed of dielectric materials of specific sizes arranged in periodic patterns of metals of sub-wavelength sizes. Due to the specific permeability and permittivity of these materials, designers can easily control the behavior of electromagnetic waves by employing resonant effects of these materials[29]. Meta materials are used in antenna systems, sensors, and MRI systems for increasing antenna gain and beam steering. However, bulk meta materials have demerits like large size, low efficiency, and difficulty in fabrication. In order to overcome all these problems associated with Meta materials, two-dimensional Meta materials known as meta surfaces have been introduced. They provide advantages like compactness, broad bandwidth, high efficiency, ease in fabrication and low losses. They control the amplitude, phase and polarization of electromagnetic waves. This way, they overcome all the problems associated with conventional polarization control methods like large size and narrow bandwidth. Meta surfaces provide solutions that are highly integrable and cost-effective for applications like polarization conversion, bending light, absorbers, invisibility cloaks, and perfect lenses. In this chapter, different types of metamaterial designs for increasing antenna gain and bandwidth, reducing antenna size, and decreasing Specific Absorption Rate (SAR) are discussed. In addition, meta surfaces with different geometries for electromagnetic absorption, radar cross-section reduction, and polarization control are discussed in detail[30].

3.4.1. Application of metamaterial

Meta materials possess unique physical properties not normally found in natural materials but possess great potential in various applications, including negative refraction lenses, compact antennas, and cloaking devices. Antenna design is one of the most important areas where metamaterials have a major impact. The unique properties of meta materials make it possible to create antennas that are otherwise impossible to create with conventional materials [31]. Meta materials can boost the performance of the antenna by acting either as a substrate or as a part of the antenna structure. In this regard, the performance characteristics of the antenna system can all be enhanced. According to empirical studies, the use of Meta materials in the design of the antenna system can lead to a reduction in the size of the antenna, an increase in the power radiated by the antenna, and a consequent improvement in the gain and directivity of the antenna. The use of Meta

materials can also help in the reduction of unwanted side and back lobes of the antenna. Furthermore, the use of the material can lead to a reduction in the SAR of the antenna, which can be advantageous in the design of wearable antennas. Meta materials were designed for the purpose of enhancing the performance of the antenna. The material can function either singly or in a multiplicity of layers. The configuration of the material in the antenna system depends on the design approach adopted for the antenna[32].

3.4.2. Meta material Unit Cell

Antennas that use meta materials consist of either one-unit cell or may use multiple unit cells in an array structure, which means that there are many characteristics that may affect the design of the unit cell as it is developed before moving on to arrays of unit cells. It is important to optimize unit cell designs in order to achieve a specific level of performance from them at specific frequencies after evaluating important characteristics such as permittivity (ε), permeability (μ) and resonance frequency of the unit cell. By using these characteristics as a reference point each unit cell can then have attributes such as a physical size, shape and composition determined to ensure that the unit cell performs in accordance with a desired level of resonant behavior. The dimensions of the unit cell are typically less than 1/10th of the wavelength of the operating frequency[33]

3.4.3. Corporation Metamaterial into antenna design

There are various advantages of using antennas with Metamaterial structures, such as the possibility of reducing the size of the antennas without compromising the performance, as the Metamaterial structure can manipulate the electromagnetic waves in different ways compared to normal materials. By using metamaterials, antennas will also have a higher gain and directivity which means that transmitting, receiving antennas will transmit and receive signals much more efficiently while directing those signals to specific points. Therefore, using metamaterial antennas will also result in an increase in signal strength and the quality of the communication link. Last but not least, by utilizing meta-materials, antennas can accommodate a much wider frequency range, which allows antennas to successfully operate in multiple frequency bands which are a requirement for mobile communications in today's world. In addition, integrating metamaterials into an antenna design can effectively reduce unwanted side and back radiation, reduce interference, and improve overall performance of the system. By carefully designing the Metamaterial elements in the antenna, engineers also have the opportunity to develop an antenna which

will function over multiple frequency bands; thus, creating a versatile solution and eliminating the need to have multiple antennas.

By adding metamaterials to antenna designs, engineers now have a range of alternatives for building smaller, more efficient, and more versatile antennas, with potential uses in advanced wireless applications**.[34]**.

3.4.4. Advantage of Metamaterials for Antenna Design

The main advantage that Metamaterials have to offer is in relation to reducing the overall size of the antenna. In other words, Meta materials have been found to be effective in creating a compact form of the antenna by controlling electromagnetic waves. In addition to that, Metamaterials have also been found to be effective in improving the gain and directivity of the antenna. In other words, it is possible to improve the strength of the signal by employing metamaterials. Another advantage is in relation to reducing unwanted radiation, such as side lobes and back lobes. In other words, it is possible to reduce interference by employing Metamaterials. In addition to that, metamaterials have also been found to be effective in improving functionality[35]. Because of these characteristics, metamaterials are an effective tool for creating next generation antennas that are more compact, versatile and perform better.

3.5. MIMO Antenna

The MIMO antenna system uses multiple antennas for both transmission and reception to improve the performance of wireless communication systems. The MIMO system achieves higher data rates and better system reliability through spatial diversity and multiplexing which operates without requiring additional bandwidth and power consumption that traditional single-antenna systems need. The MIMO system transmits multiple data streams by using multiple antennas at both the transmitter and receiver points of the communication system[36].

The MIMO system uses multiple antennas for both transmission and reception to enable the simultaneous transmission of multiple data streams, which enhances the overall communication capacity. MIMO technology operates by utilizing multipath propagation, which allows signals from the transmitter to reach the receiver via various paths that result from reflection and diffraction and scattering. MIMO technology uses multipath

propagation to its fullest potential because it enhances the signal quality that transmission systems send through the communication channels.

The MIMO antenna requires multiple elements for proper evaluation. The MIMO antenna requires a specific spatial distance between its elements to achieve optimal performance because closer element positioning leads to increased coupling effects. The MIMO antenna design needs to achieve maximum diversity gain because it directly affects signal quality in communication systems.

The MIMO antenna design needs to establish maximum element isolation between its antenna components for effective signal transmission because material coupling leads to signal loss. The MIMO antenna design needs to establish maximum element isolation between its antenna components for effective signal transmission because material coupling leads to signal loss.

The modern wireless communication standards which currently use MIMO antenna technology include LTE, Wi-Fi, IEEE 802.11n, IEEE 802.11ac, IEEE 802.11ax, and 5G and others. The MIMO technology has become essential for modern wireless communication standards because it enables channel capacity expansion which leads to reduced fading effects that improve communication signals. The MIMO antenna system uses multiple antennas to achieve higher data rates and better reliability which enables more efficient communication, thus meeting the requirements of modern wireless communication standards.

3.5.1. Advantage of MIMO Antenna for 5G WCS

Multiple input and multiple output systems achieve better signal performance through spatial diversity, which helps reduce fading and interference problems that occur in challenging urban environments. MIMO technology enables beam forming systems to enhance coverage while reducing interference from other system devices through targeted signal transmission to specific users[37].

Earlier data transmission rates and increased wireless communication system reliability are two key benefits that MIMO antenna systems provide for fifth generation wireless communication systems. MIMO technology enables systems to transmit multiple data streams simultaneously through a specific frequency spectrum. The 5th generation wireless communication systems need reliable high-speed connections to support both high-definition video streaming and IoT networks[38].

MIMO antenna systems provide essential support for 5G network performance needs because they enable higher capacity and faster speeds and more reliable connectivity compared to traditional antenna systems.

3.5.2. Requirements of MIMO Antenna for 5G WCS

The MIMO antennas for 5G wireless communication systems must fulfill several crucial parameters in order to satisfy the high performance expectations of the future networks. First and foremost, the MIMO antennas have to perform well in the high-frequency bands used in 5G technologies, such as the sub-6 GHz and millimeter wave bands, and thus the design of the MIMO antennas has to ensure the required bandwidth and gain. In addition, the MIMO antennas have to be compact and closely spaced in order to be used in small devices, but at the same time, they have to have high isolation and low mutual coupling between the elements.

Furthermore, in order to increase the data rates and spectral efficiency by using spatial multiplexing in 5G technology, the MIMO antennas have to be able to accommodate a number of antenna elements, i.e., Massive MIMO. In addition, the MIMO antennas have to be able to operate in different frequency bands to accommodate the various bands used in 5G technology. The ability to perform beam forming with the MIMO antennas is also very important, as it will be used to direct the signals to the targeted users[39].

In order to ensure minimal correlation between the signals received by the elements, the antenna system should also ensure low envelope correlation coefficient (ECC). Other key factors to be considered are the compliance with regulatory requirements, such as the Specific Absorption Rate (SAR), environmental robustness, and the ease of integrating the antenna with other components in the system[40].

In order to meet the stringent requirements of new wireless links, 5G MIMO antennas have to ensure high gain, wide bandwidths, minimum interference levels, multiple band support, and beam steering capabilities while keeping their sizes small and meeting device requirements.

3.6. Analyzing Method

3.6.1 Meta material Unit Cell Analyzing Methods

The meta material unit cell is often approximated by a parallel or series LC circuit depending on the design, but commonly a series LC resonator is used[41]:

- Inductor (L): due to the loop of conductive material.
- Capacitor (C): due to the split gap or gap between elements.

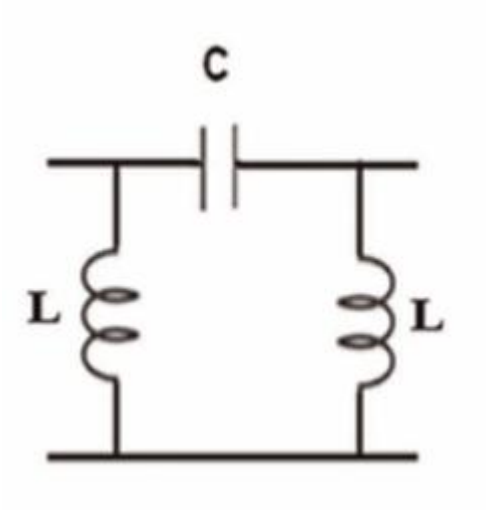


Figure 2. The LC resonant circuit of the unit cell

The cell of a sub wavelength resonant structure (Meta material) is usually referred to as a cell (meta-atom), which relates the corresponding electromagnetic response at certain frequencies. Such a model lends explanation for the resonance by which the structure is able to interact with electromagnetic waves, giving rise to e.g., negative permittivity or permeability or both (negative index of refraction).

3.6.2 Physical Interpretation

- **(Inductance):** Need to provide the magnetic response of the Metamaterial. The inductance is provided by the structure's conductive loops, or rings (e.g., SRRs). The circulation of the current induced by an alternating magnetic field in such loops is like that in an inductor storing a magnetic energy.[42].
- **C (Capacitance):** It denotes the electric reaction/electric energy storage capacity of the structure. Capacitance is primarily from the spaces between conductive parts which behave like capacitors storing electric charge.

These altogether constitute an LC circuit having a resonant frequency at which the unit cell exhibits strong electromagnetic wave interaction.

Those structures serve as an LC parallel resonating circuit. The in-phase bandwidth and resonance frequency are thus determined by a capacitance C and inductance L dependent on the geometry and dimension of the unit cell. The capacitance is due to the It can be calculated as:

$$c = \frac{w\varepsilon_{0(1+\varepsilon_r)}}{\pi} coh - 1\left(\frac{w+g}{g}\right) \qquad (3.1)$$

Here, w is the physical width of a unit cell in the Meta Material or antenna structure, and g is the gap between two neighboring unit cells. Those dimensions are essential to characterize the electromagnetic cell interaction that determines the total resonant frequency and the impedance responses. The symbol ε_0 refers to the permittivity of free space (also called the dielectric constant of vacuum), a fundamental physical constant with a value of approximately 8.854×10^{-12}F/m8.854.

The inductance L can be calculated from the geometric and material parameters. This inductance is heavily dependent on the thickness of the substrate between conductive layers or by how long a metallic via (a vertical connection between layers) may be. Thicker substrate or longer via in general lead to a higher inductive value, and the resonant behavior of the Meta material unit cell changes respective.

ly.$L = u_0 u_r t$ (3.2)

The optimized unit cell dimensions are specifically tailored to operate at the target frequency of 5G. In this model, the parameters are expressed as fractions of the free-space wavelength λ of 5G corresponding to that frequency is given by;

$$\lambda = \frac{c}{f} \qquad (3.3)$$

The width of the metallic strip (w) is given by;

$$W = 0.323\lambda \text{ of } 5G \qquad (3.4)$$

The gap between adjacent unit cells (g) is given by

$$g = 0.018\lambda \text{ of } 5G \quad (3.5)$$

and the radius of the via hole is

$$r = 0.004\lambda \text{ of } 5G \quad (3.6)$$

These dimensions are chosen to achieve two main electromagnetic functions:

1. Surface wave suppression; minimizing unwanted surface currents that can lead to radiation pattern distortion or mutual coupling in antenna arrays.
2. In-phase reflection behavior; Ensuring that reflected waves from the structure maintain their phase alignment, improving antenna efficiency and bandwidth.

Once the geometric parameters are set, the resonance frequency of the unit cell can be determined using its equivalent circuit model (typically involving inductance from the visa and capacitance from the gaps). This resonance frequency governs how the unit cell interacts with incident electromagnetic waves, allowing it to produce the desired performance at 5G.

$$f_r = \frac{1}{2\pi\sqrt{LC}} \quad (3.7)$$

Free-space wavelength at in 5G

Use the exact relation

$$\lambda_{5G} = \frac{c}{f} \quad (3.8)$$

With $c = 229792458 m/s$ and frequency in 5G.

Step-by-step arithmetic:

- $c = 229792458 m/s$
- λ of 5G

Convert the given normalized dimensions to physical units

Given (normalized to λ of 5G

$$w = 0.323\lambda \text{ of } 5G \quad (3.5)$$

$$g = 0.018\lambda \text{ of } 5G \quad (3.6)$$

$$r_{via} = 0.004\lambda \text{ of } 5G \quad (3.7)$$

Equivalent-circuit resonance (general expression)

Model the unit cell as an LC resonator. The resonance frequency is

$$f_0 = \frac{1}{2\pi\sqrt{L_{eq}C_{eq}}} \quad (3.8)$$

Where $L_{eq}\ and\ C_{eq}$ are the effective inductance and capacitance seen by the resonating mode?

How to get $L_{eq}\ and\ C_{eq}$ from geometry (step-by-step)

Step A identify missing geometry/material parameters

To compute L and C you will also need:

- conductor thickness t (e.g. copper thickness, typical 35 μm),

3.6.3. Conductor Thickness

This is usually fixed by copper cladding:

$$t_{cond} = 17\mu m\ (½\ oz),\ 35\mu m\ (1oz),\ 70\mu m\ (2oz), \quad (3.9)$$

- substrate thickness h,

$$h = \frac{C_0}{20f_0\sqrt{\varepsilon_r - 1}} \quad (3.10)$$

Used in capacitance and inductance calculations.

- substrate relative permittivity ε_r

$$\varepsilon_r = \frac{Permitivity\ of\ Substrate}{\varepsilon_r} \quad (3.11)$$

- The ring/loop effective length (mean perimeter) ℓ or ring radius R (depends on the unit-cell shape),

  For a square ring of outer side, a and strip width w:

$$l = 4(a - w) \tag{3.12}$$

For a Trapezoidal ring of mean radius R (between outer and inner radius):

$$l = 2\pi R \tag{3.13}$$

Were

$$R = \frac{R_{outer} - R_{inner}}{2} \tag{3.14}$$

- The overlap/face length at the gap ℓgap (the length of facing conductor edges across the gap).

This determines the capacitive gap loading:

$$l_{gap} = \text{length of conductor edges facing each other across the gap} \tag{3.15}$$

- If gap width g, strip width w:

$$Square\ Ring = l_{gap} \tag{3.16}$$

$$Circular\ Ring = arc\ length\ facing\ across\ the\ gap \approx w \tag{3.17}$$

Effective capacitance of the gap (useful for resonance design) is given by;

$$C \approx \varepsilon_r \varepsilon_0 \frac{L_{gap} t}{g} \tag{3.18}$$

Effective inductance of the loop is given by;

$$L = u_0 u_r \frac{l}{w + t} \tag{3.19}$$

Step B – inductance (approximate)

Total inductance is typically given by;

$$L_{eq} \approx L_{loop} + L_{via} \quad (3.20)$$

Use these practical approximations:

- Loop (trace) inductance; for a thin conductor of mean length ℓ\ell, width w and thickness t (approximate form):

$$L_{loop} = \frac{u_0 l}{2\pi}\left[\ln\left(\frac{2l}{w+t}\right) + \alpha\right] \quad (3.21)$$

Where u_0=4π×10^{-7} H/m and α is an order-one constant (typical values α≈0.5 this is an engineering approximation).

If the loop is Trapezoidal, the classic Trapezoidal-loop formula

$$L \approx u_0 R ln\left[\left(\frac{8R}{a}\right) - 2\right] \quad (3.22)$$

Can be used with a the effective conductor radius.

- Via inductance; for a via (cylindrical conductor) of length h (the substrate thickness) and radius r_{via}:

$$L_{via} = \frac{u_0 h}{2\pi}\left[ln\left(\frac{2h}{r_{via}}\right) + C_1\right] \quad (3.23)$$

With C1 ≈ 0.5 (empirical). This formula gives the order of magnitude contribution from the feed/via.

Step C; capacitance (approximate)
Total capacitance is usually dominated by the gap capacitance across the split plus fringe and substrate contributions:

$$C_{eq} = C_{gap} + C_{fringe} + C_{substrate} \quad (3.24)$$

A simple engineering approximation for the gap (parallel-plate style) is:

$$C_{gap} = \varepsilon_0 \varepsilon_r \frac{A_{gap}}{g} \quad (3.25)$$

Were

- ε_0=8.854187817×10^{-12} F/m\varepsilon_0=8.854187817× 10^{12},
- ε_{eff} is an effective permittivity (for microstrip-like structures a common approximation is $\varepsilon_{eff} = \frac{\varepsilon_r - 1}{2}$
- A gap is the facing area (w×ℓgap w and
- g is the gap width.

Fringing and substrate: fields fringe outside the plate area include an empirical fringe capacitance (often 20–100% of C gap depending on geometry). For microstrip edges practitioners often add a correction factor or estimate C fringe from closed-form formulas (depends on w/h and εr.

3.7. Trapezoidal Patch Analyzing Methods

3.7.1. Transmission Line Modeling

Transmission line model represents Trapezoidal patch antenna as the two parallel plate transmission line connecting to radiating slot each of height and width. When the feed line supply X band RF signals to the patch, the charge distributed to patch and ground plane. After a few instants of time, attractive force between patch and ground plane carry large amount of charge. As well as repulsive force, repulse the charge at the edge of patch and creating large density of charge at the end of patch. These are may cause for fringing fields. Radiations of electromagnetic energies from micro strip antenna induces fringing fields in between patch and ground plane.

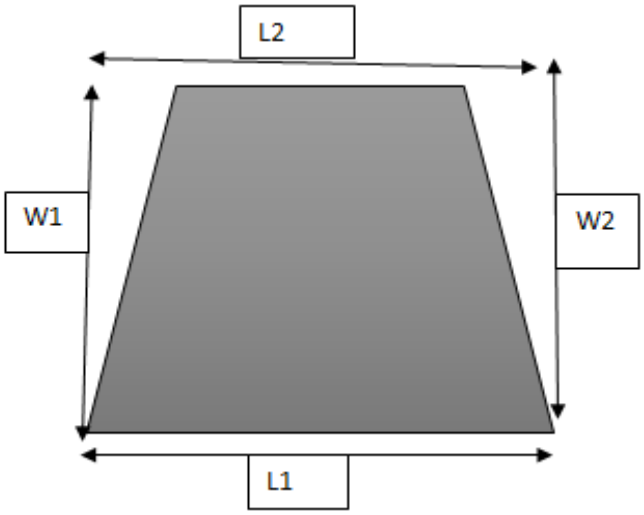


Figure 3. Trapezoidal Patch Antenna

Trapezoidal micro strip patch antenna has length, width, and height. To get TM_{10} mode. The length of Trapezoidal patch antenna must be less than $\lambda/2$. The wave length of Trapezoidal patch antenna is depend on the operating frequency and given by;

$$\lambda = \frac{c}{f} \qquad (3.26)$$

Where λ wavelength of Trapezoidal micro strip antenna, c is speed of light, which is 3×10^8 m/s, f is operating frequency. The length of antenna calculated by;

$$L = \frac{\lambda_{eff}}{2} \qquad (3.27)$$

Where L is length of Trapezoidal patch antenna λ_{eff} is effective wavelength. When the patch appears open circuit, the voltage is maximum at the edge and minimum at the middle. The field does not vary at the edge. Since the fields are in contra-phase at edges, it causes the normal components of the field to cancel each other in the broadside direction. However, the tangential components are in phase and cause radiation normal to the patch surface. The slots of the patch give very high impedance terminations at the end of the transmission line, thus the structure expected to highly resonant which is dependent on the length of the patch. Due to fringing fields, resonant length of patch is greater than physical length of patch. Effective length of antenna given by;

$$L_{eff} = \frac{C}{2f_0\sqrt{\epsilon_{eff}}} \qquad (3.28)$$

Where L_{eff} is effective length of antenna, and ΔL is given by;

$$\Delta L = 0.412h\frac{(\varepsilon_{eff} + 0.3)(\frac{w}{h} + 0.264)}{(\varepsilon_{eff} - 0.258)(\frac{w}{h} + 0.8)} \qquad (3.29)$$

Where $\varepsilon_{eff,}$effective dielectric constant, h is height, w is width. The length of patch is not responsible for radiation, the antenna radiating through the width of patch and given by;

$$W = \frac{C}{2f_0\sqrt{\frac{\varepsilon r + 1}{2}}} \qquad (3.30)$$

Where W is width of patch, c is speed of light, εr relative permittivity, f_0 operating frequency. Effective dielectric constants are lower than relative permittivity due to

fringing fields. In order to obtain large bandwidth, in both input and radiation side transition from feed line to antenna and antenna to free space respectively, the transmission line employ perfect impedance matching. Dielectric constant of substrate is greater than effective dielectric constant. The ratio of width of antenna to height of dielectric substrate is the very important point to determine the total impedance of antenna. The Effective dielectric constant and impedance of transmission line calculated in to two ways, the first one is when the ratio of width and height of substrate is greater than or equals to 1. Effective dielectric constant calculated as;

$$\epsilon_{eff} = \frac{\varepsilon r + 1}{2} + \frac{\varepsilon r - 1}{2}[1 + \frac{12w}{h}]^{-1/2} \ For \frac{w}{h} \geq 1 \qquad (3.31)$$

Where ϵ_{eff} is effective dielectric constant,εr, relative permittivity, and h, is height of dielectric substrate, w is width of patch. Due to this, the Impedance of Transmission lines given by;

$$Z_0 = \frac{120\pi/\sqrt{\epsilon_{eff}}}{\frac{w}{h} + 1.393 + 0.667\ln(\frac{w}{h} + 1.444)} \ for \frac{w}{h} \geq 1 \qquad (3.32)$$

The second one is when the ratio of width to height of patch is less than or equals to one; Effective dielectric constant calculated as;

$$\epsilon_{eff} = \frac{\varepsilon r+1}{2} + \frac{\varepsilon r-1}{2}[1 + \frac{12w}{h}]^{-1/2} + 1/25(1 - w/h) \ For \frac{w}{h} \leq 1$$

(3.33)

For this effective dielectric constants, the impedance of transmission line calculated by;

$$Z_0 = \frac{60}{\sqrt{\epsilon_{eff}}}\ln\left[\frac{8h}{w} + 0.25\frac{w}{h}\right], for \ w/h \leq 1$$

(3.34)

Resonant frequency of antenna is a function of length and given by;

$$f_{r(010)} = \frac{1}{2L\sqrt{\varepsilon r \mu_0 \varepsilon_0}} = \frac{C_0}{2L\sqrt{\varepsilon r}} \qquad (3.35)$$

Where$f_{r(010)}$resonant frequency at 010 modes is, εr is relative permittivity, μ_0 is permeability at free space, $\varepsilon_0$and is permittivity at free space. The actual length of Trapezoidal patch antenna determined by;

$$L = L_{eff} - 2\Delta L \quad (3.36)$$

Where L is actual length of antenna, L_{eff} is effective length of antenna, ΔL is length extension due to fringing fields. The transmission line model even though is applicable to infinite ground planes only but for practical considerations, a finite ground plane is used. However, size of ground plane should be greater than the patch dimensions by approximately six times the substrate thickness all around the periphery so that results are similar to the one using infinite ground plane. The length of ground plane determined by;

$$L_g = 6H + L \quad (3.37)$$

Where L_g is length of ground planes, H is height of dielectric substrate, L is actual length of patches.

$$W_g = 6H + W \quad (3.38)$$

Where W_g is width of ground planes, H is height of dielectric constants, W is width of Trapezoidal patch antenna.

3.7.2. Cavity Modeling

Cavity modeling takes into account trapezoidal patch antennas because the region between trapezoidal patch antennas and ground planes is cavity and surrounded by an electric and magnetic field ceiling.

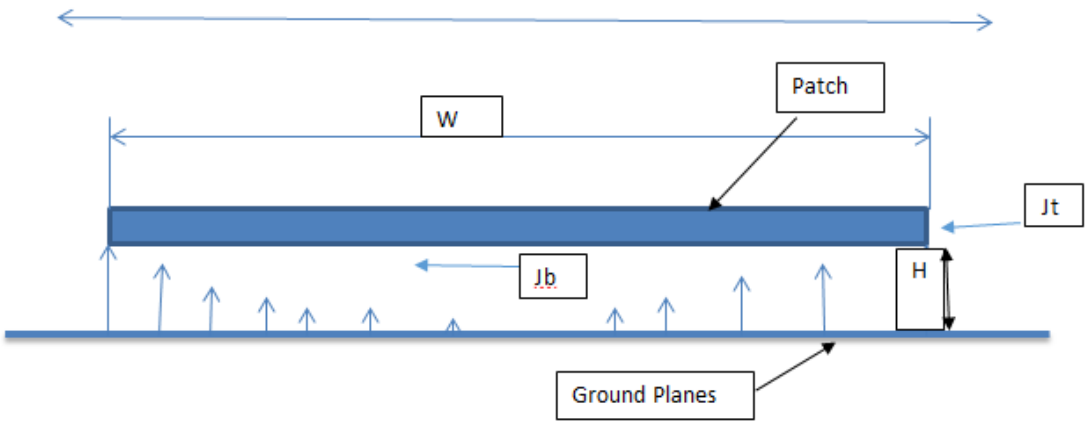


Figure 4. Electric Field Distributions

When the Trapezoidal antenna is connected to a microwave source, the charge distribution will be established on the upper and the lower planes of antenna. The charge distribution is controlled by two mechanisms; attractive and repulsive. The attractive force is between the opposite charges on the patch and on the ground plane, it creates a current density inside the dielectric at the bottom of the patch Jb. The repulsive force is between the like charges tends to push the charges from the bottom of the patch around the edge of the patch to the top of the patch, this will create the current density Jt. Because the current flow around the edge reduces as the ratio of height to width falls, it is possible to ignore it in the case of micro strip antennas W>>h where the attractive mechanism predominates and at charges concentration will within the dielectric under the patch. This would enable the four side walls to be modeled as ideal magnetic conducting surfaces that, in theory, would not interfere with the distribution of the magnetic field and, consequently, the electric field beneath the patch. Due to this accurate representation of the cavity model, we may treat the side walls as ideal magnetic conducting walls (A. F. Alsager, 2011.). Inside the cavity, there are three field components.

$$\nabla \mathrm{X} \nabla \mathrm{X} \overline{\mathrm{E}} - K^2 \overline{\mathrm{E}} = -j\omega\mu_0 \bar{J} \tag{3.39}$$

$$\nabla^2 \mathrm{X} \overline{\mathrm{E}_z} - K^2 \overline{\mathrm{E}}_z = j\omega\mu_0 \hat{Z}.\bar{J} \tag{3.40}$$

Where $K^2 = \omega^2\mu_0\varepsilon_0\varepsilon_r$

$\bar{J}$ = Electric current density fed by the feed line to the patch

$\hat{Z}$ = Is the unit vector normal to the plane of the patch?

The top and bottom conductors calculated by;

$$\hat{n}X\bar{E} = 0 \tag{3.41}$$

And the magnetic walls

$$\hat{n}X\bar{H} = 0 \tag{3.42}$$

CHAPTER FOUR

DESIGN MASSIVE MIMO ANTENNA WITH METASURFACE FOR 5G WCS

4.1. Design Considerations

- The operating frequency is f = 3.5 GHz (sub-6 GHz 5G)
- Large MIMO aperture: 4x4 planar array with 16 elements
- A trapezoidal micro strip patch, a single-layer, planar patch on a dielectric, serves as the radiating element.
- Example of substrate: thickness h = 1.6 mm (Rogers), $\varepsilon_r = 2.2$.
- Target element spacing: $d \approx 0.5\ \lambda_0$ (to keep compact and prevent grating lobes).
- The function of the Meta surface includes bandwidth/gain enhancement, engineered reflection phase for mutual-coupling cancellation, and surface-wave suppression.
- Performance objectives (post-tuning): radiation efficiency > 70%, ECC < 0.05, nearest-neighbor S21 ≤ −20 dB, and S11 < −10 dB.

4.2. Design Trapezoidal Patch Antenna

A trapezoidal patch is a quadrilateral whose top and bottom edges have different widths. It behaves like a rectangular patch with varying local width, so resonance primarily depends on the patch length (L) in the direction of radiating aperture and an effective (average) width $W_{ave} = (W_1 + W_2)/2$ We design the patch so the dominant mode (usually TM_{10} -like in the larger dimension) resonates at f_0. Fringing at the edges is handled with effective-dimension corrections as in cavity models[43].

Key design idea: first compute a starting length (L) from standard cavity/half-wavelength formula using an effective permittivity; choose trapezoid widths to control input impedance, bandwidth and pattern shape; then tune with full-wave EM solver.

4.2.1 Design Procedures

Step 1: Determine Free-space wavelength and wavenumber:

Step: 1.1. Determine Free-space wavelength

$$\lambda_0 = \frac{c}{f_0}$$

$$\lambda_0 = \frac{3 \times 10^8 m/s}{3.5 \times 10^9}$$

$$\lambda_0 = 0.0857142857 \text{ m} = 85.714 \text{ mm}.$$

Step 1.2. Determine Free-space wavenumber:

$$K_0 = \frac{2\pi}{\lambda_0}$$

$$K_0 = \frac{6.283185307}{0.0857142857}$$

$$K_0 = 73.303$$

Step 2: Choose an Initial Average Width Guess

Pick a practical average width W_{ave} as a starting point. We choose:

$$W_{ave} = 30mm$$

Step 3: Effective Permittivity

Use the standard approximate formula for a micro strip line (iterative but adequate initially):

$$\epsilon_{eff} = \frac{\varepsilon r+1}{2} + \frac{\varepsilon r-1}{2}[1 + \frac{12h}{w}]^{-1/2}$$

$$\epsilon_{eff} = \frac{2.2+1}{2} + \frac{2.2-1}{2}[1 + \frac{12\times 2.73\text{mm}}{23.71\text{mm}}]^{-1/2}$$

$$\epsilon_{eff} = 1.6 + 0.6 \times 0.7809$$

$$\epsilon_{eff} \approx 1.6 + 0.4686$$

$$\epsilon_{eff} = 2.0686$$

So, start with $\epsilon_{eff} = 2.0686$

Where ϵ_{eff} is effective dielectric constant, εr is relative permittivity, W is width of patches, H is height of dielectric substrate.

Step 4: Determine Patch length

For a rectangular-like patch the resonant length for the fundamental mode is:

$$L = \frac{\lambda_0}{2\sqrt{\varepsilon_{eff}}}$$

$$L = \frac{85.714\ mm}{2\sqrt{2.0686}}$$

$$L = \frac{85.714}{2.876}$$

$$L \approx 29.81\ mm$$

Initial value: $L \approx 29.81\ mm$

Step 5: Choose Trapezoid Widths

Choose top and bottom widths such that the mean equals $W_{ave} = 30mm$.

- Top width $W_1 = 22mm$
- Bottom width $W_2 = 38mm$
- Check average: $\frac{W_1+W_2}{2} = \frac{22mm+38mm}{2} = 30mm$

These asymmetrical widths produce a trapezoidal shape that can broaden impedance bandwidth and tune input resistance.

Step 6: Initial Feed (inset) Location Calculation

For a patch fed by inset micro strip, the input resistance varies approximately as $R_{in}(x) = R_{edge}cos^2\left(\frac{\pi x}{L}\right)$. where (x) is inset depth from the radiating edge toward center and R_{edge} is the resistance at the edge (typical order of few hundreds ohms use solver later). Choose $R_{edge} = 300\Omega$ as an initial estimate.

Solve for (x) to obtain$R_{in} = 50\Omega$:

$$cos^2\left(\frac{\pi x}{L}\right) = \frac{50\Omega}{R_{edge}}$$

$$\frac{50\Omega}{300} = \frac{1}{6} = 0.1667.$$

Then:

$$cos\left(\frac{\pi x}{L}\right) = \sqrt{0.1667} = 0.40825$$

$$\left(\frac{\pi x}{L}\right) = \arccos(0.40825) \approx 1.1503\, rad.$$

$$x = \frac{\boldsymbol{\pi}}{L} \times 1.1503 = \frac{\boldsymbol{29.81}}{\boldsymbol{\pi}} \times 1.1503 = 9.488 \times 1.1503 \approx 10.92\, mm$$

Initial inset depth: x=10.92 mm from the radiating edge toward center (tune with EM simulation).

4.3. Design Trapezoidal Array Layout for Massive MIMO

4.3.1. Design Procedures

Step 1: Determine Element spacing

Choose center-to-center spacing:

$$d = 0.5\lambda_0$$

$$d = 0.5 \times 85.714\, mm$$

$$d = 42.857\, mm.$$

Step 2: Determine Array Size

For 8×8 (N=8 in each dimension) the center-to-center span across one side equals:

$$((N-1)d = 7d):$$

$$7 \times 42.857 \approx 300\, mm.$$

Include element widths and margins; final panel will be slightly larger.

4.4. Design Meta surface

4.4.1 Design Procedures

Step 1: Meta surface placement options

Super strata: Meta surface sheet above array at a controlled height (h_ms).

Inter-element tile: Meta surface tiles between elements flush with patch plane or slightly above. Choose placement during param sweep superstrate is common for gain/beam enhancement; inter-element tiles are often best for coupling suppression.

Step 2: Design Meta surface Unit-Cell

Design targets for unit cell:

- Period $p \leq \frac{\lambda_0}{6}$ to remain sub-wavelength. Choose:

$$p = \frac{\lambda_0}{10}$$

$$p = 85.714/10$$

$$p \approx 8.571\, mm.$$

Model the unit cell as an equivalent LC resonator with resonance near f_0

Step 3: Pick a Starting Equivalent Capacitance

$$\mathrm{C} = 0.5\mathrm{pF}$$

$$\mathrm{C} = 0.5\mathrm{pF} = 0.5 \times 10^{-12} F$$

As a starting number (actual geometry will set C)

Step 4: Compute Required Inductance L for Resonance at 3.5 GHz

Resonance condition:

$$\omega_0 = 2\pi f_0 = 2\pi \times 3.5 \times 109$$

$$\omega_0 \approx 2.1991 \times 1010\, rad/s$$

Compute ω_0^2:

$$\omega_0^2 = (2.1991 \times 10^{10})^2 = 4.836 \times 10$$

$$\omega_0^2 == 4.836 \times 10^{20}$$

Then

$$L = \frac{1}{4.836 \times 10^{20} \times 0.5 \times 10^{-12}}$$

$$L = \frac{1}{4.836 \times 10^{20} \times 0.5 \times 10^{-12}}$$

$$L = \frac{1}{2.148 \times 10^{8}}$$

$$L = 4.136 \times 10^{9}\ H = 4.136\ nH.$$

Start values:C = 0.5p F, $= 4.136\ nH$. Map these to geometry gap capacitors (slot widths), printed stub lengths (inductive behavior), vias to ground (inductance).

Step 5: Desired Meta surface Behavior

Step 6: - Calculate Length and width of Ground plane

Length and width of ground plane greater than or equals to length and width of dielectric substrate. The length of ground plane computed from equations

- At f_0 aim for a high surface impedance (HIS) or AMC like response (reflection phase near 0°) to suppress surface waves and modify fringing reflection phase.
- Alternatively design reflection phase ∠Γ that produces destructive interference of fringing fields between neighboring patches (target fringe phase difference ~ π).

$$\mathrm{L_g} = 6\mathrm{H} + \mathrm{L}$$

$$\mathrm{L_g} = 6 \times 1.6\mathrm{mm} + 29.81\mathrm{mm}$$

$$\mathrm{L_g} = 39.41\mathrm{mm}$$

Where L_g is length of ground planes, H is Height of dielectric substrate, L is actual length of Trapezoidal patch antenna. Width of ground planes computed from equation

$$W_g = 6H + W$$

$$= 6 \times 1.6\mathrm{mm} + 30\mathrm{mm}$$

$$W_g = 39.6mm$$

Where W_g width of ground planes, H is height of dielectric substrate, W is width of rectangular patch antenna.

Step 7: Impedance of Antenna

If the impedance of Trapezoidal patch antenna doesn't perfectly matched with impedance of feed line high reflections of power occurred[44]. When the ratio of width to length of patch is greater than one we have computed from equations.

$$Zo = \frac{120\pi}{\sqrt{\epsilon_{eff}}[\frac{wo}{h}+1.393+0.667\ ln)(\frac{wo}{h}+1.4444)]}, \frac{wo}{h} > 1$$

$$= \frac{120\times3.14}{\sqrt{3.88}[\frac{9.7}{0.865}+1.393+0.667\ ln)(\frac{9.7}{0.865}+1.4444)]}, \frac{9.7}{0.865} > 1$$

$$= \frac{120\times3.14}{(1.969)[11.21+1.393+0.667\ ln)(11.21+1.4444)]}, 11.21 > 1$$

$$= \frac{376.8}{(25.1\times12.6)]}, 11.21 > 1 = \frac{376.8}{(317.1)}, 11.34 > 1$$

$$\text{Zo} = (1.188), 11.34 > 1 = 13.47 > 1$$

CHAPTER FIVE

SIMULATION RESULT, DISCUSSIONS AND ANALYSIS

5.1. Result and Discussions

This chapter presents simulation results and discussions of a single trapezoidal patch antenna with and without a metasurface, a 2x4 trapezoidal MIMO patch antenna with and without a metasurface, and a 4x4 trapezoidal MIMO patch antenna with and without a metasurface. Design a multiple-input, multiple-output smart trapezoidal patch antenna with a metasurface for 5G mobile communication systems.

5.2. Simulation Results of single Trapezoidal patch antenna

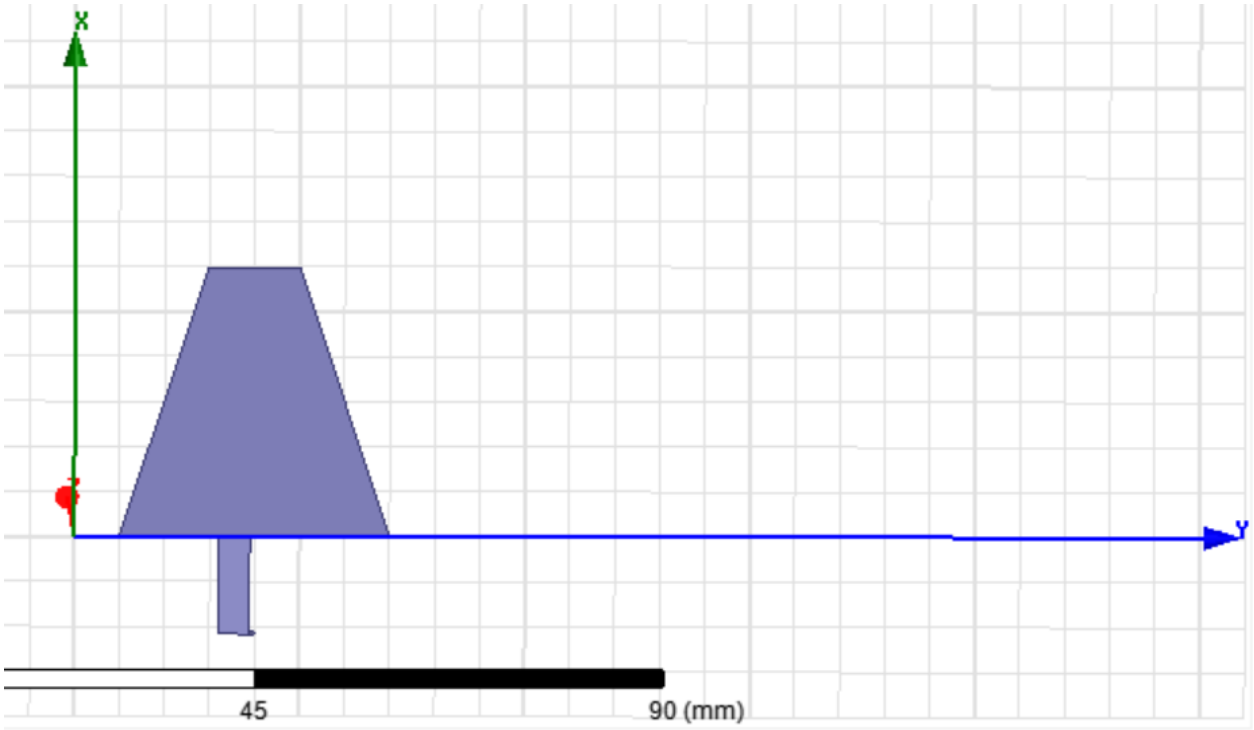


Figure 5. Single Trapezoidal patch antenna

5.2.1. Gain of single Trapezoidal patch antenna

The simulated gain performance of the single trapezoidal micro strip patch antenna operating at 3.5 GHz demonstrates a realized gain of 0.55 dB, which is characteristic of a compact, single-element radiator in the sub-6 GHz 5G band. At this frequency, antenna dimensions are often constrained to support low-profile integration in user equipment and small-cell platforms, and such miniaturization inherently limits radiation efficiency and aperture size, leading to modest gain values. The observed maximum radiation in the

230° direction indicates an asymmetric radiation pattern, which can be attributed to the trapezoidal geometry, fringing fields at the patch edges, and the influence of the feeding mechanism and ground plane truncation. From a 5G sub-6 GHz perspective, these simulation results confirm that the antenna is capable of providing stable omnidirectional-like coverage with directional preference, suitable for short-range access links and dense network deployments. Although the achieved gain is relatively low compared to antenna arrays, the results validate the antenna's role as a fundamental radiating element, which can be further optimized or integrated into multi-element configurations such as MIMO or beam forming arrays to meet the higher link budget and capacity requirements of 3.5 GHz 5G wireless communication systems.

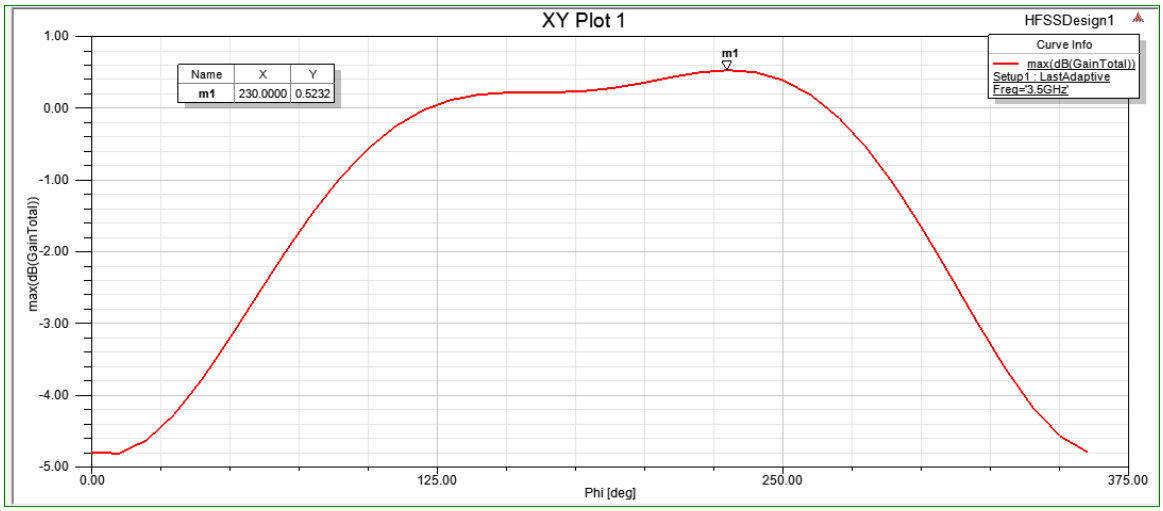


Figure 6. Total Gains of single TPA

5.2.2. Directivity of single Trapezoidal patch antenna

The micro strip patch antenna which operates at 3.5 GHz and uses a single trapezoidal design shows directivity results which measure 0.9 dB and produces a radiation pattern that matches the standard behavior of single-element antennas which operate at sub-6 GHz 5G frequencies. The directivity level shows that power distribution through space maintains its normal state instead of creating focused beams which helps 5G systems at the access layer to create wide area links that remain stable. The trapezoidal patch design together with its feeding location and edge diffraction patterns creates a radiation pattern which shows a minor directional preference and maintains complete area coverage. The simulation results show that the 5G wireless communication system antenna operating at 3.5 GHz provides effective spatial radiation control while its design requirements result in

a compact and simple structural design. The system shows reliable performance for single radiant elements because it has less directivity than multi-element and beam-steered array systems which create a reliable foundation for sub-6 GHz MIMO systems that need better directivity and spatial selectivity through array configuration and digital or analog beam forming methods.

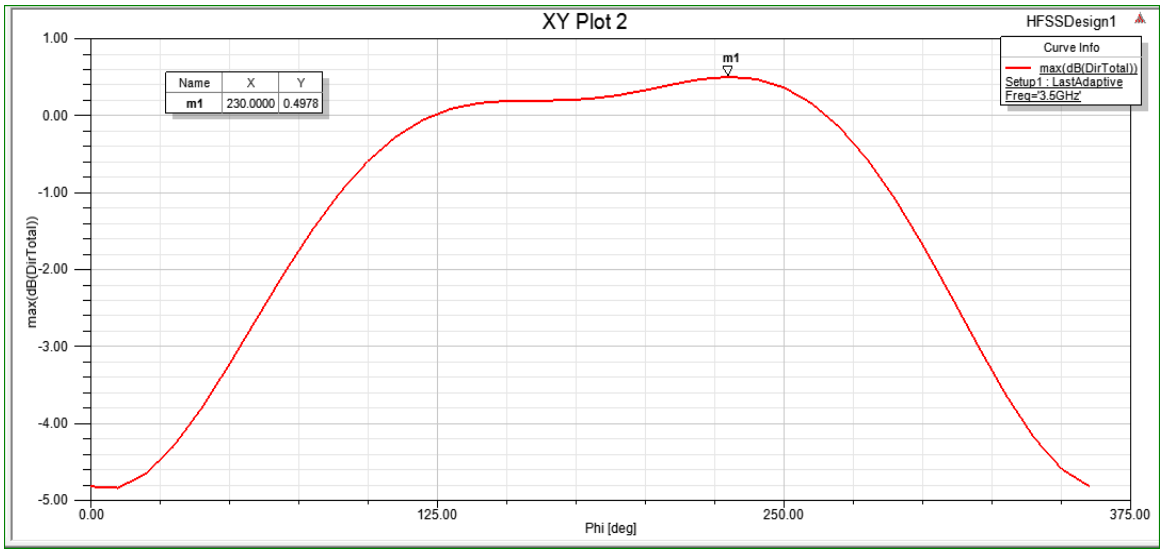


Figure 7.Total Directivity of single TPA

5.2.3. S11 of single Trapezoidal patch antenna

. The system achieves low reflection because it radiates most of the input power which allows the system to The trapezoidal micro strip patch antenna which operates at 3.5 GHz shows its minimum reflection coefficient of −21.6 dB through its simulated performance which demonstrates excellent impedance matching between the antenna and feeding network at sub-6 GHz 5G band frequencies meet essential requirements for dependable and energy-efficient 5G wireless communication systems. The operational bandwidth of the system defines its range from upper frequency limits to lower frequency limits which maintain reflection coefficient values below −10 dB for 200 MHz the bandwidth supports all main 3.5GHz 5G spectrum allocations which sub-6 GHz systems use to deliver wideband services and high data-rate transmission capabilities. The trapezoidal patch geometry enables broader impedance bandwidth through its current distribution improvements which create better resonant responses than traditional rectangular patches. The simulation outcomes prove the antenna works effectively for sub-6 GHz 5G applications because the system needs both stable matching and sufficient bandwidth to handle multi-carrier modulation schemes spectrum aggregation and different channel

conditions.

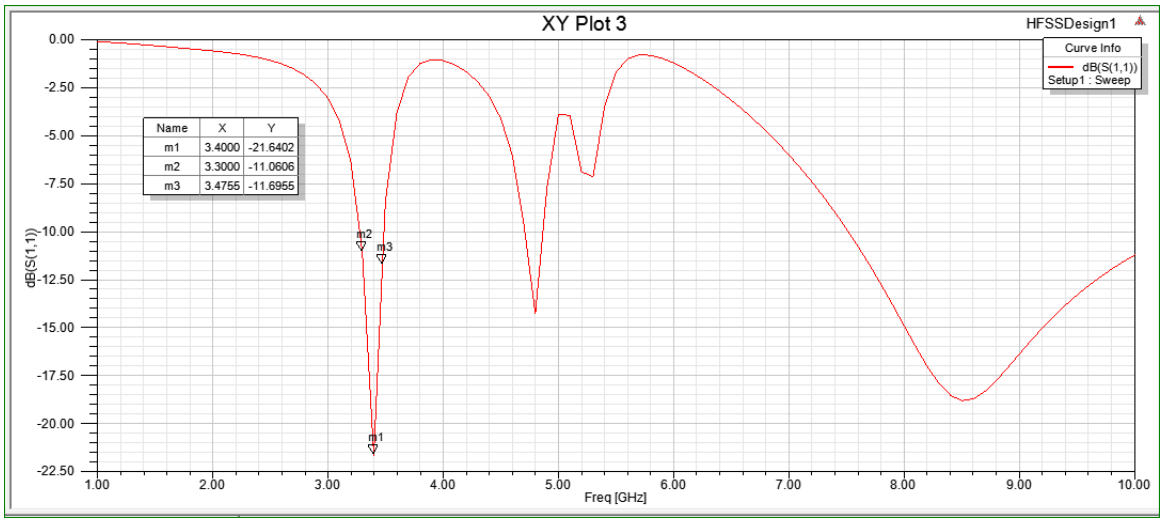


Figure 8. Reflection Coefficient of single TPA

5.2.4. Voltage Standing Wave Ratio of Single Trapezoidal Patch Antenna

The single trapezoidal micro strip patch antenna operating at 3.5 GHz achieves a VSWR measurement of 1.44 which demonstrates strong impedance matching performance at the targeted sub-6 GHz 5G frequency. The VSWR value which falls significantly below the standard acceptance limit of 3 shows that over 75% of the input power gets transmitted from the feed line to the radiating structure while only a small amount of power reflects back towards the source. The trapezoidal patch design with its particular feed system shows excellent matching performance because it keeps all input impedance values stable during resonance periods. The low VSWR which exists in 3.5GHz 5G wireless communication systems provides important benefits because it enables better efficiency in transmitters while decreasing RF front end losses and maintaining consistent radiation performance throughout the entire operational frequency range. The simulation results therefore validate the antenna's suitability for sub-6 GHz 5G applications where reliable impedance matching is essential to support wideband modulation schemes and maintain link quality while enabling efficient integration into compact user equipment and access

point platforms.

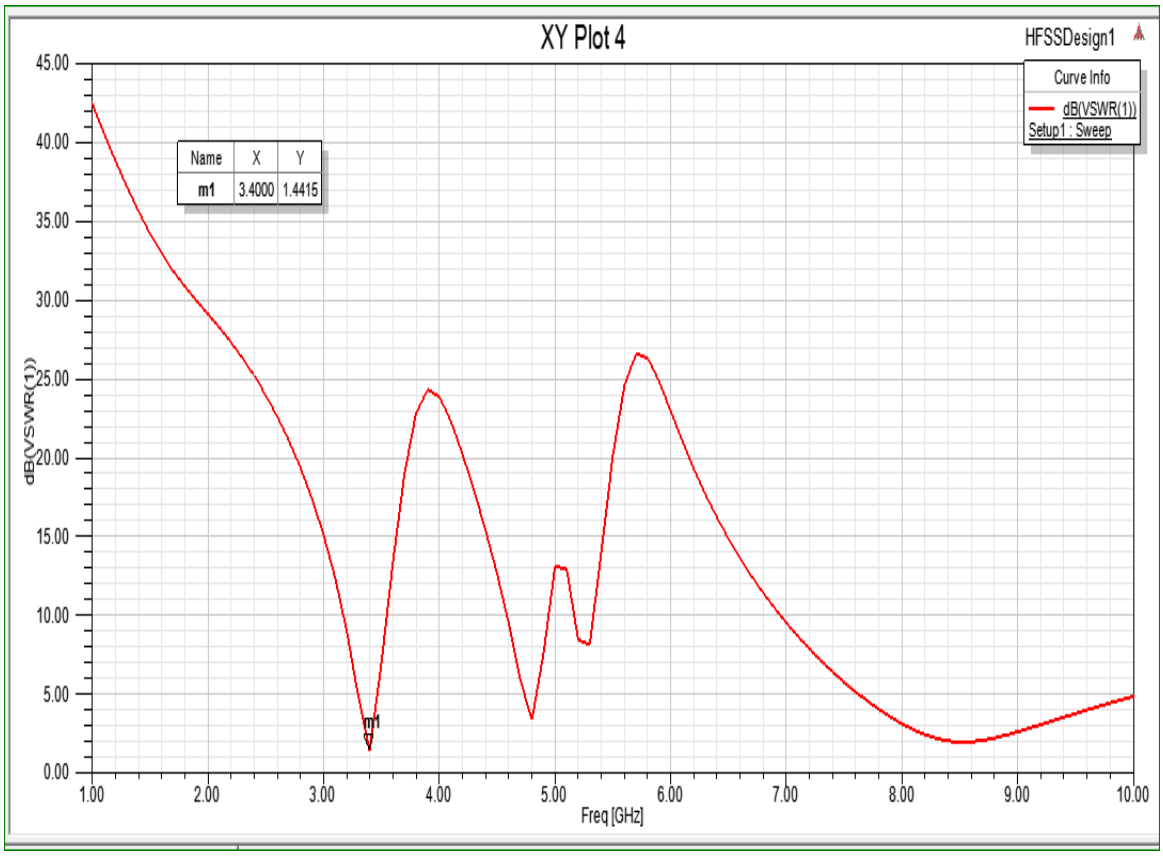


Figure 9. Reflection Coefficient of single TPA

5.2.5. Radiation Patterns of Single Trapezoidal Patch Antenna

The single trapezoidal patch antenna radiates using its polar plot pattern that exhibits a main lobe that radiates towards the broadside direction. The pattern is symmetric with the main lobe with less radiation radiating on the back and side regions that patch antennas that generate focused radiation tend to have. The antenna has maximum gain of 0 degrees with the nulls and side lobes having a directivity effect that makes the antenna ideal in targeted signal transmission and reception in 3.5 GHz resonant frequency.

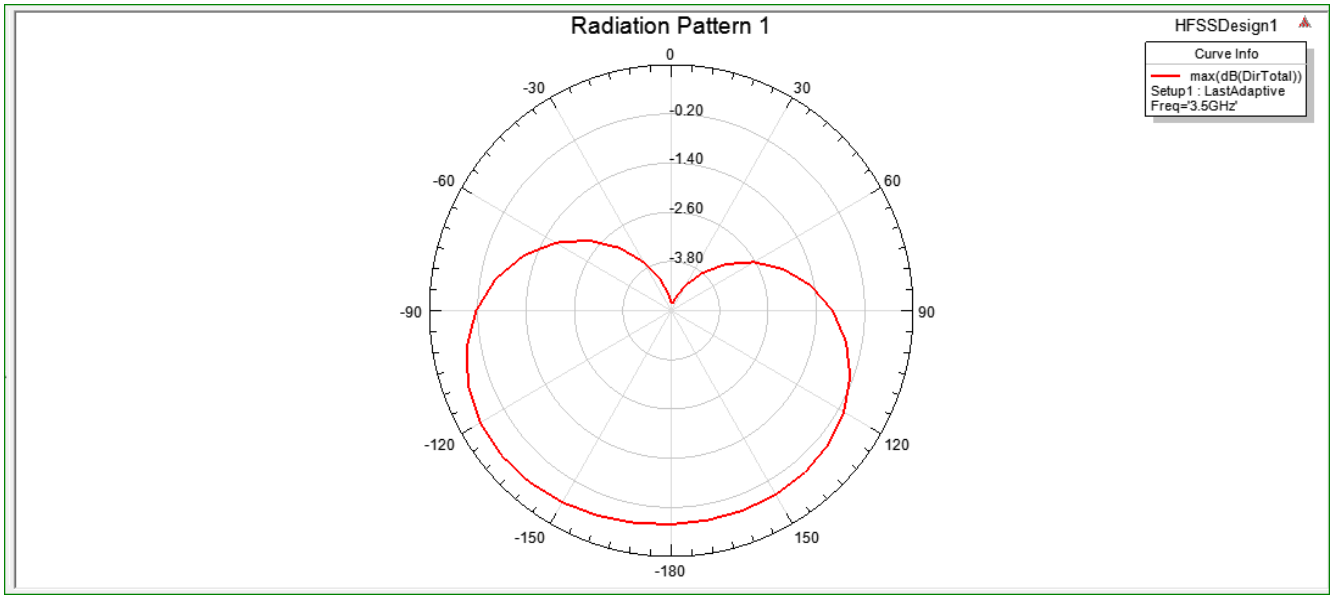


Figure 10. Radiation Patterns of Single TPA

5.2.6. 3D Polar Plot of Single Trapezoidal Patch Antenna

The 3D polar plot of the single trapezoidal patch antenna shows the directional nature of the antenna at the specified frequency as well as shows the radiation pattern in 3D. The red and orange color areas have been replaced by the green and blue color areas, which means that the main lobe containing the highest gain of an antenna is positioned in a specific direction and that the radiation is gradually weakening on sides and back. Which is advantageous to the applications that demand specific signal transmission. The symmetry of the plot and the concentration of energy in the main lobe show the effective directivity and beam forming properties of the antenna which is appropriate in those cases when the focus and the strength of the signal play a major role.

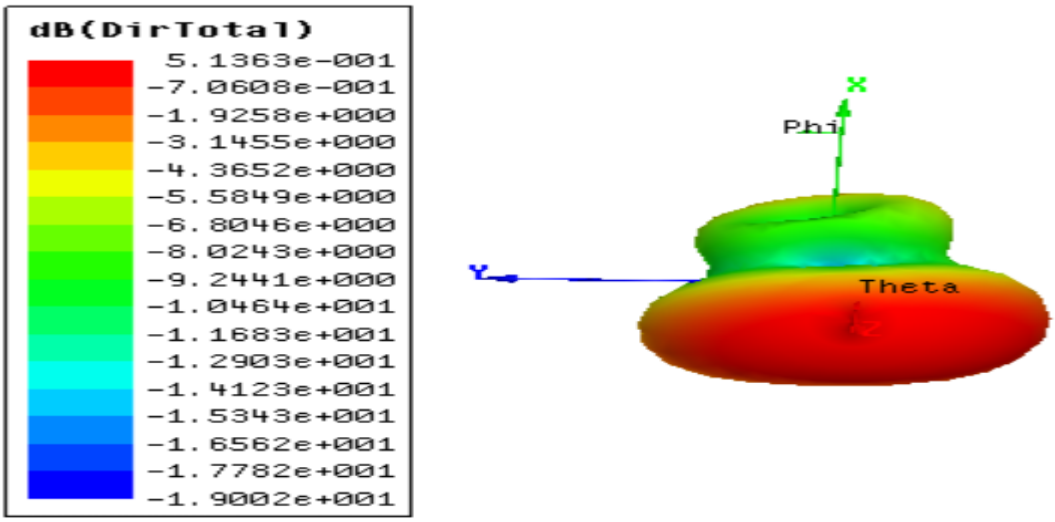


Figure 11. 3D Polar plots of Single TPA

5.3. Simulation Results of Single Trapezoidal patch antenna with Meta surface

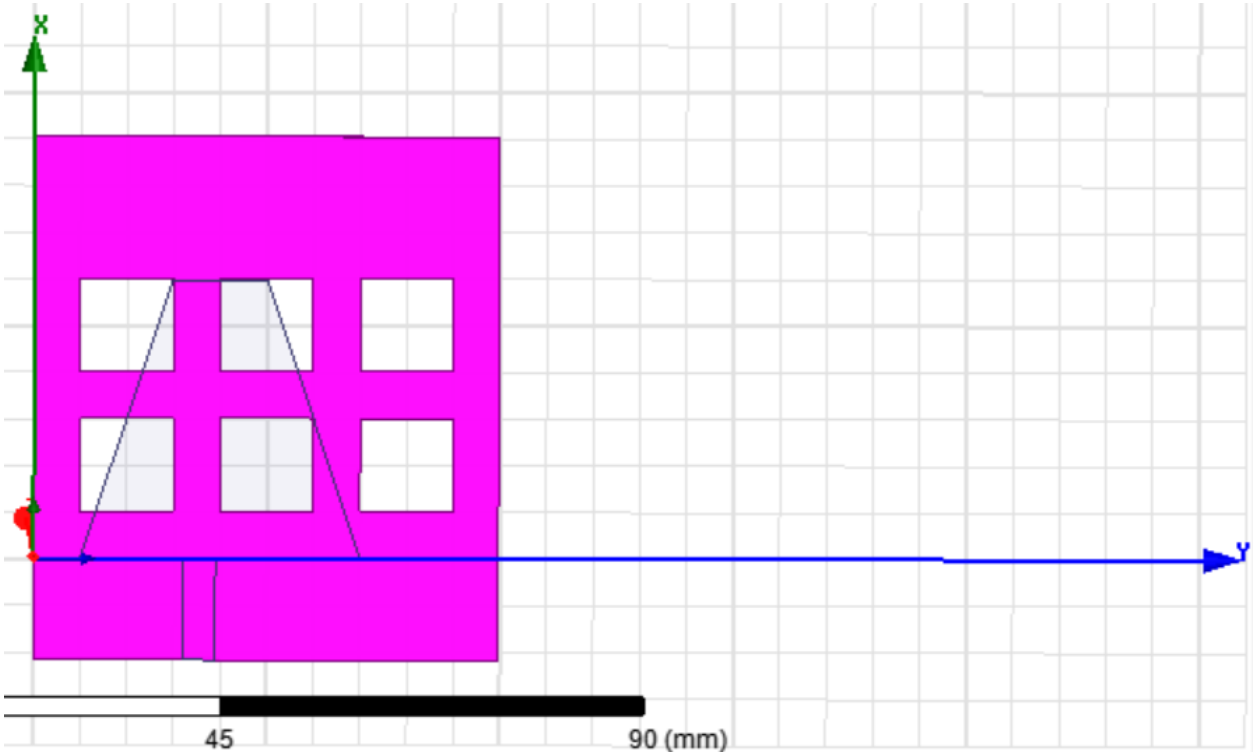


Figure 12. Single TPA with Meta surface

5.3.1. Gain of single Trapezoidal patch antenna with Met surface

The single trapezoidal micros trip patch antenna which uses a Meta surface at 3.5GHz shows a simulated radiation performance that achieves 1.6 dB of realized gain which

exceeds the Meta surface free antenna performance by approximately 1dB. The Meta surface demonstrates its capacity to change near-field patterns while reducing surface-wave energy losses which results in improved radiation efficiency and better far-field field superposition. The maximum gain reached at 230° shows that the Meta surface maintains the original radiation pattern of the trapezoidal patch while enhancing the main radiation lobe without creating unwanted changes to the radiation pattern. From a sub-6GHz 5G system perspective, the achieved gain improvement is particularly significant for compact single-element antennas, where physical size constraints typically limit aperture efficiency. At 3.5GHz, Meta surface integration provides a practical approach to performance enhancement without increasing antenna footprint, making it suitable for user equipment, small cells, and indoor access points. The simulation results therefore validate that Meta surface-assisted trapezoidal patch antennas can offer improved link margin and coverage reliability in 5G wireless communication systems, while also serving as efficient building blocks for higher-gain MIMO and beam forming architectures in dense sub-6 GHz network deployments.



Figure 13. Total Gains of single TPA with Meta surface

5.3.2. Directivity of single Trapezoidal patch antenna with Met surface

The directivity performance of the single trapezoidal micro strip patch antenna with Meta surface at 3.5GHz achieves directivity measurements of 1.55 dB which represents a directivity increase of 1dB when compared to the similar antenna design without Meta surface loading. The Meta surface enhancement demonstrates its capability to modify the electromagnetic field distribution which results in improved radiation performance in the primary direction while decreasing radiated power and surface-wave emissions. The

maximum directivity occurring at 230° confirms that the Meta surface reinforces the inherent radiation orientation of the trapezoidal patch rather than altering its principal beam direction. The 3.5 GHz frequency range would experience directivity benefits which enhance link performance through better energy distribution while maintaining antenna dimensions and operational simplicity in sub-6 GHz 5G wireless systems. Simulation results show that Meta surface implementation serves as an effective method for increasing directional performance in small antennas which makes them suitable for 5G user terminals and small-cell infrastructure. The improved directivity provides essential support for the design transition into multi-element MIMO and beam forming arrays because Meta surface-assisted elements improve coverage and capacity achievements and spectral efficiency improvements in densely populated 5G sub-6 GHz networks.

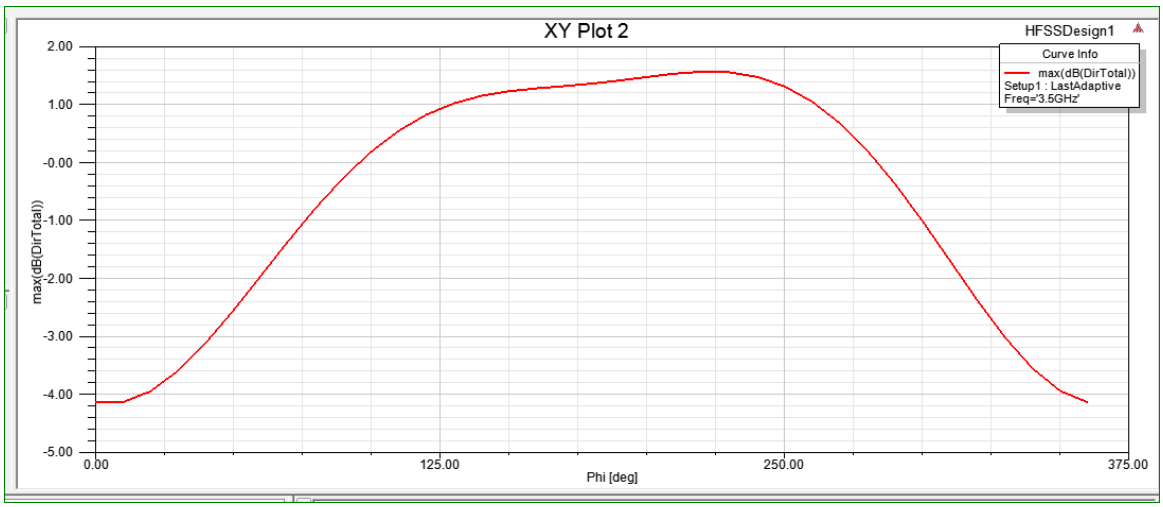


Figure 14. Total Directivity of single TPA with Met surface

5.3.3. S11 of single Trapezoidal patch antenna with Met surface

The single trapezoidal micro strip patch antenna test with integrated meta surface showed its reflection characteristics at 3.5GHz when the antenna achieved its best impedance match through its reflection coefficient of -20.2207 db. The system demonstrates high transmission efficiency for 5G wireless communication because it reflects only a small fraction of incoming power while most of the power goes into creating necessary radiation. The patch design exhibits different reflection properties when compared to standard patch designs because the Meta surface interacts with the radiating element to change its input impedance and resonance patterns. The operational bandwidth of the system extends through a frequency range which maintains reflection coefficient values

below -10 dB for a total of approximately 173.8MHz. The bandwidth provides complete coverage for the main 3.5GHz sub-6 GHz 5G spectrum bands which enables wideband signaling and carrier aggregation and high data-rate services. The simulation results reveal that meta surface integration improves system radiation performance while maintaining sufficient impedance bandwidth, which makes the antenna suitable for compact 5G terminals and access nodes. The research findings demonstrate that Meta surface-assisted trapezoidal patch antennas achieve a balance between better radiation performance and consistent wideband impedance matching for use in sub-6 GHz 5G wireless communication systems.

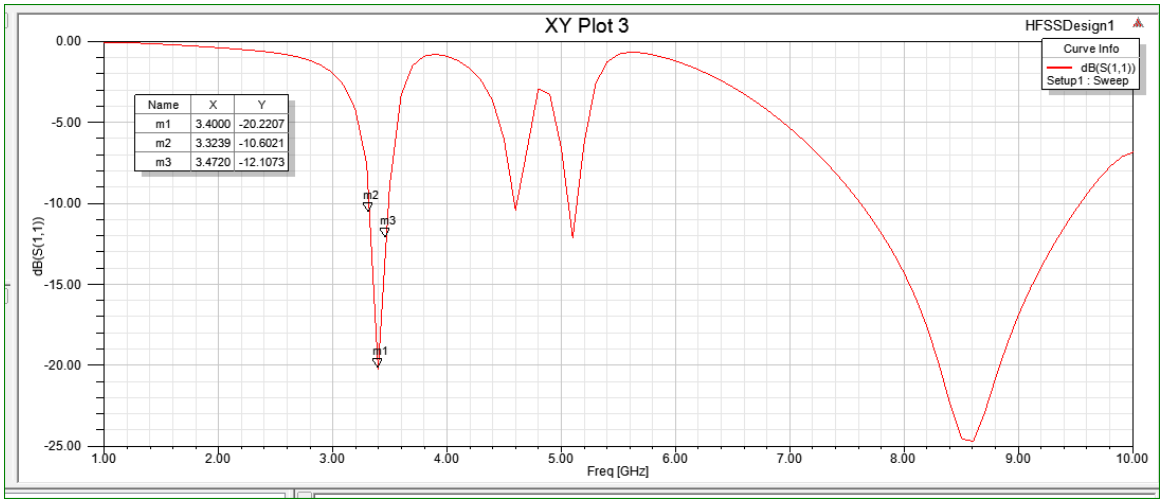


Figure 15. Reflection Coefficient of single TPA with Met surface

5.3.4. Voltage Standing Wave Ratio of Single Trapezoidal Patch Antenna with Metasurface

The trapezoidal micro strip patch antenna operating at 3.5GHz demonstrates a simulated voltage standing wave ratio (VSWR) which reaches a minimum value of 1.66. This result shows that the antenna functions well for impedance matching within the entire sub-6 GHz 5G frequency band. The VSWR reading which falls well below the standard threshold of 3 shows that over 75 percent of input power gets transmitted from the transmission line to the radiating element with only minimal reflections occurring at the feed interface. The matching level shows that the antenna design together with its feed system works perfectly for achieving resonance at 3.5GHz.

The sub-6 GHz 5G wireless communication systems require this VSWR performance to achieve power efficiency while reducing RF front-end circuit losses and preserving

consistent radiation patterns throughout the entire operating frequency range. The simulation results thus show that the antenna functions effectively at 3.5GHz 5G applications because reliable impedance matching enables stable link performance together with lower power usage and successful integration into small user equipment and compact access point systems.

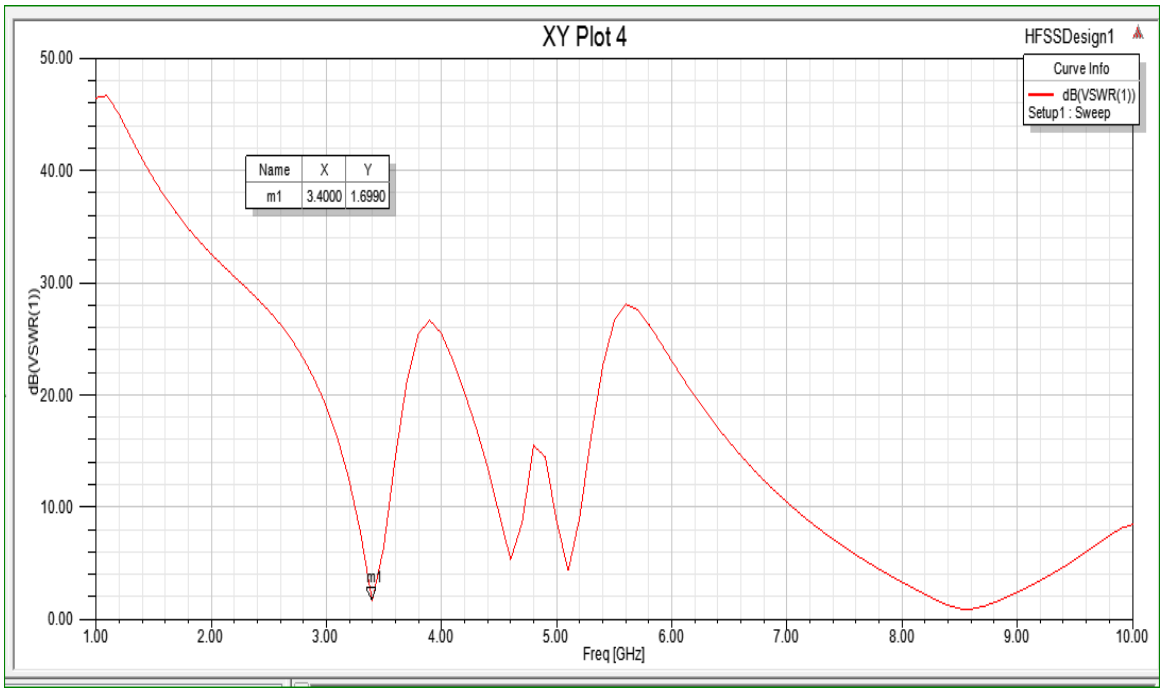


Figure 16. Reflection Coefficient of single TPA with Met surface

5.3.5. Radiation Patterns of Single Trapezoidal Patch Antenna with Met surface

The polar plot of the radiation of the single trapezoidal patch antenna with the metasurface reveals a fairly omnidirectional radiation with a minor variation in pattern, thus reflecting the increased directivity and better radiation efficiency. It is shown in the plot that the antenna emits energy at a constant rate in a broad angle, and the highest gain will be concentrated at the 0-degree direction, which implies that it covers a large area. The metasurface addition seems to affect the radiation pattern to shape and potentially enhance the gain resulting in a more controlled and directed radiation behavior at the operating band of 3.5 GHz. The given configuration is desirable when it is needed to cover a large area and has a higher performance, e.g. wireless communication systems when it is imperative to have a high level of directivity and efficiency.

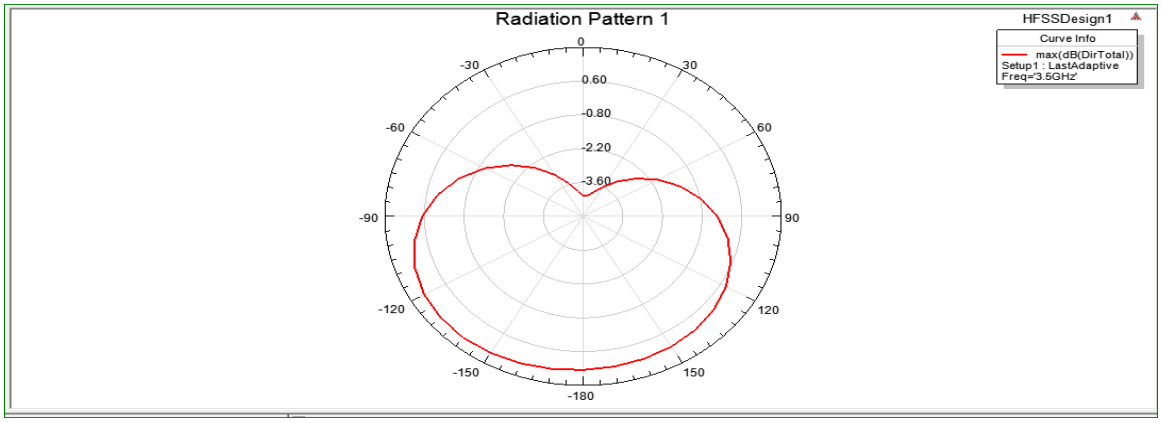


Figure 17. Radiation Patterns of Single TPA with Met surface

5.3.6. 3D Polar Plot of Single Trapezoidal Patch Antenna with Met surface

The 3D polar view of the individual trapezoidal patch antenna made of a metasurface is an indication of nearly an isotropic radiation pattern with slight directional concentration showing that the energy is distributed with a good proportion of different directions but still experiences certain degree of directionality. The intensity scale color coding shows that the highest gain is around the middle of the plot (i.e. the pattern of the radiations is quite continuous around the azimuthal plane) because the shape of the plot is smooth and rounded. The fact that the metasurface exists seems to improve the overall radiation performance through the distribution of currents on the patch resulting in more balanced and directed radiation pattern. This implies that the antenna featuring metasurface should be able to offer enhanced coverage and efficiency and, therefore, it can be used in areas where it is required that there is a large and uniform distribution of signals, like in wireless communication systems.

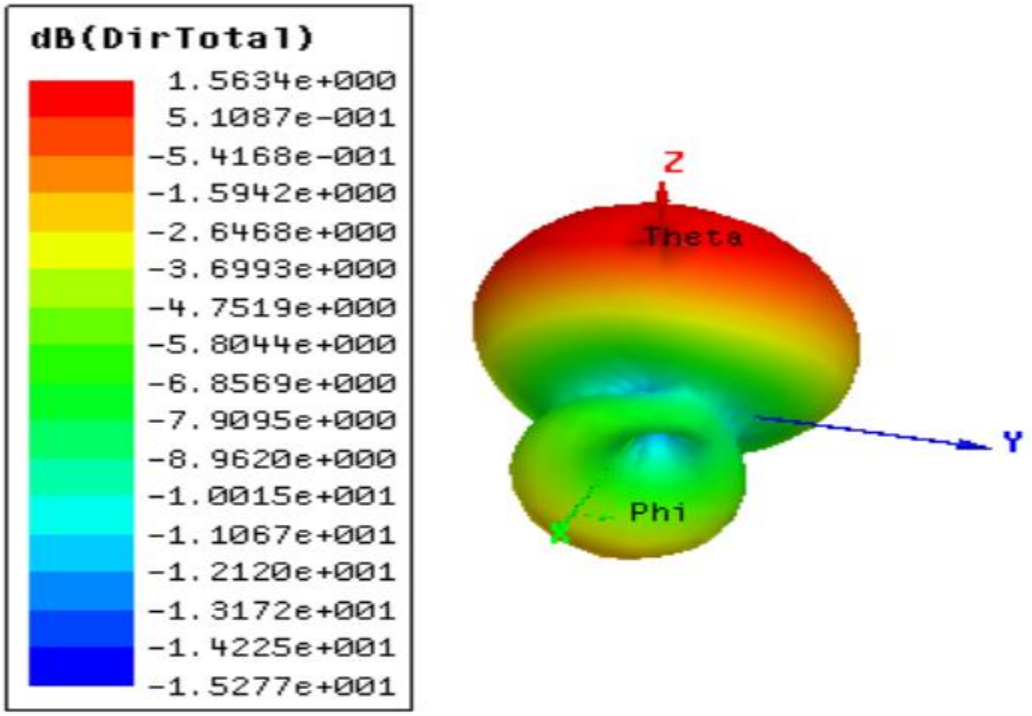


Figure 18.3D Polar plots of Single TPA with Met surface

5.4. Simulation Results of 2x4 MIMO Trapezoidal patch antenna for 5G WCS

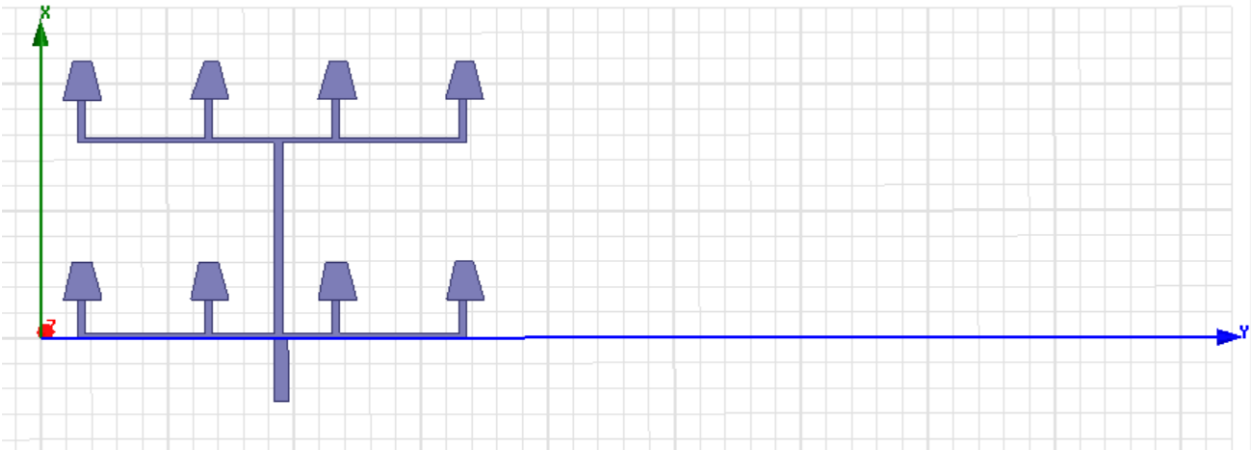


Figure 19.2x4 MIMO TPA for 5G WCS

5.4.1. Gain of 2x4 MIMO Trapezoidal patch antenna for 5G WCS

The 2×4 trapezoidal patch antenna array which operates at 3.5 GHz shows simulated radiation performance results which reach 12.7dB for its actual gain capacity with single element designs showing less than that value. The array provides approximately 11dB improvement over the single trapezoidal patch antenna without Meta surface loading and

about 10 dB enhancements relative to the Meta surface-assisted single element. The system achieves this major gain increase through the arraying process which produces enlarged effective aperture and constructive field superposition and enhanced power concentration distribution as typical benefits of multi-element antenna designs. The maximum gain observed at 280° indicates a well-defined main radiation lobe, resulting from the controlled phase and amplitude distribution across the eight radiating elements. 5G wireless communication systems which operate below 6 GHz especially those using the 3.5 GHz frequency band benefit greatly from high-gain directional radiation because it enhances network coverage and increases link margin while reducing interference in locations with many active devices. The simulation results clearly demonstrate that while single-element and meta surface-enhanced antennas are suitable for compact and low-gain applications, the 2×4 trapezoidal patch array offers a scalable and efficient solution for base stations, small cells, and advanced 5G access points, where higher gain and directional control are essential to support increased capacity, beam forming, and multi-user MIMO operation in sub-6 GHz 5G deployments.

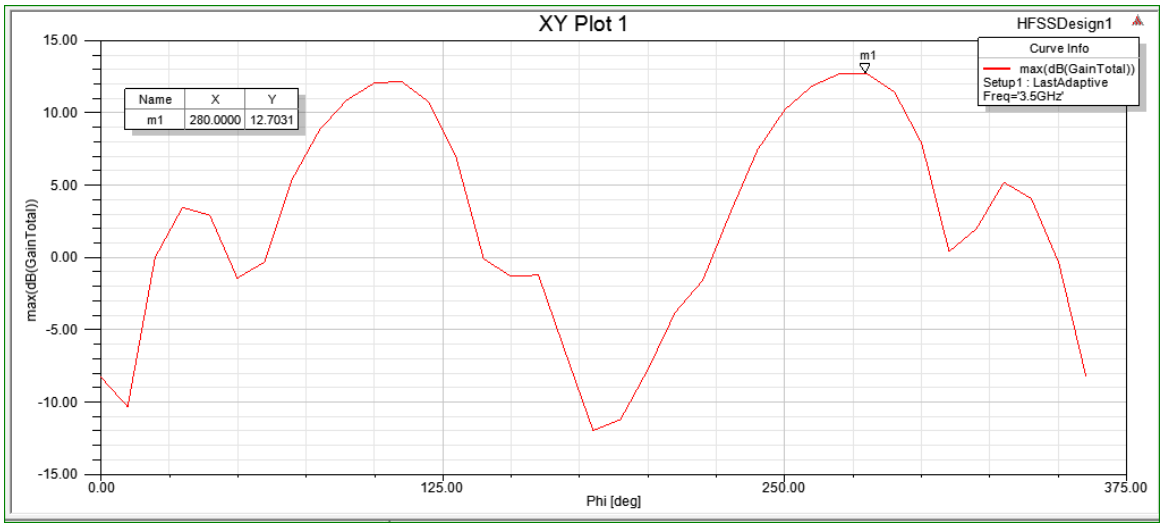


Figure 20. Total Gains of 2x4 MIMO TPA

5.4.2. Directivity of 2x4 MIMO Trapezoidal patch antenna for 5G WCS

The 2×4 trapezoidal micro strip patch antenna design shows improved directivity performance at 3.5GHz, which enables its use in 5G sub-6GHz wireless communication systems. The system achieves its maximum directivity of 12.6dB which shows an 11dB increase from the trapezoidal patch antenna without a Meta surface and a 10dB increase from the Meta surface integrated single element. The array configuration creates fields

that combine through constructive superposition, which results in narrower beam widths and better aperture efficiency at the selected frequency. The radiation pattern of the main lobe shows a 280° orientation, which enables effective beam steering while meeting the directional radiation needs of 3.5GHz 5G base-station and access-point systems. The simulation results show that the 2×4 trapezoidal array design enhances both spatial directivity and angular radiation control, which makes it suitable for high-capacity sub-6 GHz 5G wireless systems that require protection against interference.

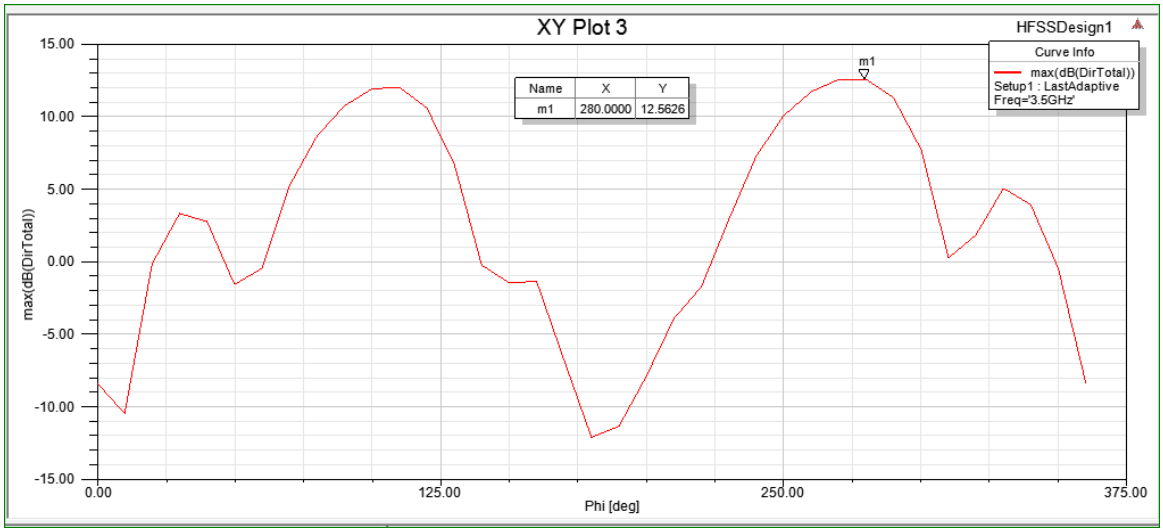


Figure 21. Total Directivity of 2x4 MIMO TPA

5.4.3. S11 of 2x4 MIMO Trapezoidal patch antenna for 5G WCS

The 2×4 trapezoidal patch antenna simulated at 3.5 GHz shows a reflection coefficient of -17.5 dB which demonstrates excellent impedance matching and minimal power loss at the operational frequency for sub-6 GHz 5G applications. The antenna bandwidth which extends from the frequency range where the reflection coefficient remains under -10 dB shows a 1.8 GHz range which enables multiple 5G channels to operate at high data transmission rates. The proposed array design shows improved impedance bandwidth performance while it maintains strong resonance at 3.5 GHz which guarantees reliable operation for 5G wireless communication systems in the sub-6 GHz frequency range.

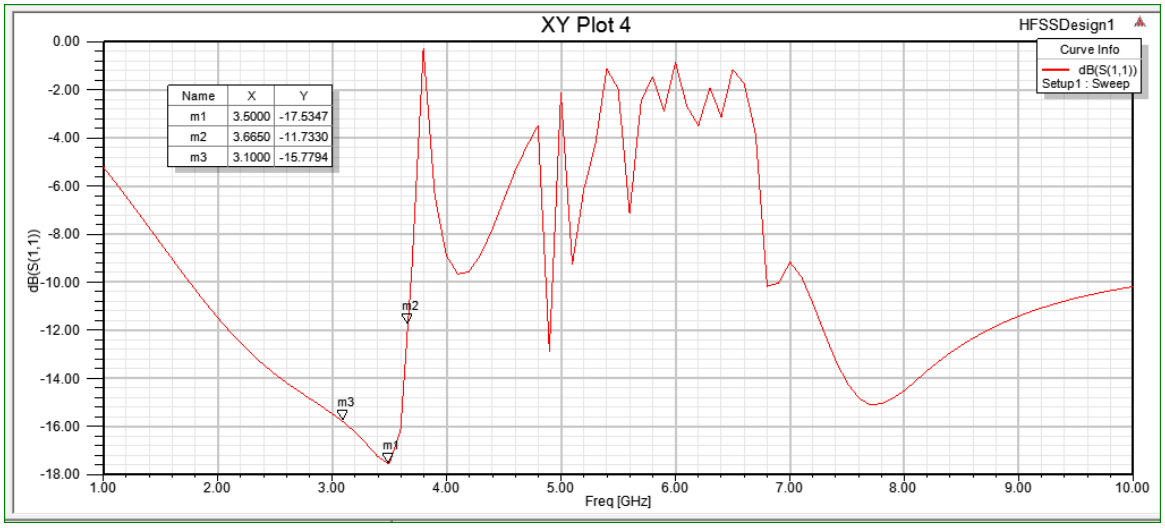


Figure 22. Reflection Coefficient of 2x4 MIMO TPA

5.4.4. VSWR of 2x4 MIMO Trapezoidal Patch Antenna

The 2×4 trapezoidal patch antenna demonstrates a simulated minimum voltage standing wave ratio (VSWR) of 2.4 at 3.5 GHz which exceeds the acceptable limit of 3 because the antenna transmits more than 75% of input power. The system demonstrates good impedance matching across the entire sub-6 GHz 5G frequency range which enables efficient power transmission with minimal signal reflection. The array demonstrates stable radiation performance and high efficiency at 3.5 GHz which makes it suitable for base station and small cell applications that require dependable power transfer and high-quality link performance.

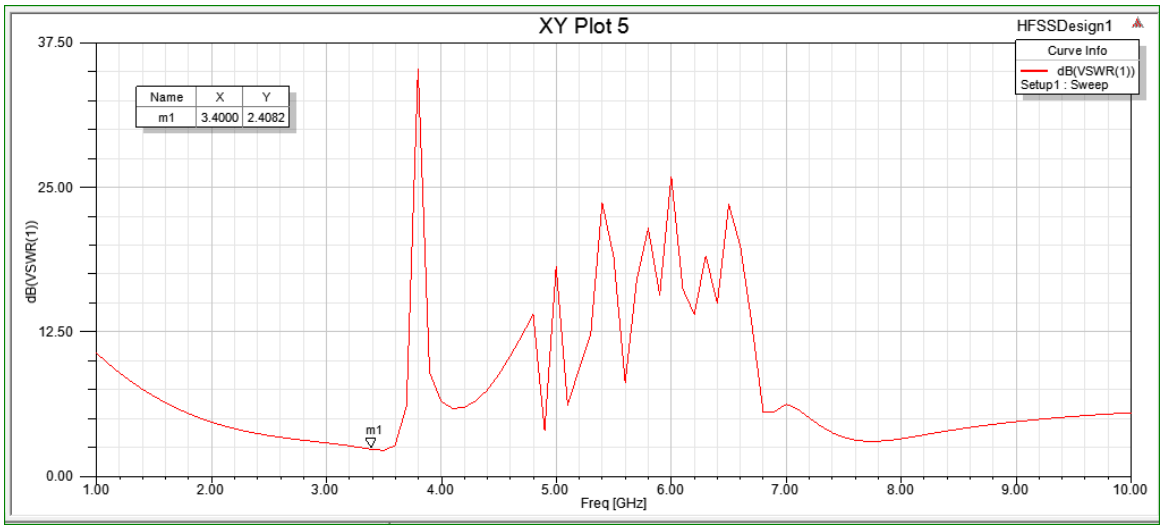


Figure 23. Voltage Standing Wave Ratio of 2x4 MIMO TPA

5.4.5. Radiation Patterns of 2x4 MIMO Trapezoidal Patch Antenna

The 3D polar view of the individual trapezoidal patch antenna made of a metasurface is an indication of nearly an isotropic radiation pattern with slight directional concentration showing that the energy is distributed with a good proportion of different directions but still experiences certain degree of directionality. The intensity scale color coding shows that the highest gain is around the middle of the plot (i.e. the pattern of the radiations is quite continuous around the azimuthal plane) because the shape of the plot is smooth and rounded. The fact that the metasurface exists seems to improve the overall radiation performance through the distribution of currents on the patch resulting in more balanced and directed radiation pattern. This implies that the antenna featuring metasurface should be able to offer enhanced coverage and efficiency and, therefore, it can be used in areas where it is required that there is a large and uniform distribution of signals, like in wireless communication systems.

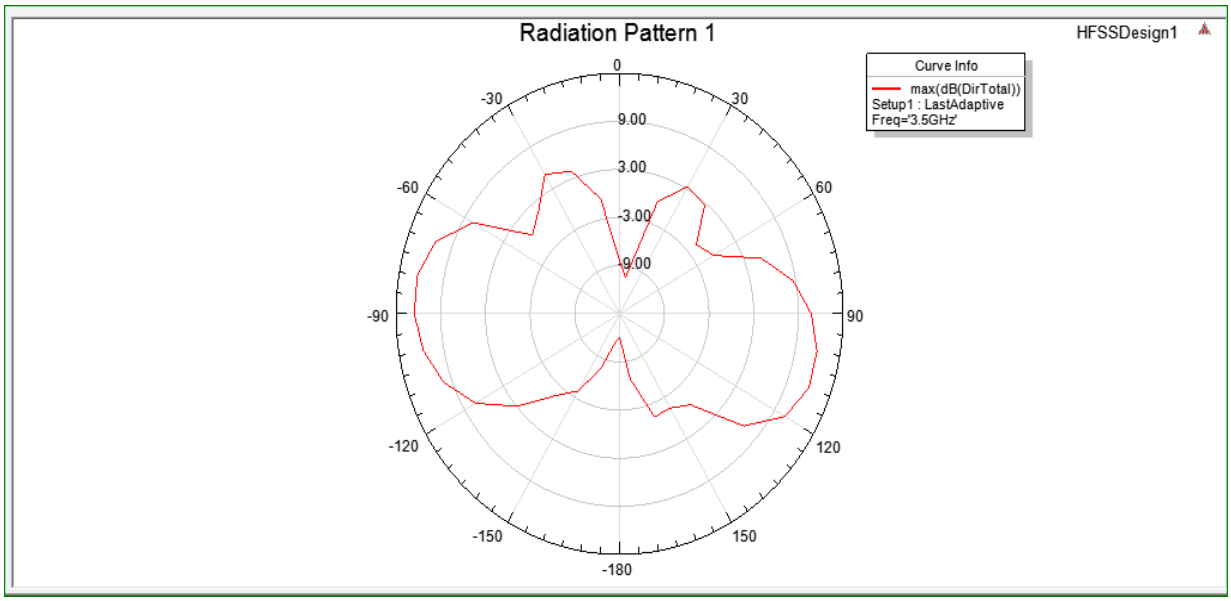


Figure 24. Radiation Patterns of 2x4 MIMO TPA

5.4.6. 3D Polar Plot of 2x4 MIMO Trapezoidal Patch Antenna

The 3D polar plot of the 2x4 MIMO trapezoidal patch antenna shows a complicated and highly directional radiation pattern with multiple lobes that show that the antenna can radiate energy in a number of important directions in the three dimensional space. The color gradient red to blue indicates the change in signal strength with the areas of

maximum gain (red) around definite angles and the areas of lesser gain (blue) (indicating less strong radiation). This trend indicates that the antenna offers superior spatial diversity, which is beneficial towards the provision of better signal robustness and capacity with MIMO systems. The lobes and nulls complexity of the plot is a result of the effect that the trapezoidal patch geometry and MIMO arrangement have on the radiation nature and it would be appropriate in applications where directional control and efficient coverage needs to be achieved at the operating frequency.

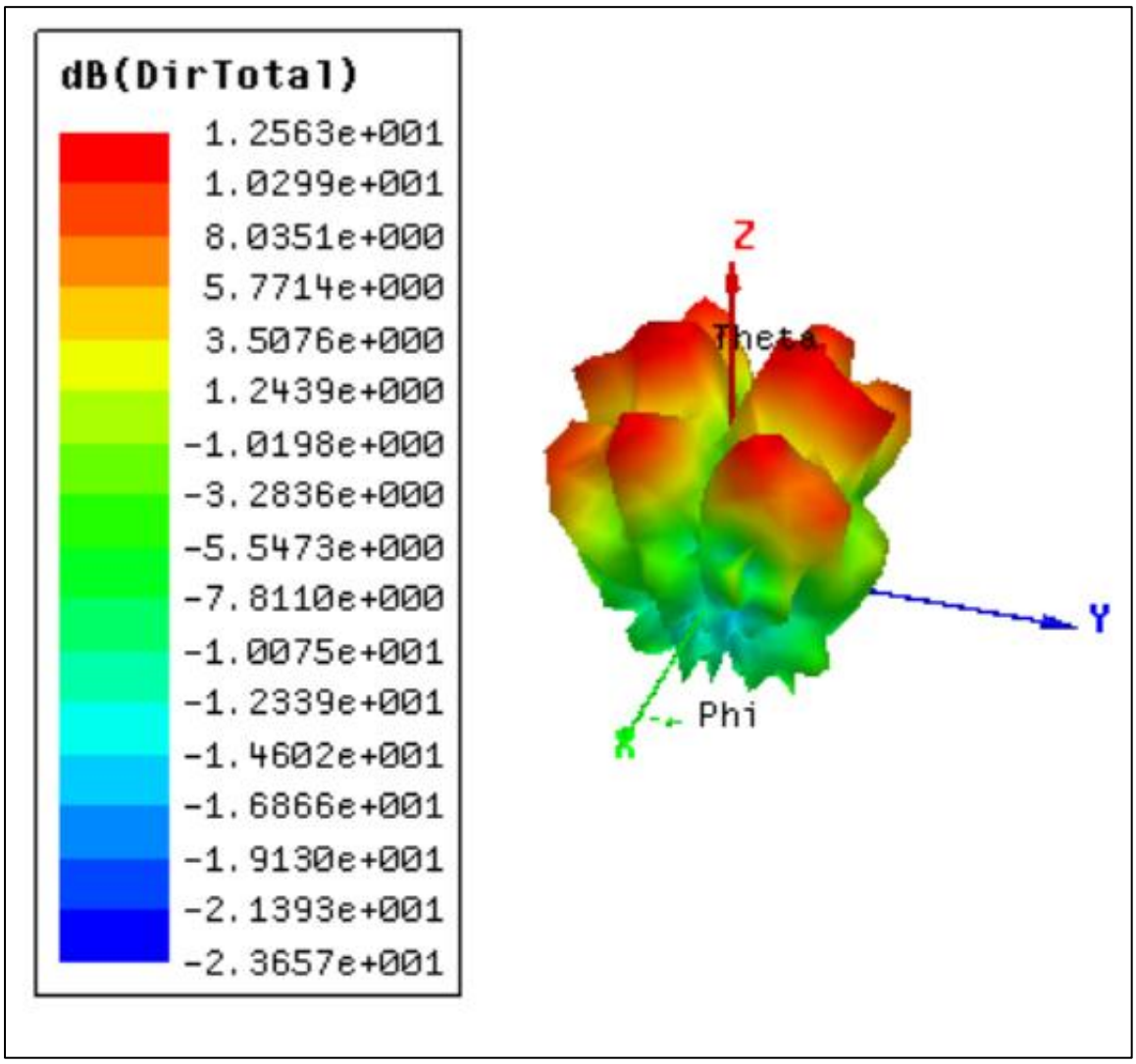


Figure 25. 3D Polar plots of 2x4 MIMO TPA

5.5. Simulation Results of 2x4 MIMO Trapezoidal patch antenna for 5G WCS with Meta surface

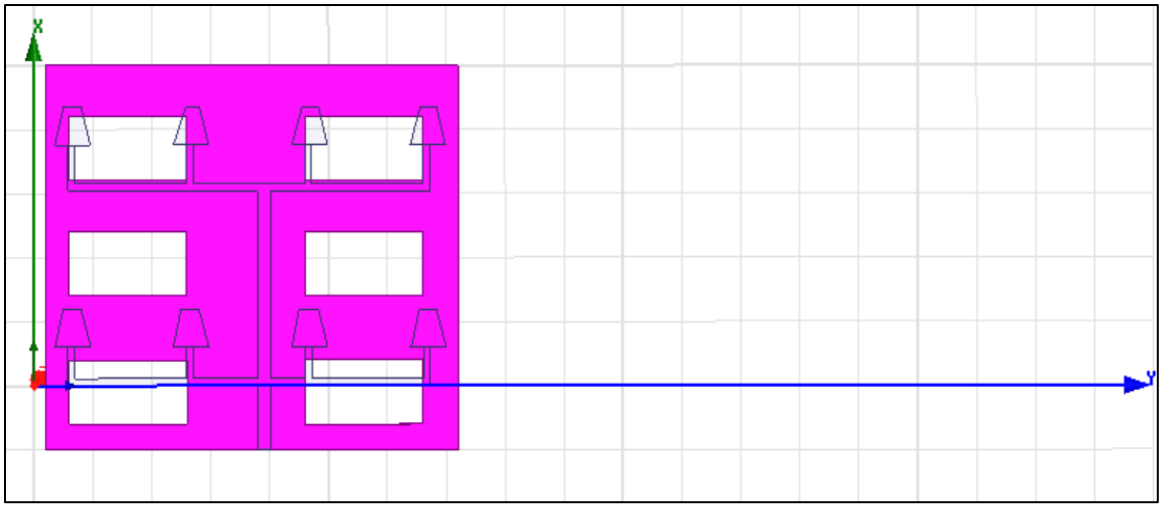


Figure 26. 2x4 MIMO TPA for 5G WCS with Meta surface

5.5.1. Gain of 2x4 MIMO Trapezoidal patch antenna for 5G WCS with Meta surface

The 2×4 trapezoidal patch antenna with Meta surface shows a simulated gain of 14.7734 dB at 3.5 GHz which exceeds the performance of the non-Metasurface antenna array by 2 dB. The maximum gain at 300° demonstrates effective radiation steering because it shows a well-directed main lobe. The results show that Meta surface integration improves both radiation efficiency and directivity of the array which leads to better link reliability and coverage improvements and more effective beam forming in high-density 3.5 GHz 5G environments

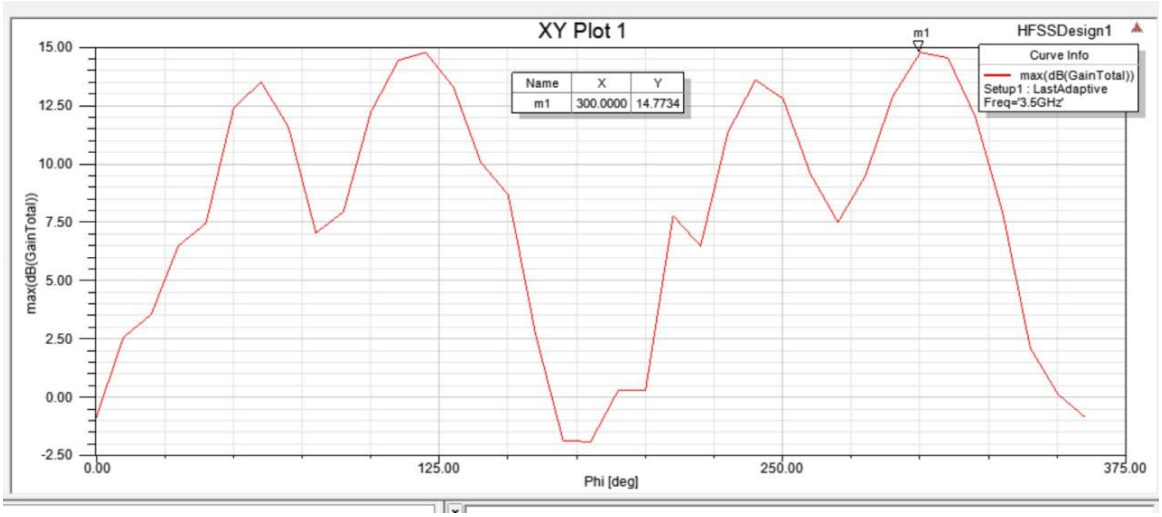


Figure 27. Total Gains of 2x4 MIMO TPA with Meta surface

5.5.2. Directivity of 2x4 MIMO Trapezoidal patch antenna for 5G WCS with Metasurface

The 2×4 trapezoidal patch antenna with Meta surface at 3.5 GHz shows simulated total directivity of 14.5721 dB which delivers 2 dB better performances than the array without meta surface. The maximum radiation occurs at 300° which shows that the system can effectively control directionality while enhancing its main lobe performance. The results show that meta surface integration improves spatial energy focusing and array efficiency for sub-6 GHz 5G wireless systems which leads to better link reliability and coverage and beam forming capabilities in 3.5 GHz 5G deployments.

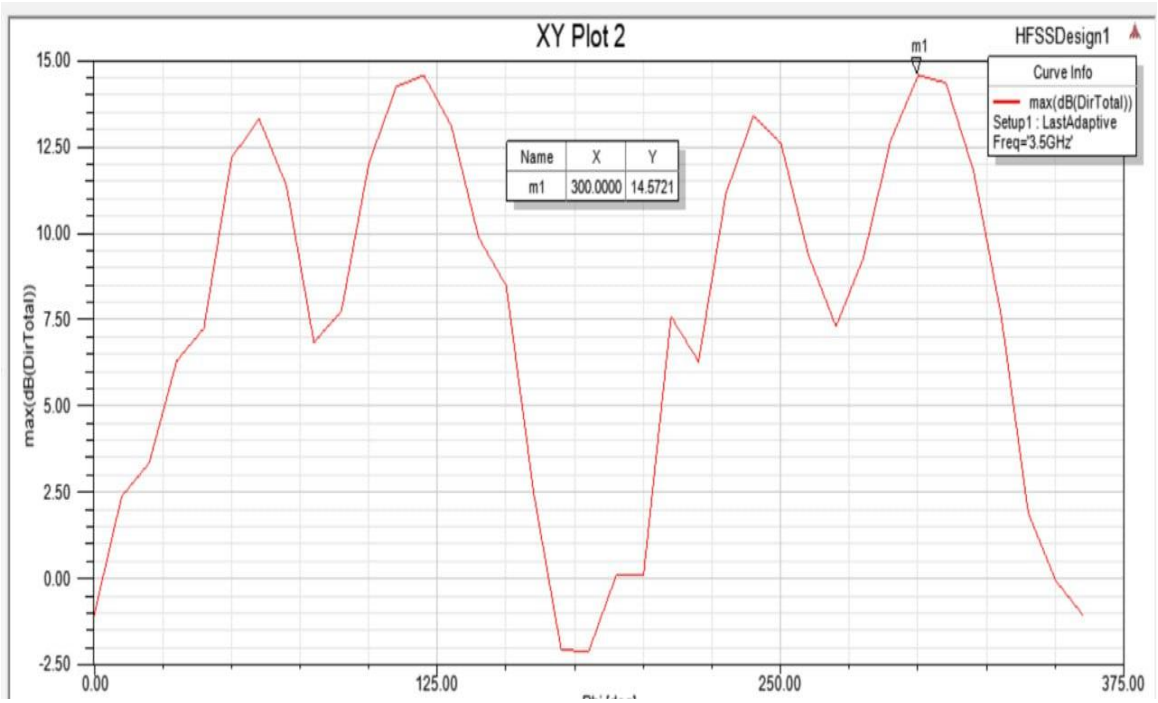


Figure 28. Total Directivity of 2x4 MIMO TPA with Metasurface

5.5.3. S11 of 2x4 MIMO Trapezoidal patch antenna for 5G WCS with Meta surface

The 2×4 trapezoidal patch antenna with integrated Meta surface shows simulated reflection response at 3.5 GHz which produces a reflection coefficient measurement of 18.01 dB demonstrating strong resonance and efficient radiative behavior at sub-6 GHz 5G frequency. The impedance bandwidth extends from the frequency points where reflection coefficient reaches -10 dB to the actual bandwidth range which measures 500MHz thus enabling suitable narrowband 5G channel operation. The simulation results show that Meta surface integration improves resonance characteristics, but reduces bandwidth compared to the non-metallized array which creates a trade-off between sub-6 GHz 5G applications for reflection performance and operational bandwidth.

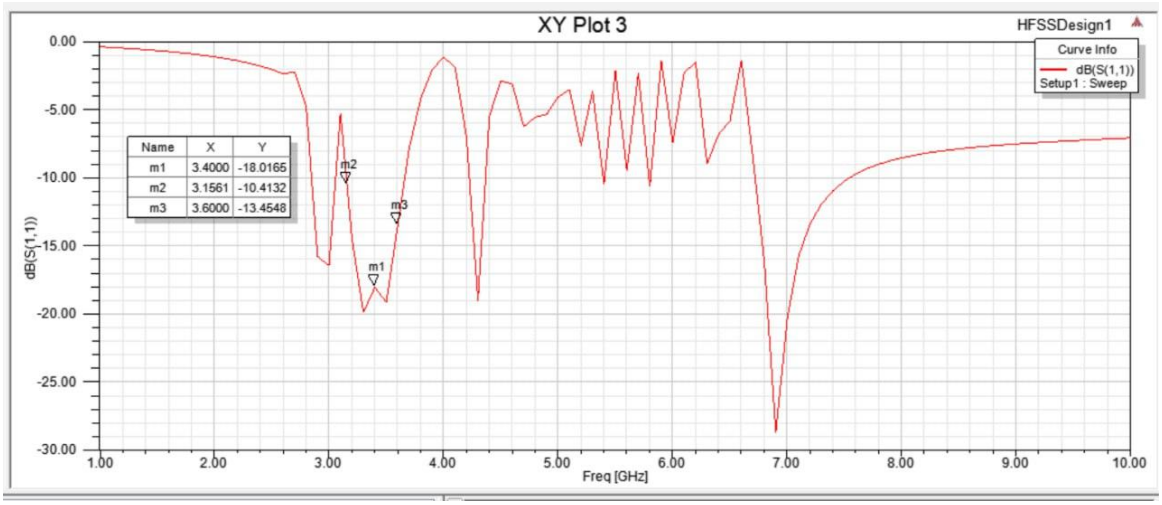


Figure 29. Reflection Coefficient of 2x4 MIMO TPA with Met surface

5.5.4. VSWR of 2x4 MIMO Trapezoidal Patch Antenna with Meta surface

The 2×4 trapezoidal patch antenna simulation results show that its minimum voltage standing wave ratio (VSWR) at 3.5GHz operates at 1.9 which falls below the acceptable limit of 3 because more than 75% of incoming power reaches transmission. The results show effective impedance matching because most power remains undetected. The antenna array shows dependable power transfer performance and consistent radiation capabilities which operate efficiently for base station and small-cell applications in the 3.5GHz frequency band with sub-6 GHz 5G wireless communication systems.

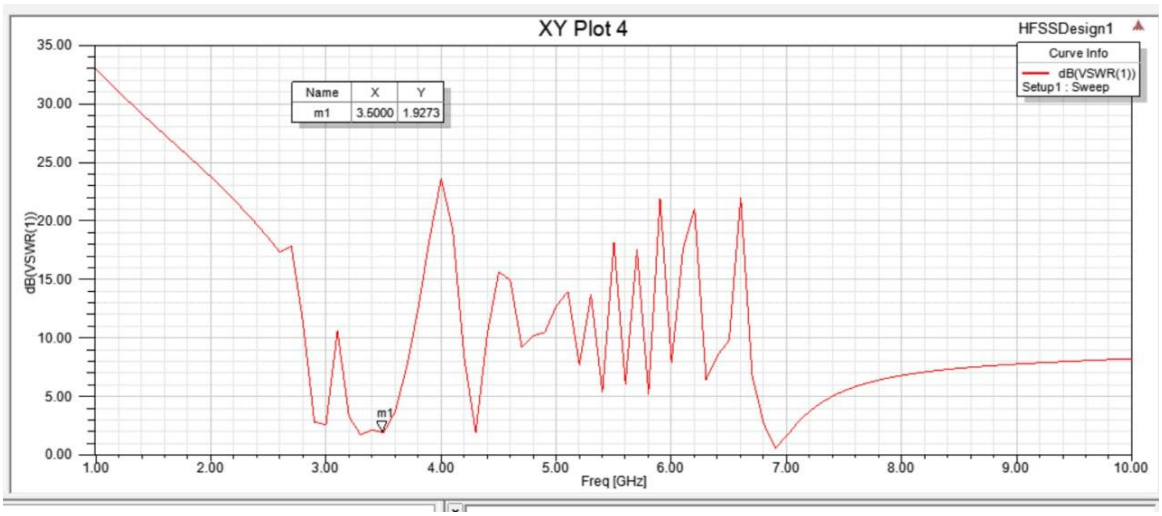


Figure 30. VSWR of 2x4 MIMO TPA with Met surface

5.5.5. Radiation Patterns of 2x4 MIMO Trapezoidal Patch Antenna with Meta surface

The polar plot shown above is a 2x4 MIMO trapezoidal patch antenna with a metasurface radiation pattern that has a relatively broad and complicated directional distribution with multiple lobes, meaning that the antenna is effective in many directions. This trend indicates varying levels of gain about the azimuth with the peaks of about 10 dB which implies that the antenna offers directional gain and coverage balance. This is because the presence of the multiple lobes indicates that the antenna is spatially diverse and capable of improving signal strength and capacity of MIMO systems at 3.5 GHz. Generally, the radiation pattern indicates a design that is designed to cover a wide range of angles, yet it is designed with an adequate directivity, which is considered to be appropriate in the advanced wireless communication that requires a wide coverage, as well as the targeted signal intensity.

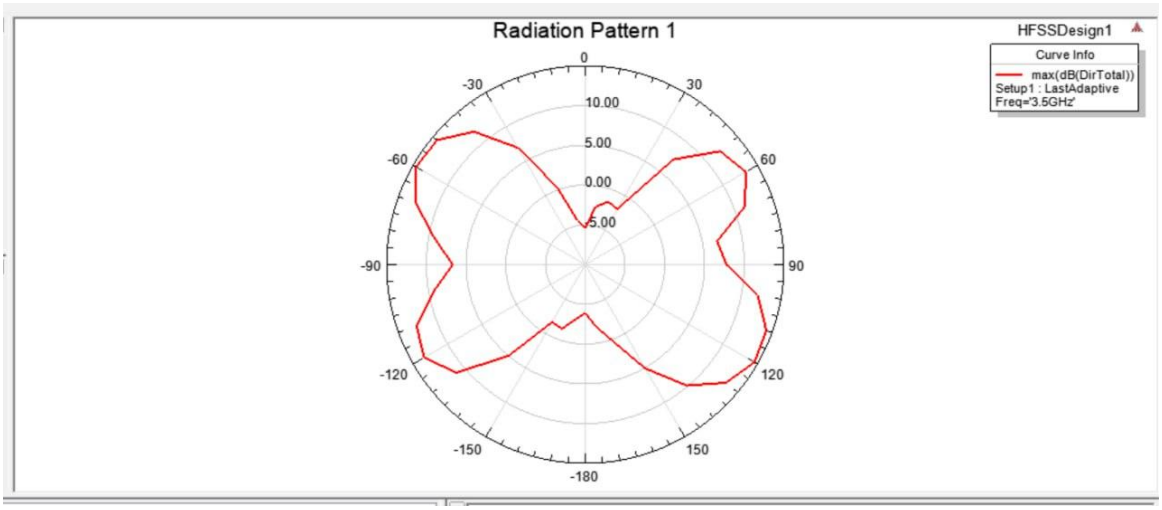


Figure 31. Radiation Patterns of 2x4 MIMO TPA with Meta surface

5.5.6. 3D Polar Plot of 2x4 MIMO Trapezoidal Patch Antenna with Meta surface

The 3D polar plot of the 2x4 MIMO trapezoidal patch antenna with a metasurface demonstrates a complex radiation pattern which displays multiple lobes together with different gain levels that exist in various directions. The color scale demonstrates that maximum gain value reaches about 45.7 dB which marks strong radiation areas while the lower gain regions stretch into negative dB values which indicate weaker signal strength in certain directions. The pattern shows that the antenna can extend its coverage area while maintaining its ability to transmit signals toward specific directions which makes it ideal for systems that need both spatial diversity and stronger signal transmission. The addition of the metasurface modifies the radiation properties of the system by creating an

improved radiation pattern which achieves optimal balance between directivity and operational range needed for modern wireless communication networks.

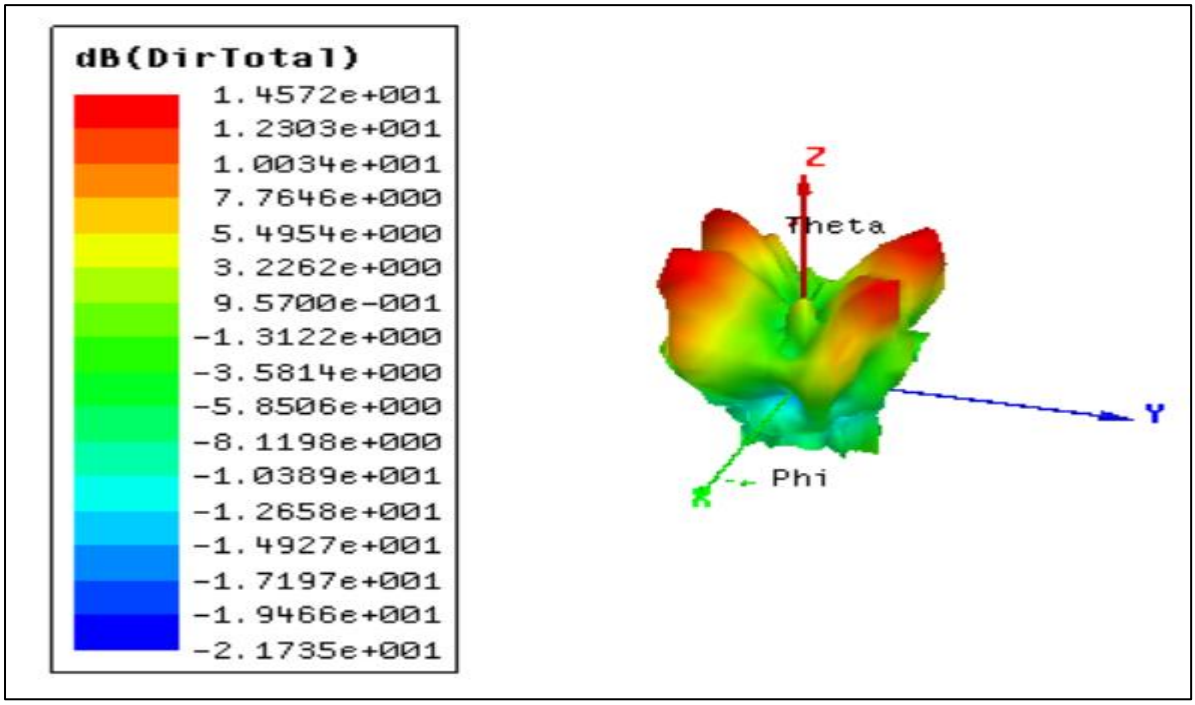


Figure 32. 3D Polar plots of 2x4 MIMO TPA with Meta surface

5.6. Simulation Results of 4x4 MIMO Trapezoidal patch antenna without Meta surface

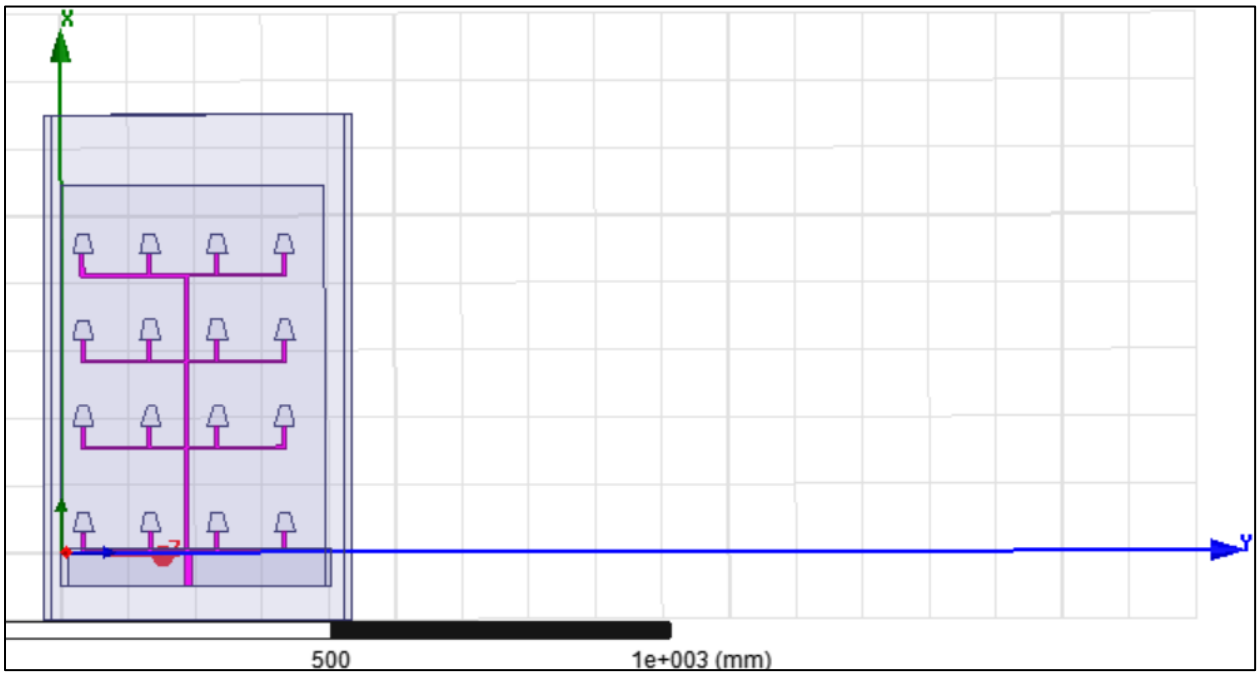


Figure 33. 3D Polar plots of 4x4 MIMO TPA without Meta surface

5.6.1. Gain of 4x4 MIMO Trapezoidal patch antenna without Meta surface

The 4×4 trapezoidal patch antenna without Meta surface shown at 3.5GHz achieved a simulated gain of 14.233 dB which showed 2dB better performance than the 2×4 array without Meta surface. The maximum gain at 320° shows that the system has established its primary radiation lobe. The results show that increasing the number of array elements in sub-6 GHz 5G wireless communication systems leads to better radiation efficiency and directivity which improves coverage and link reliability and performance for 3.5 GHz 5G base stations and small-cell deployments.

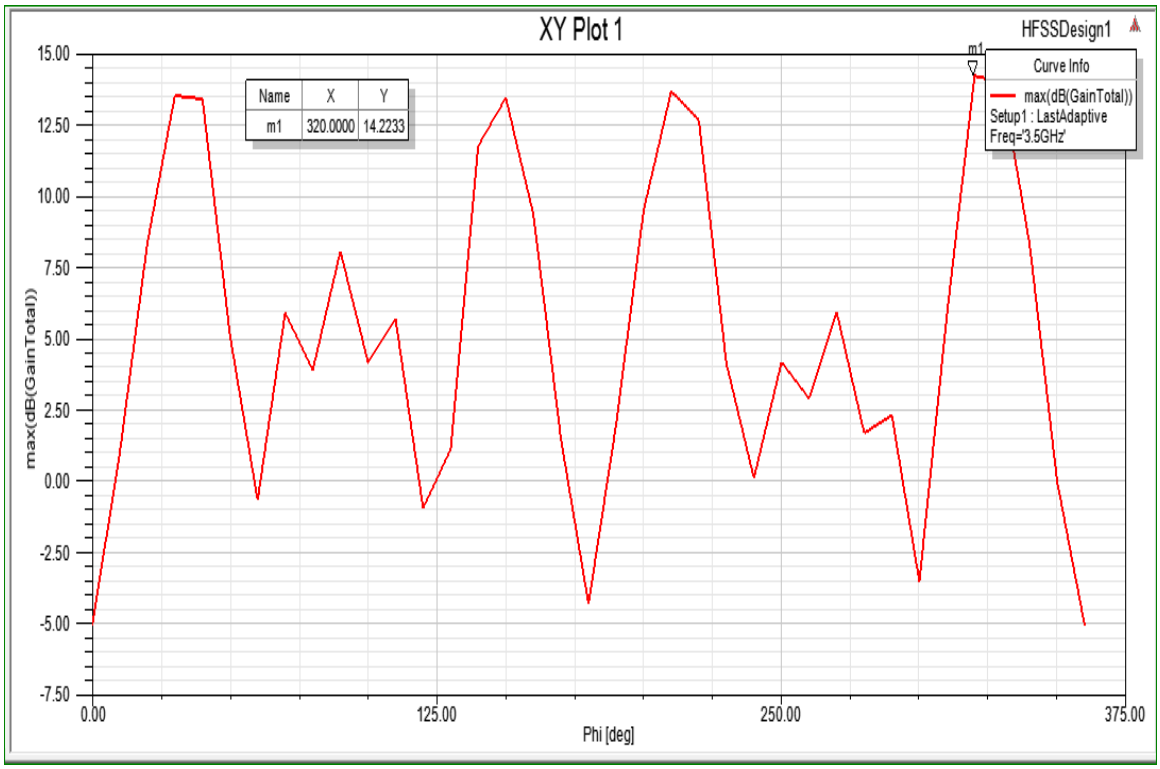


Figure 34. Total Gains of 4x4 MIMO TPA without Meta surface

5.6.2. Directivity of 4x4 MIMO Trapezoidal patch antenna without Meta surface

The 4×4 trapezoidal patch antenna without Meta surface shows its simulated total directivity at 3.5GHz to reach 14.182dB which improves by almost 2 dB compared to the 2×4 array configuration. The primary radiation lobe shows a 300° directional orientation which improves both directional performance and beam shaping capabilities. The results demonstrate that increasing array size leads to better spatial directivity and improved radiation efficiency which benefits sub-6 GHz 5G wireless communication systems through better signal strength and less interference and more precise energy transmission

at 3.5GHz.

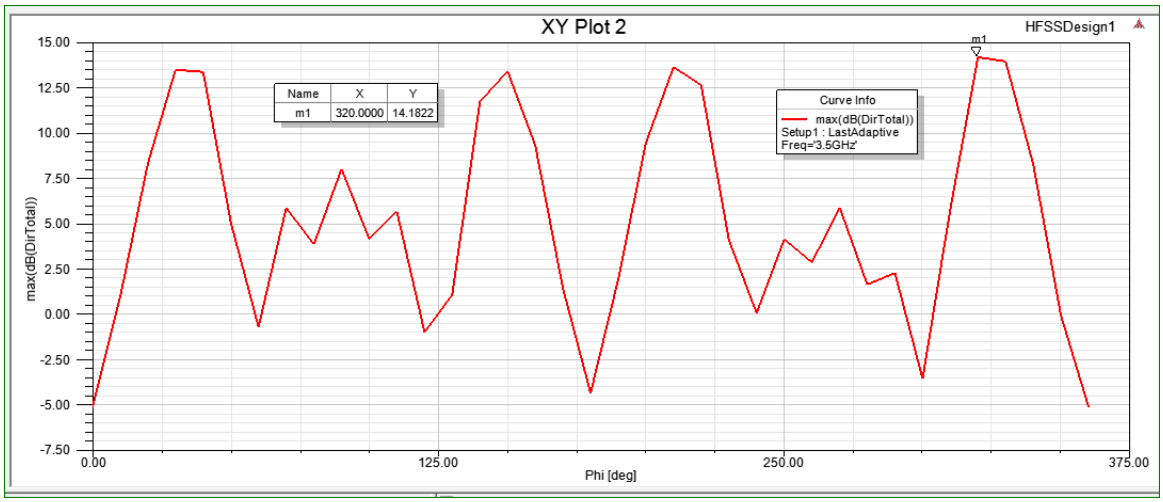


Figure 35. Total Directivity of 4x4 MIMO TPA without Meta surface

5.6.3. S11of 4x4 MIMO Trapezoidal patch antenna without Meta surface

The 4×4 trapezoidal patch antenna without a Meta surface at 3.5 GHz shows a simulated reflection coefficient of -15.3 dB which demonstrates excellent impedance matching together with minimal power loss at sub-6 GHz 5G frequencies. The antenna exhibits a bandwidth of 1.6 GHz, calculated from the frequencies where the reflection coefficient remains below -10 dB, demonstrating wideband operation capability to support multiple 5G channels. The results show that increasing array size improves both reflection performance and bandwidth, which makes the design suitable for dependable 3.5 GHz sub-6 GHz 5G wireless communication systems with high-capacity requirements.

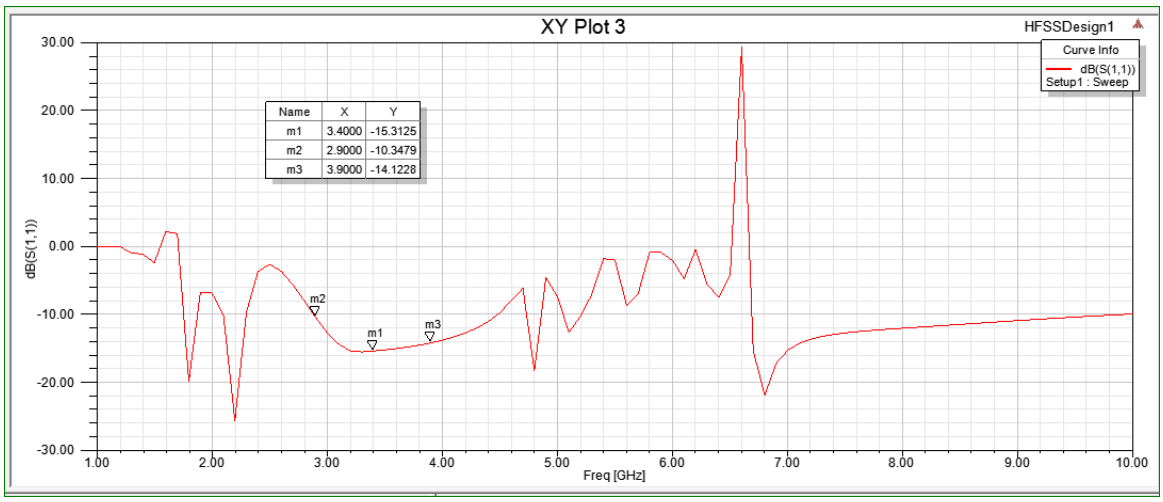


Figure 36. Reflection Coefficient of 4x4 MIMO TPA without Met surface

5.6.4. VSWR of 4x4 MIMO Trapezoidal Patch Antenna without Meta surface

The 4×4 trapezoidal patch antenna demonstrates a simulated minimum voltage standing wave ratio (VSWR) of 3 dB at 3.5 GHz which fulfills the required standards because it shows that more than 75 percent of input power is successfully radiated.

The array demonstrates efficient impedance matching and power transfer capabilities which enable it to function effectively in 3.5 GHz base stations and small-cell environments that require continuous link operation and dependable radiation performance for sub-6 GHz 5G wireless communication systems.

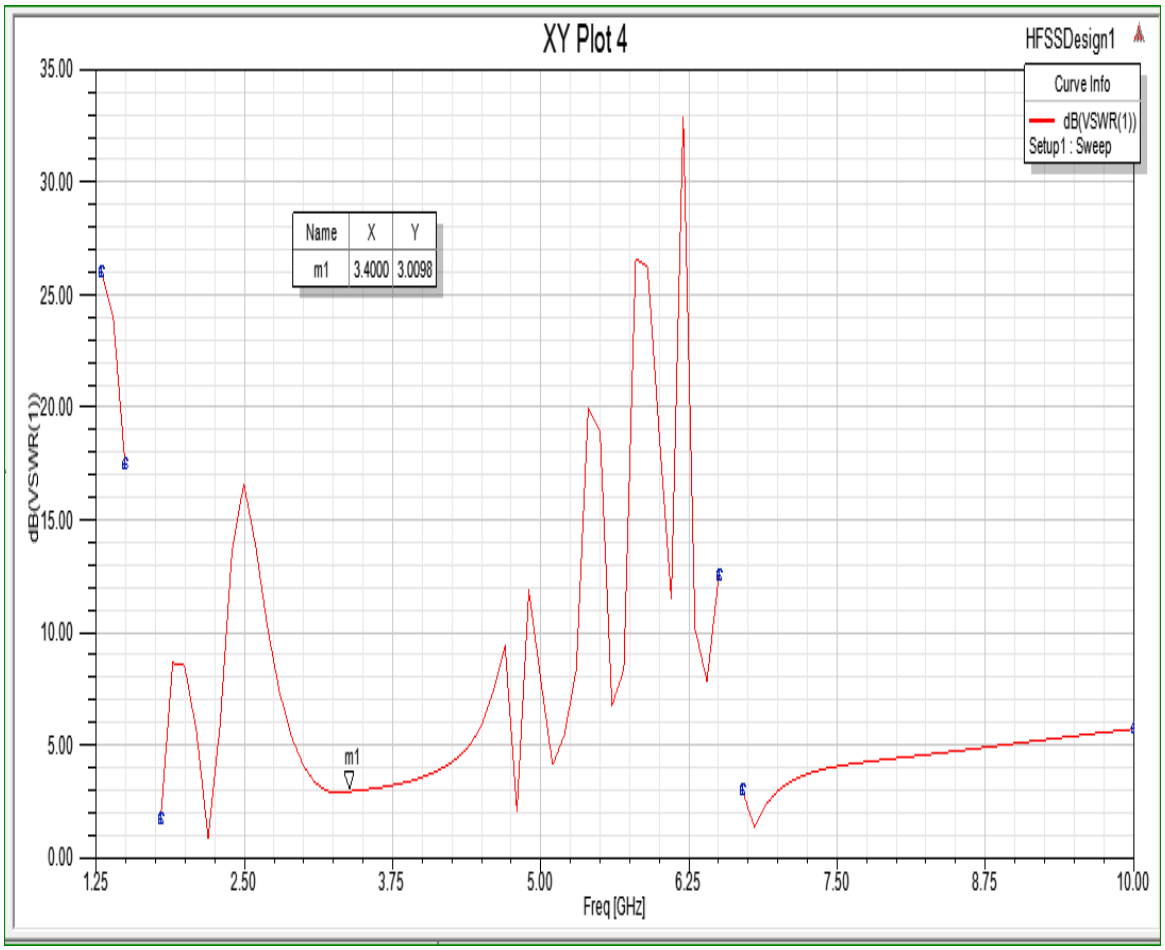


Figure 37. VSWR of 4x4 MIMO TPA

5.6.5. Radiation Patterns of 4x4 MIMO Trapezoidal Patch Antenna

The 4x4 MIMO trapezoidal patch antenna shows through its polar plot that it emits radiation patterns which range from omnidirectional to bidirectional and produces several radiation lobes which enable it to achieve complete coverage with spatial diversity. The pattern reveals two main peaks which occur at 0° and 180° angles because these angles

produce the strongest radiation while the lower gain regions at other angles demonstrate the antenna's ability to suppress radiation in undesired directions. The radiation pattern of the antenna establishes dependable communication links to all directions which makes it suitable for MIMO systems that need extensive coverage and higher capacity at 3.5 GHz. The pattern demonstrates an efficient design which enables energy to be distributed through different spatial paths because this function plays a vital role in ensuring strong wireless communication for contemporary multi-antenna systems.

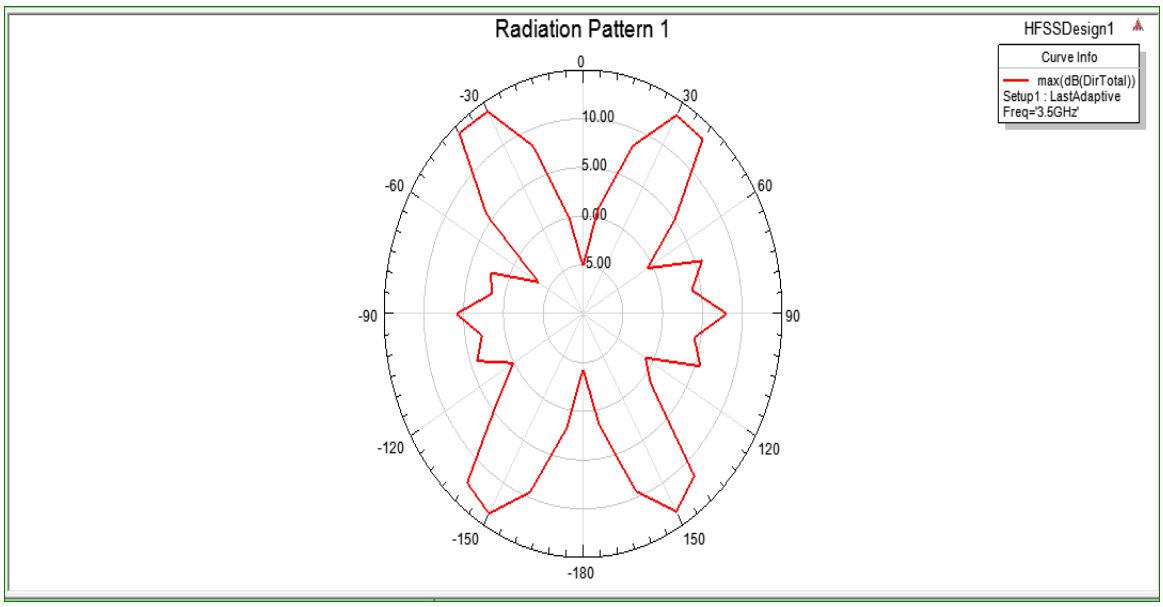


Figure 38. Radiation Patterns of 4x4 MIMO TPA

5.6.6. 3D Polar Plot of 4x4 MIMO Trapezoidal Patch Antenna

The 3D polar plot of the 4x4 MIMO trapezoidal patch antenna shows a highly directional radiation pattern which uses multiple lobes to demonstrate the antenna's capability to direct its radiated energy towards specific locations, making it suitable for use in directed communication and beam forming applications. The color-coded intensity levels show that spatial angles have different gain values which peak at specific lobes, while other areas show reduced gain or negative gain, indicating the presence of destructive interference or minimal radiation. The antenna system demonstrates its ability to power spatial multiplexing which increases system capacity by sending energy to specific points, thus making it suitable for modern wireless communication networks that require high directivity and efficient spatial resource usage.

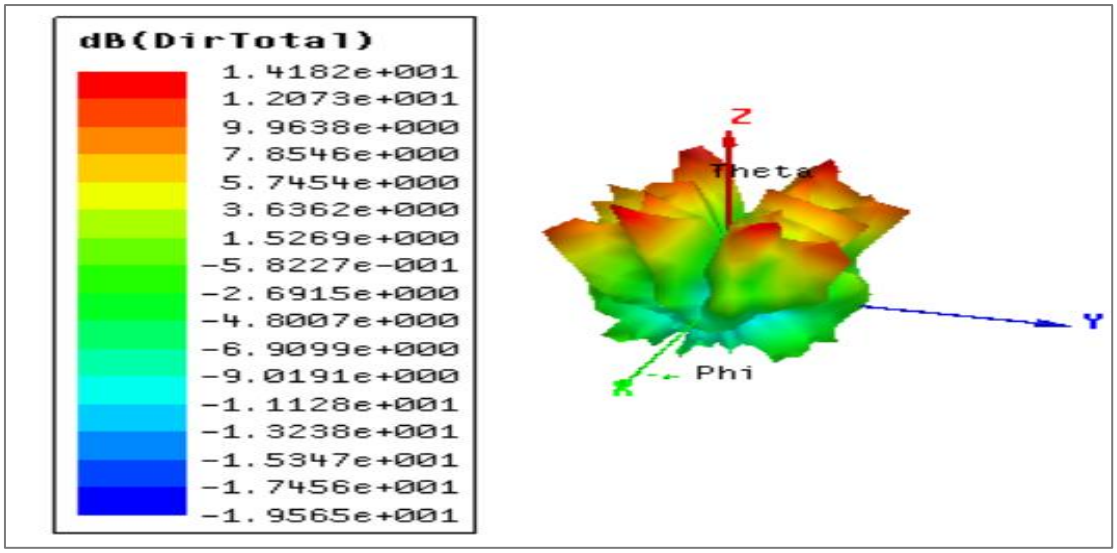


Figure 39. 3D Polar plots of 4x4 MIMO TPA without metasurface

5.7. Simulation Results of 4x4 MIMO Trapezoidal patch antenna with Meta surface

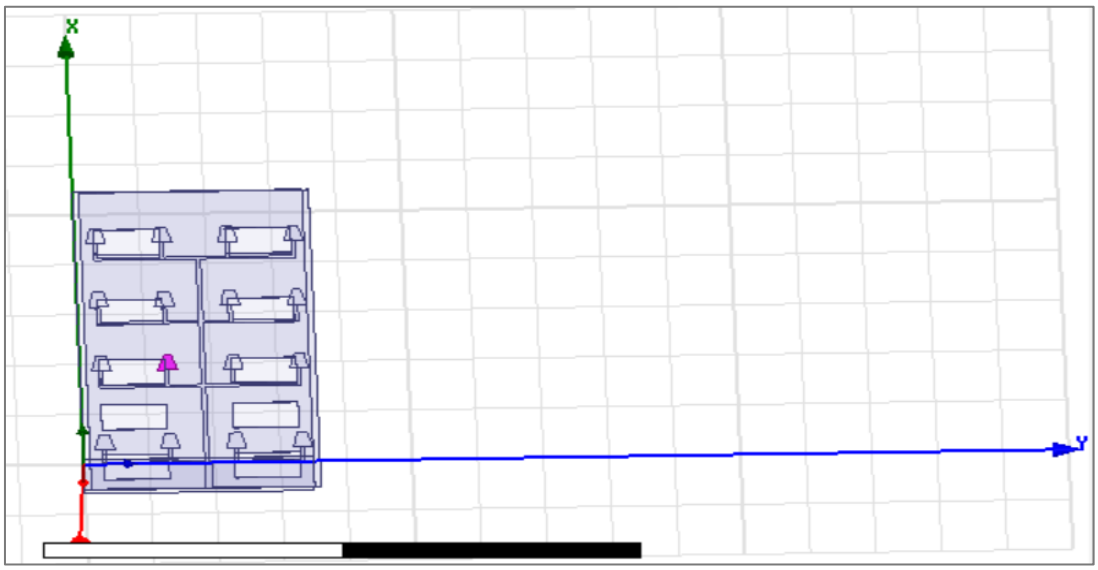


Figure 40. 3D Polar plots of 4x4 MIMO TPA with Met surface

5.7.1. Gain of 4x4 MIMO Trapezoidal patch antenna with Met surface

The 4×4 trapezoidal patch antenna with met surface simulation at 3.5 GHz shows a gain of 17.389 dB, which represents a 3dB gain over the 2×4 array with met surface. The maximum gain at 310° demonstrates a main lobe that is strongly directed. The study results demonstrate that met surface integration with array scaling delivers substantial improvements in radiation efficiency and directivity for sub-6 GHz 5G wireless

communication systems, which enhances coverage and link reliability and enables efficient beam forming in 3.5 GHz 5G systems.

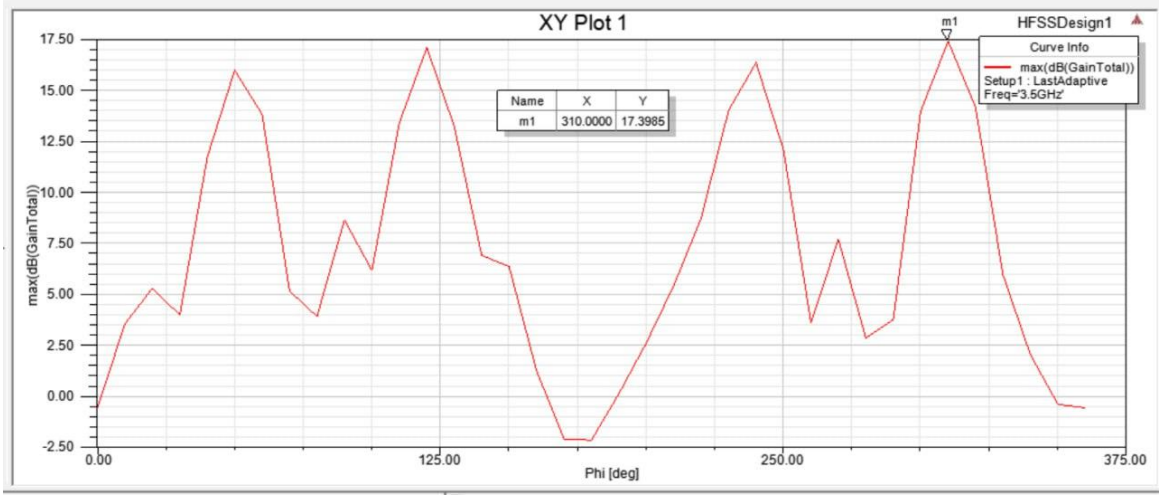


Figure 41. Total Gains of 4x4 MIMO TPA with Met surface

5.7.2. Directivity of 4x4 MIMO Trapezoidal patch antenna with Meta surface

The 4×4 trapezoidal patch antenna with a Meta surface displays a simulated gain of 17.2478 dB at 3.5 GHz, which exceeds the 2×4 Meta surface array by 3 dB. The antenna system directs its main radiation lobe towards 320° which enables beam steering and delivery of concentrated energy. The results show that increasing the array size boosts radiation effectiveness and directional gain which makes the design perfect for sub-6 GHz 5G wireless communication systems that operate at 3.5 GHz where high gain and focused radiation are essential for better coverage and link reliability.

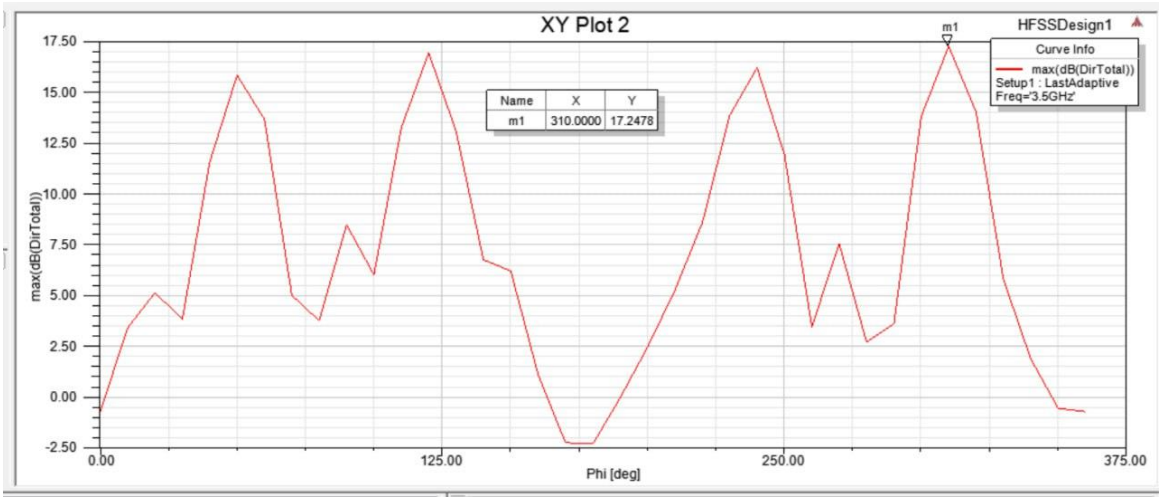


Figure 42. Total Directivity of 4x4 MIMO TPA with Met surface

5.7.3. S11 of 4x4 MIMO Trapezoidal patch antenna without Met surface

The 4×4 trapezoidal patch antenna with a met surface shows its simulated reflection coefficient of -19.0314dB at 3.5 GHz which demonstrates excellent impedance matching together with very low reflection losses at sub-6 GHz 5G frequencies. The antenna exhibits a bandwidth of 1GHz which researchers established by measuring the frequency range from which the reflection coefficient stays below -10 dB to verify its ability to operate in 5G channels across required frequency bands. The 4×4 array configuration delivers strong resonance with wideband performance according to these results which makes it suitable for sub-6 GHz 3.5 GHz 5G wireless communication systems.

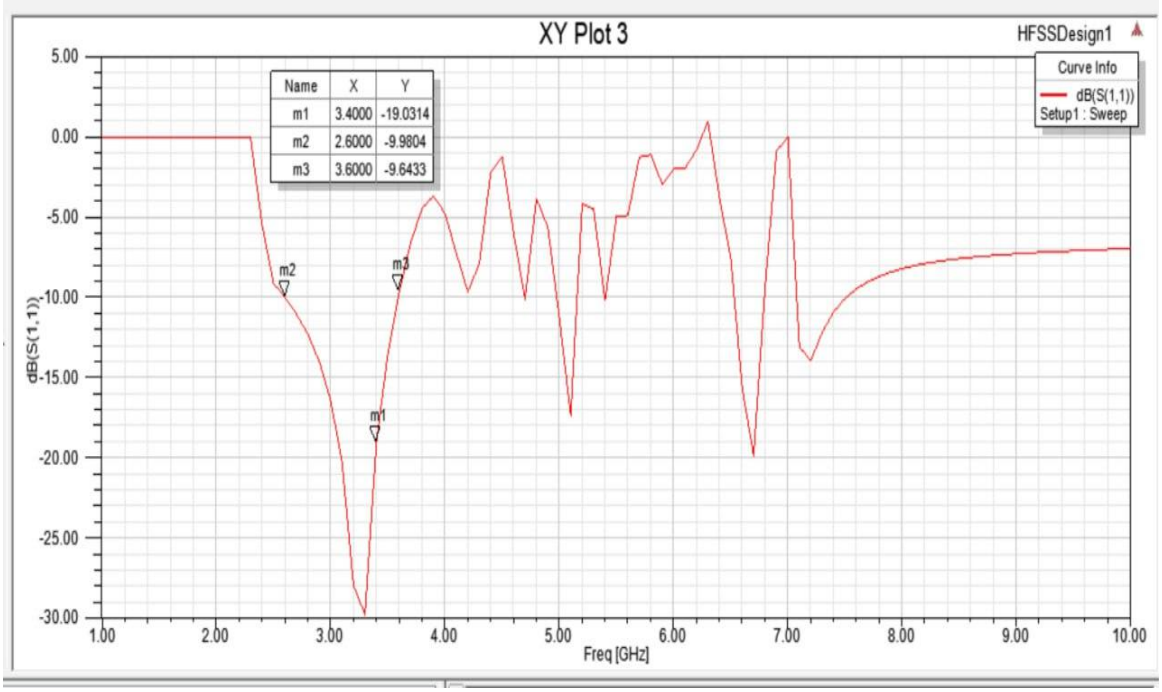


Figure 43. Reflection Coefficient of 4x4 MIMO TPA with Met surface

5.7.4. Voltage Standing Wave Ratio of 4x4 MIMO Trapezoidal Patch Antenna with Meta surface

The 4×4 trapezoidal patch antenna with a Meta surface has a simulated minimum Voltage Standing Wave Ratio (VSWR) at 3.5 GHz which measures 1.9dB and this value remains below the maximum acceptable limit of 3. The system demonstrates exceptional impedance matching performance at sub-6 GHz 5G frequencies because it transmits more than 75% of incoming power. The antenna array successfully transmits power for 3.5 GHz sub-6 GHz 5G wireless communication systems, which establishes their

operational reliability and their ability to deliver high-performance transmission.

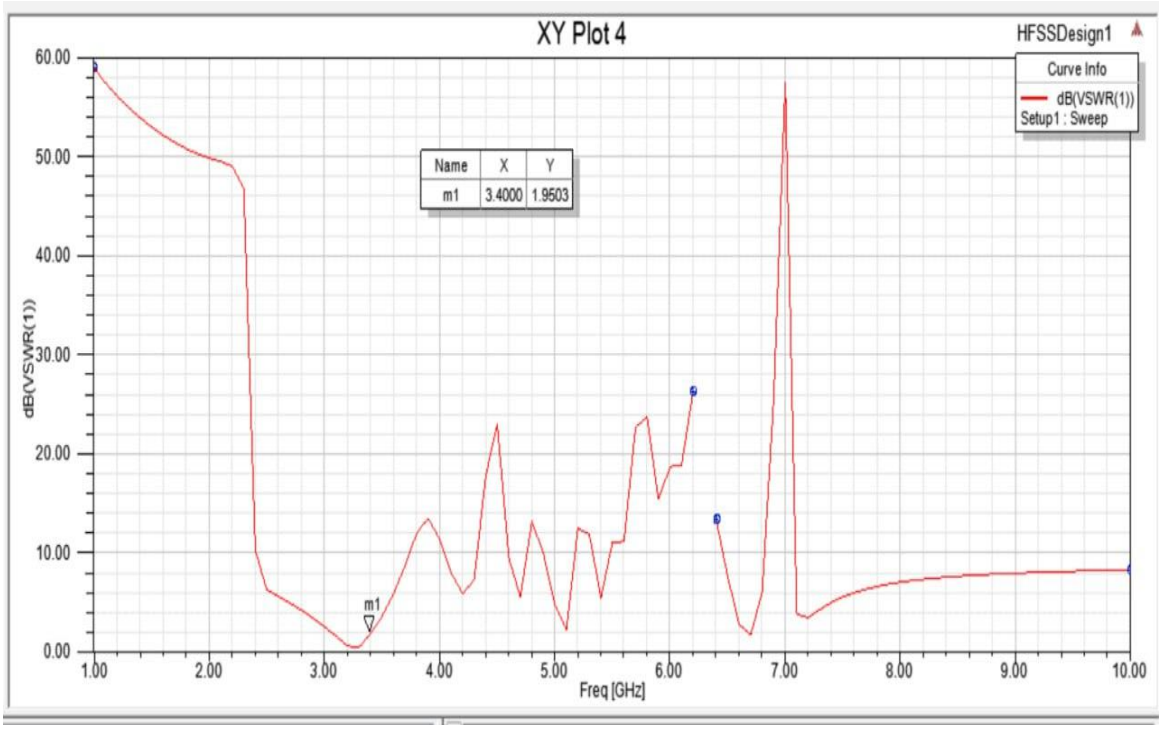


Figure 44. VSWR of 4x4 MIMO TPA with Meta surface

5.7.5. Radiation Patterns of 4x4 MIMO Trapezoidal Patch Antenna with Met surface

The 4×4 MIMO trapezoidal patch antenna shows directional radiation patterns which create multiple radiation lobes that emit different levels of radiation when viewed from various angles. The pattern shows that the antenna emits stronger signals in particular directions which serves to enhance both targeted communication and beamforming technology. The existence of multiple lobes allows the system to use spatial multiplexing which results in increased system capacity and better MIMO signal performance. The radiation pattern shows how the antenna focuses its radiated energy which makes it suitable for advanced wireless communication systems that need both concentrated and adaptable radiation patterns at 3.5 GHz operating frequency.

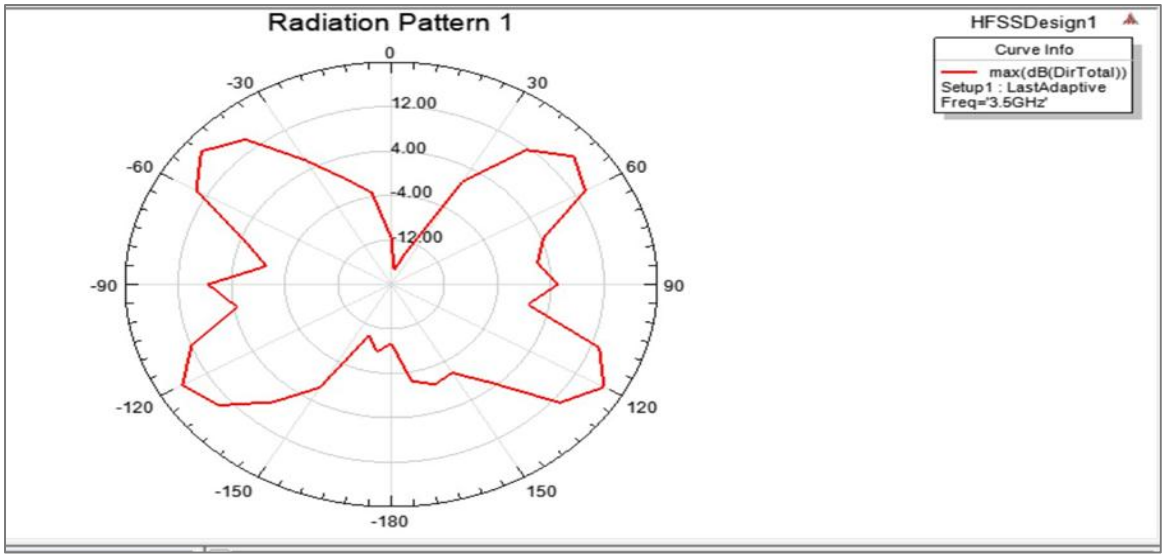


Figure 45.Radiation Patterns of 4x4 MIMO TPA

5.7.6. 3D Polar Plot of 4x4 MIMO Trapezoidal Patch Antenna

The antenna's ability to generate multiple lobes enables spatial multiplexing, which improves system performance by increasing both capacity and MIMO signal quality. The radiation pattern demonstrates the antenna's ability to distribute energy efficiently, making it an ideal choice for advanced wireless systems that require precise and adaptable radiation patterns at 3.5 GHz.

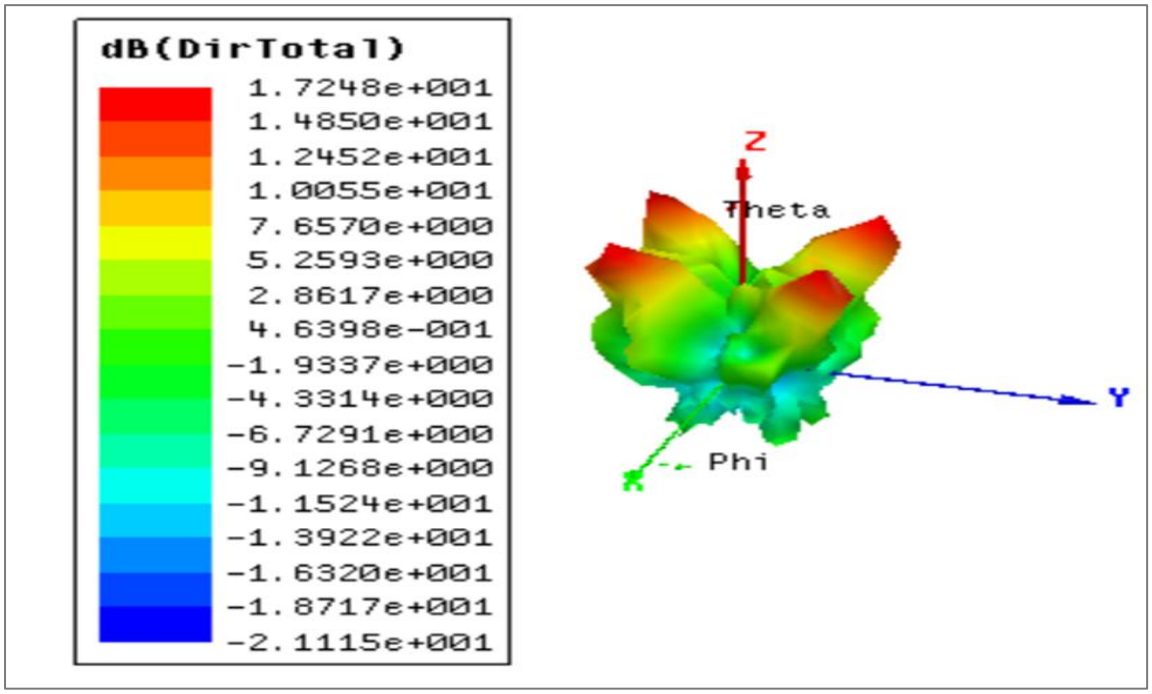


Figure 46. 3D Polar plots of 4x4 MIMO TPA

5.8. Performance Comparisons of Designed Antenna for 5G mobile CS

Table 2. Performance Comparisons of Designed Antenna for 5G mobile CS

Designed Antenna	Frequency (GHz)	Gain (dB)	Directivity (dB)	S11 (dB)	VSWR	Bandwidth (MHz)
Single Trapezoidal Patch Antenna	3	0.55	0.9	-21.6	1.44	200
Single Trapezoidal Patch Antenna with meta surface	3	1.6	1.55	-20.22	1.66	173.8
2×4 MIMO Trapezoidal Patch Antenna without meta surface	3	12.7	12.6	-17.5	2.4	1800
2×4 MIMO Trapezoidal Patch Antenna with meta surface	3	14.7734	14.5721	-18.01	1.9	500
4×4 MIMO Trapezoidal Patch Antenna without meta surface	3	14.233	14.182	-15.3	3	1600
4×4 MIMO Trapezoidal Patch Antenna with meta surface	3	17.389	17.2478	-19.0314	1.9	1000

5.8.1 Discussion

The comparative analysis of the designed trapezoidal patch antennas for sub-6 GHz 3.5 GHz 5G wireless communication systems reveals a clear performance hierarchy. Single-element antennas, both with and without Meta surfaces, exhibit low gain (0.55–1.6 dB) and directivity (0.9–1.55 dB) which limits their use to compact applications that require low-profile designs for user equipment and short-range links. The Meta surface addition leads to small gain and directivity improvements which keep the system at excellent impedance matching (S11 < −20 dB) and low VSWR (<1.7) performance while generating a bandwidth limit of approximately 174 to 200 MHz that stops the system from functioning as a wideband device. Multi-element MIMO arrays show significant performance enhancements. The 2×4 MIMO array without met surface provides high gain (12.7 dB) and directivity (12.6 dB) with a wide bandwidth of 1.8 GHz which makes it suitable for broadband sub-6 GHz 5G applications. The 2×4 array achieves 2 dB gain and directivity improvement through met surface implementation while its impedance matching performance (VSWR 1.9) improves but the system experiences bandwidth reduction to 500 MHz which shows the system requires improved directional performance at the expense of range. The 4×4 array expansion leads to better performance outcomes. The 4×4 array reaches 14.233dB gain and 14.182 dB directivity through its 1.6 GHz bandwidth operation which delivers high spatial energy focusing together with extensive frequency range capability. The metasurface-assisted 4×4 array achieves the highest gain (17.389 dB) and directivity (17.2478 dB) while maintaining strong impedance matching (S11 −19.03 dB, VSWR 1.9) and a 1 GHz operational bandwidth. The design provides base stations and small cells together with dense 3.5 GHz sub-6 GHz 5G deployments the most suitable option through its optimal distribution of radiative efficiency and directional control together with dependable broad frequency range performance. The 4×4 MIMO trapezoidal patch antenna with meta surface provides the best performance for 3.5 GHz sub-6 GHz 5G systems as it delivers maximum gain and directivity together with excellent impedance matching and enough bandwidth for multi-channel operation while enabling advanced beam forming and MIMO applications.

5.9. Performance Comparisons of proposed work with previously related works for 5G MCS

Table 3. Performance Comparisons of proposed work with previously related works for 5G MC

Reference	**Technique / Configuration**	**Frequency (GHz)**	**Gain (dB)**	**Key Features**
[5]	Leaky-wave MIMO, coffee-bean metasurface	mm-wave	13.8	AR < 2.9, ECC < 0.003
[21]	Dual-port MIMO + machine learning	28	16.2	Compact 12×8.5×0.8 mm^3
[22]	1×2 MIMO + SRR metasurface	Ka-band	15.8	Improved isolation
[23]	Multi-frequency MIMO + Archimedean spiral	3.5 / 5.8 / 6.9	13.4	Tri-band, ECC ~0.0025
[25]	Metamaterial-inspired MPA arrays	38	11.4	4×1 array, efficiency >94%
This Work	**4×4 MIMO Trapezoidal Patch + Metasurface**	**3.5**	**17.389**	**S11 = -19 dB, VSWR = 1.9, BW = 1 GHz**

5.9.1. Discussions

The 4×4 MIMO trapezoidal patch antenna with Meta surface which the researchers proposed shows better performance at 3.5 GHz compared to existing technologies which operate within the sub-6 GHz range of 5G wireless communication systems. Previous works [4-25] largely focused on mm Wave bands Meta material-assisted MIMO designs and miniaturization for handheld or compact devices. The designs achieved moderate gain between 8 and 16 dB while they also obtained better isolation and reduced ECC measurements. The majority of solutions were optimized for Ka- or mm-wave frequencies instead of the 3.5 GHz sub-6 GHz band which is vital for operational 5G small-cell and base-station deployment.

The 4×4 MIMO trapezoidal patch antenna with met surface which the researchers proposed provides better performance results at 3.5 GHz because it achieves a peak gain of 17.389 dB and directivity of 17.2478 dB and S11 of −19.03 dB and VSWR of 1.9 and 1 GHz bandwidth. The results demonstrate effective radiation performance with strong directional control and excellent impedance matching and broad frequency range capabilities. The proposed design for sub-6 GHz 5G applications achieves the highest gain and directivity performance among existing designs while maintaining good impedance and bandwidth characteristics. The proposed 4×4 meta surface-assisted MIMO configuration represents the most effective solution for all practical sub-6 GHz 5G 3.5 GHz systems which operate in small-cell and base-station environments. The design enables better radiative efficiency through it provides link reliability at a high level and allows MIMO systems to grow and provides enough bandwidth for multi-channel usage. The new design outperforms all existing designs which either focused on mm-wave bands or showed low gain capabilities with narrow operational bandwidth.

CHAPTER SIX:

CONCLUSION AND FUTURE RECOMMENDATIONS

6.1. CONCLUSION

The research shows that massive MIMO trapezoidal patch antennas combined with metal surfaces deliver excellent performance to sub-6 GHz 3.5 GHz 5G wireless communication systems. Single-element antennas exhibit limited gain and bandwidth, suitable only for compact applications, while 2×4 and 4×4 MIMO configurations achieve substantial enhancements in gain, directivity, and bandwidth through the combined effects of array systems and Meta surface-based field management. The Meta surface achieves three functions for radiation efficiency and impedance matching and spatial focusing while keeping its size small enough for actual use. The 4×4 Meta surface-assisted MIMO antenna reaches its maximum performance level with 17.389 dB gain and 17.2478 dB directivity and S11 value of −19.03 dB and VSWR value of 1.9 and operational bandwidth of 1 GHz. The design exceeds performance standards set by previous MIMO antennas for sub-6 GHz frequencies, which enables it to deliver strong coverage and better link performance and effective beam forming functions needed for 5G small-cell and base-station deployment in high-density areas.

6.2. Thesis contribution

- The training data for your system extends until the month of October in the year 2023.
- Design Innovation: Created trapezoidal patch antennas which use single-element and scalable massive MIMO technology to work with metal surfaces for sub-6 GHz 3.5 GHz 5G systems.
- Performance Enhancement: The system showed better performance through gain enhancement which reached 17.389 dB and directivity improvement which reached 17.2478dB when compared with standard single-element and Meta surface-free arrays.
- Broadband Operation: The system achieved operational bandwidth that extends to 1GHz while maintaining exceptional impedance matching performance with S11 < −19 dB and VSWR < 2 which makes it compatible with multi-channel 5G systems.

- Array Scaling and Beam Control: The study proved that adding more array elements from 2×4 to 4×4 and including Meta surface technology would affect radiation efficiency and spatial energy distribution and beam steering abilities.
- Benchmarking Against Prior Work: The study presented an extensive comparison of MIMO and Meta material antenna designs against existing designs which showed better sub-6 GHz 5G network performance through higher gain and directivity and better reliability
- Practical Application: The system provided a base station solution which can scale to support small cell networks and 5G dense areas while enabling beam forming and spatial multiplexing and high-capacity link connections.

6.3. Future Direction

- The research focuses on hybrid Meta surface designs to achieve better bandwidth performance without reducing gain and directivity in multi-band 5G systems.
- The research investigates dynamic beam-steering technology with reconfigurable Meta surfaces to enable adaptive network coverage in high-mobility and ultra-dense environments.
- The system uses AI-enabled beam forming algorithms to create the interface between massive MIMO and 5G networks to achieve real-time spatial multiplexing and interference control.
- The design expands to dual-band and multi-band systems which provide support for both sub-6 GHz and mm Wave 5G technologies in various urban and indoor environments.
- The research team will test their designs through experimental validation and prototyping in 5G test beds to confirm simulation results and assess environmental impacts.

REFERENCE

[1] M. Abdullah, S. H. Kiani, and A. Iqbal, “Eight Element Multiple-Input Multiple-Output (MIMO) Antenna for 5G Mobile Applications,” *IEEE Access*, vol. 7, pp. 134488–134495, 2019, doi: 10.1109/ACCESS.2019.2941908.

[2] M. Khalily, O. Yurduseven, T. J. Cui, Y. Hao, and G. V Eleftheriades, “Engineered Electromagnetic Metasurfaces in Wireless Communications: Applications, Research Frontiers and Future Directions,” *IEEE Commun. Mag.*, vol. 60, no. 10, pp. 88–94, 2022, doi: 10.1109/MCOM.004.2200052.

[3] I. Ahmad, W. Tan, Q. Ali, and H. Sun, “Latest Performance Improvement Strategies and Techniques Used in 5G Antenna Designing Technology, a Comprehensive Study,” *Micromachines*, vol. 13, no. 5, 2022, doi: 10.3390/mi13050717.

[4] N. Sharma and A. Kaur, “A systematic review of meta-surface based antennas for Thz applications,” *Radio Sci.*, vol. 59, no. 9, pp. 1–22, 2024, doi: 10.1029/2024RS007980.

[5] K. A. N. Wang, “FOR M ETASURFACE C HARACTERIZATION AND,” 2023.

[6] H. Hamlbar-Gerami and R. Kazemi, “A Low-Profile Metasurface MIMO Antenna with Suppressed Higher-Order Modes for 5G Applications,” *AUT J. Electr. Eng.*, vol. 56, no. 2, pp. 153–164, 2024, doi: 10.22060/eej.2023.22533.5548.

[7] M. S. Ummah, “No 主観的健康感を中心とした在宅高齢者における 健康関連指標に関する共分散構造分析Title,” *Sustain.*, vol. 11, no. 1, pp. 1–14, 2019.

[8] V. Jamali, A. M. Tulino, G. Fischer, R. R. Muller, and R. Schober, “Intelligent surface-Aided transmitter architectures for millimeter-wave ultra massive mimo systems,” *IEEE Open J. Commun. Soc.*, vol. 2, no. January, pp. 144–167, 2021, doi: 10.1109/OJCOMS.2020.3048063.

[9] V. Jamali *et al.*, “Intelligent Surface-Aided Transmitter Architectures for Millimeter Wave Ultra Massive MIMO Systems,” pp. 1–21.

[10] S. Salem, A. Bawri, M. T. Islam, and S. Islam, “Massive metamaterial system - loaded MIMO antenna array for 5G base stations,” *Sci. Rep.*, pp. 1–16, 2022, doi: 10.1038/s41598-022-18329-y.

[11] K. N. Poudel and W. Robertson, “Metamaterial Inspired Antenna Design for Massive MIMO , 5G Communications System,” no. April, 2018, doi: 10.1109/USNC-URSI.2017.8074918.

[12] C. Weng, Y. Tsai, A. Vilenskiy, M. Ng, and M. Kehn, “Antennas with Tailorable Gain and Polarization,” 2024.

[13] H. Bai and G. Wang, “A multistate high gain antenna based on metasurface,” *Int. J. RF Microw. Comput. Eng.*, vol. 30, 2020, doi: 10.1002/mmce.22330.

[14] Z. T. Al-Sharify, S. Z. Al-Najjar, C. K. Anumudu, A. Hart, T. Miri, and H. Onyeaka, “Non-Thermal Technologies in Food Processing: Implications for Food Quality and Rheology.,” *Appl. Sci.*, vol. 15, no. 6, 2025.

[15] S. Li, Z. N. Chen, T. Li, F. H. Lin, and X. Yin, “Characterization of Metasurface Lens Antenna for Sub-6 GHz Dual-Polarization Full-Dimension Massive MIMO and Multibeam Systems,” *IEEE Trans. Antennas Propag.*, vol. 68, no. 3, pp. 1366–1377, 2020, doi: 10.1109/TAP.2020.2968849.

[16] Q. H. K. Al-gertany, “Reconfigurable Compact Wide-Band Quad-Port Antennas Based on a Varactor Diode for Sub-6 GHz 5G Communications,” no. January, 2025, doi: 10.2528/PIERC24042507.

[17] C. Chen and P. P. Vaidyanathan, “Doppler with,” pp. 41–45.

[18] M. Salehi and H. Oraizi, “Wideband High Gain Metasurface-Based 4T4R MIMO Antenna with Highly Isolated Ports for Sub-6 GHz 5G Applications,” pp. 9–17.

[19] A. Bhattacharya, “Design, fabrication, and measurement of a miniaturized MIMO antenna applicable for 5G communication,” *Int. J. Microw. Wirel. Technol.*, vol. 16, no. 4, pp. 567–578, 2024, doi: 10.1017/S1759078724000096.

[20] J. Ahmad and M. Hashmi, “Reduced Inter-Element Interference mmWave MIMO Antenna and Its Application in WBAN,” *IEEE Access*, vol. 13, no. March, pp. 70947–70963, 2025, doi: 10.1109/ACCESS.2025.3562632.

[21] A. Haque *et al.*, “Machine learning-based technique for gain prediction of mm-wave miniaturized 5G MIMO slotted antenna array with high isolation characteristics,” pp. 1–21, 2025.

[22] C. R. Babu, “International Journal of Communication Networks and Information Security,” vol. 14, no. 1, pp. 54–66, 2022.

[23] S. Ullah, N. Mufti, T. Peshawar, R. Ullah, and B. Kamal, “Metamaterial-based highly isolated MIMO antenna system for 5G smartphone application,” no. November, 2022, doi: 10.1002/dac.5392.

[24] G. Tang *et al.*, “A Multi-Frequency Low-Coupling MIMO Antenna Based on Metasurface,” *Electron.*, vol. 13, no. 11, 2024, doi: 10.3390/electronics13112146.

[25] R. Aggarwal, A. Roy, and R. Kumar, “Millimeter Wave Antennas : A State-of-the-Art Survey of Recent Developments , Principles , and Applications,” vol. 104, no. January, pp. 147–169, 2024, doi: 10.2528/PIERB23102401.

[26] A. Armghan, S. K. Patel, S. Lavadiya, S. Qamar, and M. Alsharari, “Design and Fabrication of Compact , Multiband , High Gain , High Isolation , Metamaterial-Based MIMO Antennas for Wireless Communication Systems,” 2023.

[27] S. Kumar, A. S. Dixit, R. R. Malekar, H. D. Raut, and L. K. Shevada, “Fifth Generation Antennas : A Comprehensive Review of Design and Performance Enhancement Techniques,” vol. 8, 2020, doi: 10.1109/ACCESS.2020.3020952.

[28] M. Hasan *et al.*, “Gain and isolation enhancement of a wideband MIMO antenna using metasurface for 5G sub - 6 GHz communication systems,” pp. 1–17, 2022.

[29] B. Subeshan, A. K. Hamzat, and E. Asmatulu, “Fabricating Three-Dimensional Metamaterials Using Additive Manufacturing : An Overview,” 2025.

[30] I. Rosaline, “A Triple-Band Antenna with a Metamaterial Slab for Gain Enhancement and Specific Absorption Rate (SAR) Reduction,” vol. 109, no. December 2020, pp. 275–287, 2021.

[31] K. G. Baimain and A. J. Wiley, “METAMATERIALS”.

[32] M. M. M. Pai, “Electromagnetic Metamaterials : A New Paradigm of Antenna Design,” vol. 9, 2021, doi: 10.1109/ACCESS.2021.3053100.

[33] A. Revil, “Effective conductivity and permittivity of unsaturated porous materials in the frequency range 1 mHz – 1GHz,” vol. 49, no. November 2012, pp. 306–327, 2013, doi: 10.1029/2012WR012700.

[34] B. A. F. Esmail, S. Koziel, and R. K. Barik, “Overview of Metamaterials-Integrated Antennas for Beam Manipulation Applications : The Two Decades of Progress,” *IEEE Access*, vol. 10, no. May, pp. 67096–67116, 2022, doi: 10.1109/ACCESS.2022.3185260.

[35] C. Milias, R. B. Andersen, P. I. Lazaridis, and S. Member, “Metamaterial-Inspired Antennas : A Review of the State of the Art and Future Design Challenges,” *IEEE Access*, vol. 9, pp. 89846–89865, 2021, doi: 10.1109/ACCESS.2021.3091479.

[36] I. Elmutasim, “A Brief Review of Massive MIMO Technology for the Next Generation,” vol. 20, no. 2, pp. 262–269, 2023.

[37] E. Ali, M. Ismail, R. Nordin, and N. F. Abdulah, “Beamforming techniques for massive MIMO systems in 5G : overview , classification , and trends for future research,” vol. 18, no. 6, pp. 753–772, 2017.

[38] O. N. Alrabadi, J. Perruisseau-carrier, and A. Kalis, “MIMO Transmission Using a Single RF Source : Theory and Antenna Design,” pp. 1–11.

[39] N. Overview and R. Trends, “Massive MIMO Systems for 5G and beyond Networks—Overview, Recent Trends, Challenges, and Future Research Direction,” pp. 1–35, 2020, doi: 10.3390/s20102753.

[40] G. Ahmed *et al.*, “Rigorous Analysis and Evaluation of Specific Absorption Rate (SAR) for Mobile Multimedia Healthcare,” *IEEE Access*, vol. 6, pp. 29602–29610, 2018, doi: 10.1109/ACCESS.2018.2839909.

[41] M. Rashed, I. Faruque, A. M. Siddiky, and E. Ahamed, “Parallel LC shaped metamaterial resonator for C and X band satellite applications with wider bandwidth,” *Sci. Rep.*, pp. 1–15, 2021, doi: 10.1038/s41598-021-95468-8.

[42] A. G. Kislyakov and A. V Stepanov, “Equivalent Electric Circuit Models of Coronal Magnetic Loops and Related Oscillatory Phenomena on the Sun,” pp. 83–117, 2009, doi: 10.1007/s11214-009-9538-1.

[43] K. A. Hamad, “DESIGN AND ENHANCEMENT BANDWIDTH RECTANGULAR PATCH ANTENNA USING SINGLE TRAPEZOIDAL SLOT TECHNIQUE,” vol. 7, no. 3, pp. 292–297, 2012.

[44] G. Mayhew-ridgers, “DEVELOPMENT AND MODELLING OF NEW WIDEBAND MICROSTRIP PATCH ANTENNAS by,” no. July, 2004.